



NFPA
Education and
Technology
Foundation

California Polytechnic State University, San Luis Obispo

NFPA Fluid Power Vehicle Challenge

Project Report

April 19, 2017

California Polytechnic State University, San Luis Obispo

1 Grand Ave.

San Luis Obispo, CA, 93410

Submitted by: Anthony Fryer, Tyler Momberger, Jonathan Sather, Daniel Schletewitz

Advisors: Dr. Jim Widmann, George Leone



Table of Contents

1. Introduction	3
2. Background	3
2.A Competition Background	3
2.B Possible Design Solutions and Consideration	4
2.C Previous Cal Poly Designs.....	5
3. Objectives	7
3.A Goals	8
3.A.i Design Goals.....	8
3.A.ii Source of Goals	9
4. Design Development.....	10
4.A Preliminary Analyses/ Design Concepts.....	10
4.A.i Bike Layout Analysis.....	10
4.A.ii Hydraulic Circuit Analysis.....	15
4.A.iii Max Pressure Analysis.....	20
4.A.iv Pump/Motor Analysis	21
4.A.v Display Analysis.....	22
4.A.vi Tubing Analysis.....	25
4.A.vii Accumulator Analysis	26
4.A.viii Clutch Analysis	27
4.A.ix Clutch Disc FEA.....	30
4.A.x Tire Analysis	33
4.A.xi Aerodynamic Analysis	34
5. Final Design Considerations	35
5.A Bike Geometry	35
5.B Hydraulic System.....	39
5.B.ii Tubing Selection.....	39
5.B.iii Accumulator Selection	39
5.B.iv Pump/Motor Selection.....	40
5.C Freewheel Mechanism.....	40
5.D Electromechanical System	41
5.D.i Components.....	42
5.D.ii Layout	43
5.D.iii Printed Circuit Board Design.....	46
5.E Cost Analysis	47
6. Management Plan	48
6.A Construction and Validation Timeline	48
7. Concept Hazard Identification Checklist	49

8. Manufacturing	50
8.A Hydraulic Circuit Fabrication	50
8.A.i Bending Hard Lines.....	50
8.A.ii Hydraulic Circuit Assembly.....	52
8.B Electromechanical Circuit Fabrication	52
9. Testing	53
9.A Clutch Tests	53
9.B Hydraulic System Tests	54
9.C Electronic System Tests	54
9.C.i Solenoid Power Testing.....	54
9.C.ii Logic Testing.....	54
9.D Integrated System Tests	55
9.D.i Flow and Leak Testing.....	55
9.D.ii Competition-Specific Performance Testing.....	56
9.D.iii Reliability Testing.....	56
9.D.iii Other Metrics	56
9.E Bike Layout Analysis	56
10. Conclusions	59
Appendices	61
Appendix A: Works Cited	62
Appendix B: Comparison Plots	63
Appendix C: QFD House of Quality	66
Appendix D: Current Gantt Chart	67
Appendix E: Hydraulic Circuit Configurations (With Flow Directions)	71
Appendix F: Precharge and Work Calculators (Matlab Code)	73
Appendix G: Maximum Charge Pressure Calculations	75
Appendix H: Integrated System Tests	77
Appendix I: Tubing Friction Analysis	79
Appendix J: Cost Analysis and BOMs	85
Appendix K: Solidworks Models	91
Appendix L: Clutch Diagram	94
Appendix M: Hydraulic Components	100
Appendix N: Mechatronics Power Supplies	108
Appendix O: Clutch Analysis	109
Appendix P: Patterson Control Model	111
Appendix Q: Keyway Analysis	118
Appendix R: Eagle Schematic and Board for Custom PCB	119
Appendix S: Concept Design Hazard ID Checklist	121

1. Introduction

The purpose of our project is to design and manufacture a human-powered, hydraulically or pneumatically driven vehicle and enter it in the Fluid Power Vehicle Challenge (FPVC) competition. The inspiration for this competition stemmed from the Parker Hannifin and the National Fluid Power Association's (NFPA) desire to support and educate the next generation of Fluid Power engineers. The Challenge was designed to combine the bicycle, which provides a familiar platform, with fluid power to offer an interactive educational experience to engineering students. Per the competition guidelines, any direct mechanical connection between the driving force (the crank set) and the rear wheel will be penalized. Thus, instead of using chains or gears, teams must utilize either hydraulic or pneumatic modes of power transfer. *How* they utilize those modes of power transfer is the essence of the design challenge, and is what separates the successful designs from the blunders. Our team name, 0 Chainz, was selected to emphasize our commitment to avoiding the usage of chains in our design. 0 Chainz will compete with other universities in a series of races and presentations in April of 2017. The goal of 0 Chainz is to produce an entry that will outperform Cal Poly's 2015 and 2016 Challenge entries in all sub-competitions as well as finish within the top three overall.

The project benefits the fluid power industry, the NFPA, California Polytechnic State University-San Luis Obispo, and 0 Chainz. The fluid power industry benefits by fostering a good relationship with young engineers as well as having the opportunity to identify exceptional students to recruit. The NFPA succeeds at increasing the knowledge and excitement for fluid power. Cal Poly benefits from increased visibility as well as any winnings the entry may be awarded. Lastly, 0 Chainz benefits from gaining the engineering experience of taking a project through the steps to design, build, and test on a specific timeline.

2. Background

2.A Competition Background

The Chainless Challenge (CC) Competition was developed by Parker and first held in 2005. Select universities were invited to participate in the annual competition featuring hydraulic and pneumatic vehicles. The competition, however, was suspended from 2009-2011. The NFPA took over the Challenge in the 2015/2016 school year and renamed it the Fluid Power Vehicle Challenge. We initially used the previous year's rules and specifications to design the entry that will represent Cal Poly in the 2017 competition.

The competition has traditionally consisted of a midway design review, competition races, and design judging. The midway design review determined if sufficient changes have been made to the bike from the previous year. Points can be added to the design score based on the team's vehicle design, circuit design, selection of hardware, analysis, and building stage.

The competition consists of three races: a sprint, a time trial, and an efficiency event. The sprint race takes place on a 200-meter straight course and is essentially a drag race. Teams are given 10 minutes to charge their accumulator before racing in heats of two from a standing start. The endurance event consists of a longer course with maneuvering required. It is not uncommon for vehicles to fail during this event. During the efficiency event, teams charge their accumulator and release it. Pedaling is not allowed and the accumulator is the only source allowed to power the motor. The winner is determined using Equation 1 below where the distance the bike went in relationship to the amount of pre-charge in the accumulator is used to gauge efficiency; W is the weight of the bike, L is the distance traveled, P is the pre-charge, and V

is the volume of the accumulator. Points are awarded for placing well in each of the races; monetary awards are given also.

$$score = \frac{W * L}{P * V} \quad (1)$$

The last aspect of the Challenge is the judging of the designs. Designs are evaluated based on four categories: innovation, reliability, manufacturability, and safety. New designs and features that add to the competition score points for innovation. Reliability is judged on how well the bike faired during the endurance race. System failure or leaks negatively affect judging. When grading manufacturability, judges take into consideration the construction of the bike and how well components are packaged on the frame. Lastly, safety is judged by ensuring that the bike does not have and inherently dangerous design flaws, pinch points, or sharp edges. All components must be operated with in their designed specification range.

Other CC specifications typically include:

- Use of bio-degradable hydraulic fluid
- Each rider must wear a helmet
- Any vehicle leaking at a rate above 50 drops per minute will be eliminated
- Max vehicle weight of 210 pounds
- Max vehicle speed of 45 mph

2.B Possible Design Solutions and Consideration

The design specifications mandate that no belt or chain may be used to connect the pedals to the drive wheel, and prohibit internal combustion engines and electric motors. These specifications effectively left 0 Chainz with two options to choose from: utilize pneumatic or hydraulic power.

First, the viability of a pneumatic circuit was explored. Pneumatic vehicles have not done well at the competition in the past because, unlike the fluid in hydraulic systems, air is compressible. This means that some of the energy in the fluid is being lost as heat instead of moving through the motor and producing work. 0 Chainz therefore determined that it was not worth pursuing a pneumatic power system and decided to continue with a hydraulic system, keeping in line with previous Cal Poly entries and the advice of our advisors.

After landing on a hydraulic power system, we still needed to determine what kind of components we wanted to use. Looking at the big picture, the basic circuit consists of a way to transfer energy from the pedals directly to the driving wheel (direct drive), and a way to store and release energy to the driving wheel (charging and discharging the accumulator). To accomplish these tasks, rotational pumps or linear actuators are typically used to transfer energy from the pedals, and a bladder, piston, or spring accumulator is typically used for energy storage. The benefits of pumps are their high efficiency and smoother operation, which make the vehicle more rideable. The drawback, however, is that piston pumps are relatively heavy and only operate efficiently at high rpm, so they require additional gearing. Linear actuators act as pistons that pump fluid out of phase based on how they are attached to the crankshaft. It is more difficult to achieve a consistent pedaling force and therefore harder to maintain a cadence. Specific design decisions regarding these components are elaborated in the Pump/Motor Analysis (Section 4.A.iv).

Another consideration is minimizing the amount of fittings within the hydraulic circuit to reduce system power losses. Conversely, it is beneficial to add a method of additional power gain, or a regeneration

mode, to the system. Such a method would allow for power gain in already-used operations like braking, as well as adding points to our overall score per the Competition specifications.

Another important aspect of the system is the maximum pressure. All components must be rated for at least the maximum system pressure, noting that overrated components would add unnecessary weight. As a guideline, the higher the pressure that can be attained in our system, the more energy we can store in the accumulator. Through vehicle modeling and analysis of previous results, more energy storage in the accumulator positively correlates to better performance in the sprint race. An upper bound on our maximum attainable pressure rating will be dependent on our physical ability to charge the accumulator as discussed later (Section 4.A.iii). Lastly, some sort of freewheel mechanism is beneficial to move the vehicle around and to coast during the efficiency challenge. This can be achieved using a clutch or an internally geared hub on the drive wheel. The challenge of using a clutch is that it may be prone to slipping before the desired pressure is reached when charging the accumulator. The challenge of using internally geared hubs is possible failure from the greater than human torque produced by charging or by dumping the accumulator.

Vehicle layout is another important design consideration. Entries in the past have varied between standard touring bicycle and recumbent configurations. Depictions of these geometries are shown in the Bike Layout Analysis (Section 4.A.i). In general, recumbent vehicles offer better aerodynamics and a lower center of gravity than the standard touring geometry. Three-wheeled recumbents also offer increased stability for the rider. The drawbacks, however, are that the vehicle typically becomes heavier and is difficult to configure without using a chain due to the weight of the pump that would need to attach to the pedals. In comparison, standard touring bicycles are easier to manufacture, and are lighter. Aerodynamic fairings are also an option to add to either design for drag reduction.

2.C Previous Cal Poly Designs

Historically, Cal Poly has done very well at the CC competition. This has resulted in a large amount of resources left behind by the previous teams, and insight into their successes and shortcomings to use while designing our vehicle. An overview of significant designs is presented below.

For the first competition, in 2005, Cal Poly utilized a cam follower with a linear piston pump shown below in Figure 1.



Figure 1: 2005 Cal Poly CC Entry

This design used a gear pump and chain to power to the rear wheel. The accumulator was towed behind the bike on a trailer allowing the bike itself to remain relatively light and compact. The use of a trailer to pull any component of the bike has since been outlawed. The cam follower and liner piston pump were determined to be inefficient methods and were replaced by a centrifugal piston pump the next year.

For the 2007 competition, Cal Poly's entry featured a variable displacement piston motor coupled with a spiral bevel gear attached to the rear hub. This produced an infinitely variable speed ratio. The bike, however, was underbuilt and as well as having misaligned gears. Ultimately, the drive shaft broke during the sprint race. This emphasized the importance of doing proper analysis and having sufficient time to test and train on the bike prior to competition. The bike is shown below in Figure 2.



Figure 2: 2007 Cal Poly CC Entry

The 2014 entry returned to linear actuators in an attempt to make the bike lighter while remaining robust. The actuators were attached to offset arms on the pedal axle to convert the rotational input to linear motion. The motor was also a hydraulic cylinder but set out of phase with the front one and eccentrically fastened to the drive shaft. Hydraulic lines connected both pistons to the actuator bore and connecting both cylinders together in the correct combination allowed the bike to act like a fixed gear bike. The bike, however, was not completed in time to attend the competition. It proved difficult to properly time the front and back linear actuators and became limited at high speeds. The bike ultimately served as lesson against linear actuators by demonstrating the performance reduction compared to previous designs. A picture of this bike could not be found.

The 2015 entry was a complete redesign of the CC bike. A new frame was constructed using 4130 steel tubing for increased strength and featured customized mounting plates for the pump and motor assemblies. The bike utilized two Parker F-11 5cc/rev bent axis piston pumps, one acting as the pump and the other as the motor. It was also capable of regeneration through the correct valve combination in the circuit. A planetary gear set with a 5:1 ratio was purchased to work in conjunction with the pump. The team attempted to add a clutch but struggled to apply enough clamping force at the handle. They also reported bike cable used to attach the clutch to the handle frequently snapping under load.

Lastly, the 2016 entry shows the current state of Cal Poly's CC bike. This year's team built upon the 2015 entry and made the clutch to the rear drive shaft functional to allow the bike to freewheel. They achieved this by replacing the springs in the clutch to ones with a lower spring constant. The clutch, however, slips when charging to higher pressures and effectively limits how much the accumulator can be charged. The

team had also intended to add electronically controlled solenoids and reconstruct the circuit with solid tubing but was unable to because of shipping delays. The bike can be seen below in Figure 3.



Figure 3: 2016 Cal Poly CC Entry

3. Objectives

The overall objective of this project is to outperform the 2015 and 2016 Cal Poly CC entries in every category of competition and finish within the top three overall. It is also the intention of 0 Chainz to have a net positive income, spending less on the project than we receive in winnings. By doing this, we will maintain a high level of competition as well as leaving sufficient resources for the next Cal Poly team.

Using information about past competitions from online research, discussion with the previous team, and discussion with our sponsor, we defined a set of qualitative requirements in order to satisfy the goals of the project. In order to qualify the sponsor and team requirements, a Quality Function Deployment was used as seen in Figure 4.

In the House of Quality, each requirement was ranked based on perceived importance to the sponsor and to the competition judges. Next, the 2015 and 2016 Cal Poly Chainless Challenge entries were graded on each requirement based on a score from one to five, with five being the best score. In order to define the correlations between qualitative specifications and customer requirements, each requirement was related to each specification with a blank (no correlation), a one (small correlation), a three (medium correlation), or a nine (strong correlation).

Once the requirements and specifications were related, the specifications were correlated to each other in the top pyramid. A symbol showing the favorable trend direction was indicated below each specification, and correlations between specifications were denoted as various degrees of positive or negative, or left blank if there was no significant correlation. Finally, the design targets were quantified by relating them to the 2015 and 2016 Cal Poly Chainless Challenge entries in the bottom three rows.

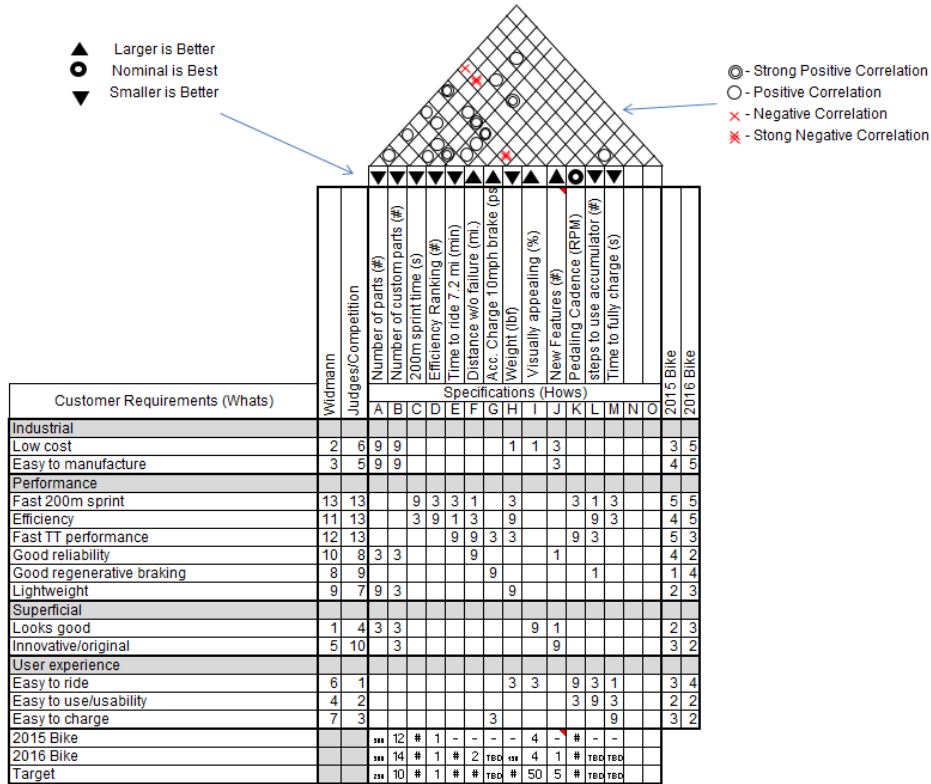


Figure 4: QFD House of Quality [Appendix C]

This QFD revealed valuable, overarching relationships and restrictions that would be fundamental to our design methodology. This visually showed the dependencies between different design factors and performance in competition categories. To start, the team began with intuitive and "feel" based requirements that described different desirable characteristics in the design. At this stage, these requirements did not include the hard metrics of time-based challenges. We then went through each requirement and found a method to quantify each in a verifiable way.

3.A Goals

3.A.i Design Goals

To fulfill our goal of improving on Cal Poly’s 2016 results and finishing in the top three overall, 0 Chainz identified the following goals. It is important to note although a podium finish cannot be guaranteed, we feel that, based on our research of the competition and recent trends, meeting these goals will increase our likelihood of success in the Challenge.

Industrial

- Low Cost – The design shall cost no more than \$7500.
- Easy to Manufacture – The completed product will contain no more than five non-OEM parts.
- Easy to Assemble – All critical components must be able to be assembled onto frame without permanent joints.

Performance*

- Fast Acceleration – The bike must take no more than 5 seconds to reach top speed.

- Fast 200m Sprint – The bike must complete a 200m sprint in less than 29 seconds.
- Efficient – The bike must be at least 10% more efficient relative to previous year's bike, based upon Chainless Challenge efficiency formula.
- Lightweight – The bike's weight must not exceed 150 lbs.
- Good Reliability – The bike must be able to ride 50 miles without mechanical failure.
- Regeneration - The bike must be capable of regenerative breaking. The specific regeneration capabilities are to be determined.

Superficial

- Looks Good – The bike should look streamlined and have a quality surface finish on components.
- Innovative/Original - The bike will implement an electromechanical control system (as opposed to last year's manual ball valve design).

User Experience

- Easy to Ride – The bike can be pedaled at a natural cadence (80-100 RPM crank speed).
- Easy to Use – Controls will be placed in reach of the rider and useable without looking.
- Easy to Charge - One person will be capable of fully charging the accumulator within 10 minutes.

*All performance goals to be met on flat, dry pavement.

3.A.ii Source of Goals

Most of the goals were defined by benchmarks from previous Chainless Challenge teams, especially competition performance. The sprint goal, for example, was set to beat the 2015 team, which won the competition overall. Other goals such as manufacturability, reliability, originality, and cost were derived from the competition requirements and scoring categories that were not part of the race performances.

The remaining goals were defined by the desires of our team. Factors such as ease of use and rideability will make our design more conducive to good performance and therefore increase our outcome at competition. Also, aesthetic appeal was important to our team since we would like to make a product that is both visually appealing to the public while efficiently housing all of the hydraulic components.

The cost goals set a ceiling for our design costs, in that it was less than the theoretical prize money received through achieving the same benchmarks set by the 2015 Cal Poly Chainless Challenge team. The success of previous teams has resulted in a well-funded program and it is our desire to continue this for future teams.

Below is a table defining all the formal engineering specifications associated with our design goals.

Table 1: Engineering Specifications for Final Design

Specification No.	Parameter Description	Requirement or Target (units)	Tolerance	Risk	Compliance
1	Number of parts	290 (parts)	Max	L	I
2	Number of custom parts	10 (parts)	Max	L	I
3	200m sprint time	25 (seconds)	Max	H	A,T
4	TT time (6.2 mile)	40 (minutes)	Max	H	A,T
5	Efficiency	110% of 2016 (score)	Min	H	A,T

6	Target cadence	90 (RPM)	±10	M	A,T
7	Distance without failure	50 (miles)	Min	M	A,T
8	Accumulator charge from braking (10mph to dead stop)	TBD (psi)	Min	L	A,T
9	Weight	80 (lb.)	Max	H	A,T
10	New features	5 (features)	Min	M	I
11	Steps to use accumulator	TBD (steps)	Max	L	T
12	Time to “fully charge”	10 (minutes)	Max	M	A,T,S
13	Production Cost	7500 (dollars)	Max	L	A

It is important to note that while almost all specifications are derived from the competition, they can all be validated outside of the competition. The time trial can be simulated beforehand because it is simply a 2 mile flat course. An efficiency score can also be calculated prior to the competition using Equation 1. Note that a "feature" as mentioned in Specification 10, is defined by 0 Chainz as a design component that we believe will be a significant innovation in the eyes of the FPVC judges. In the event that a competition is not held, all specifications can still be validated.

4. Design Development

Based on our background research of previous Cal Poly projects, we eliminated some design ideas that were initially considered. Per the advice of Dr. Widmann and our analysis, we eliminated the potential for a pneumatic design due to their poor efficiency and power capabilities as well as using linear actuators due to their relative inefficiency compared to conventional pump and motor systems.

In determining our overall vehicle design, the first step was to consider major elements upon which much of our design was contingent, such as the vehicle layout and hydraulic circuit design. In the subsequent sections, these major elements will be considered, in addition to various components that will necessarily be included in our system.

4.A Preliminary Analyses/ Design Concepts

4.A.i Bike Layout Analysis

A quantitative comparison of several different vehicle designs was used before selecting our vehicle layout. The former Cal Poly entries have been two wheeled bicycles, although the rules do not stipulate how many wheels teams may use on their vehicles.

Vehicle weight was the first performance variable that was investigated. Dr. Widmann and Jeff Powell, a member of the 2016 Cal Poly chainless team, each advised lightening the vehicle while also increasing its charge pressure. Speed vs. Power comparisons were created to see the effects of vehicle weight on the power required to maintain a speed. This comparison is especially important in determining success in the

time trial event of the competition. All vehicle comparison plots can be found in Appendix B. Figure 5 shows the power versus speed for a standard touring bicycle.

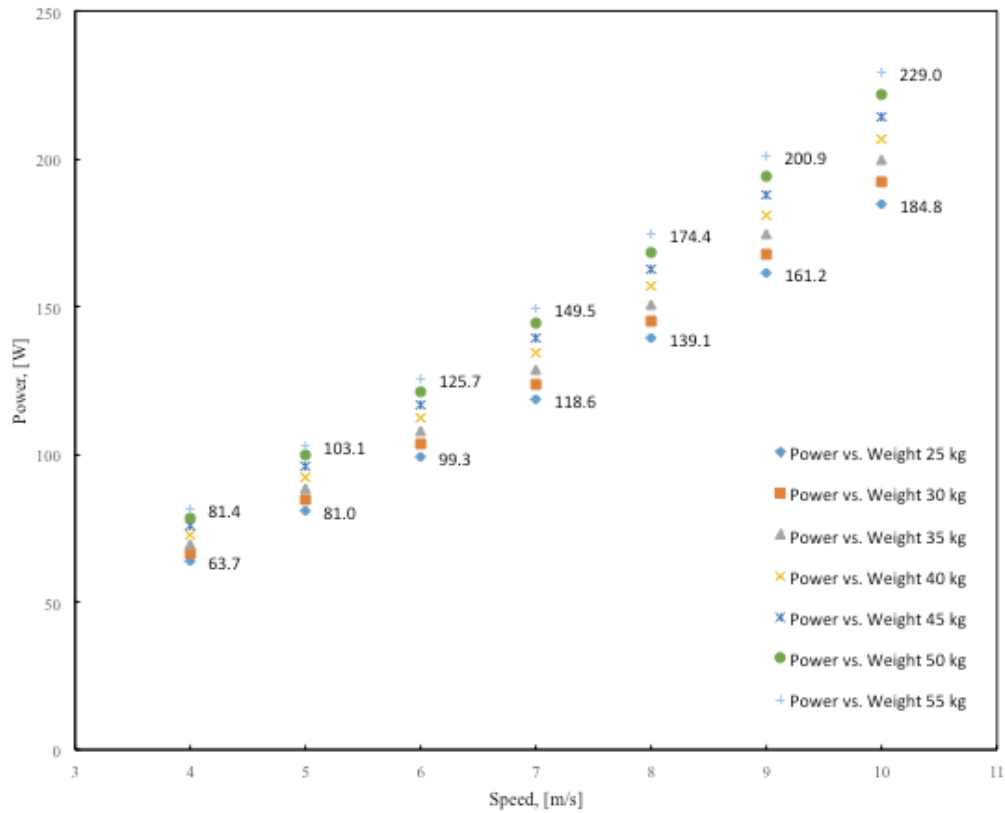


Figure 5: Power vs. Speed for Different Weights of a Standard Touring Bicycle [Appendix B]

These models contain assumptions for rolling resistance, frontal area, and vehicle drag coefficient. The assumptions, however, are carried across all four vehicle platforms. Therefore, while not an ideal model, it was suitable and the information was used in deciding the final vehicle configuration.

Figure 5 shows the power differences for a given speed between the lightest and heaviest vehicles. The power difference increases exponentially with velocity for each bicycle weight. This is due to the exponential increase in aero resistance caused by an increase in velocity. Additionally, the heaviest bicycle requires approximately 20-50 additional watts compared to the lightest bicycle for a given speed.

The first term required in calculating power required was the road load due to the weight of the vehicle as seen in Equation 2.

$$F_r = f * m * g \quad (2)$$

Where f was the rolling resistance coefficient (estimated at 0.015), m was combined mass of vehicle and rider (assume 80kg rider) and g was gravity.

Equation 3 provided the force required to overcome drag:

$$F_d = C * A * \rho \left(\frac{V^2}{2} \right) \quad (3)$$

$$F_{net} = F_r + F_d \quad (4)$$

Where C was a constant based on shape, A was the frontal area, ρ was the density of air, and V was velocity.

The power required was the net force, F_{net} calculated in Equation 4, multiplied by traveling velocity. As shown, the V term was squared, which means that the force and power exponentially increased with an increase in vehicle speed. Weight was still non-negligible.

Using these graphs, we compared different designs between a conventional upright bicycle, a time trial specific bicycle, a recumbent, and an aero recumbent (all of which can be seen in Appendix B). In brief, the aero recumbent was the fastest vehicle for a given power output, followed by the recumbent, the TT bike, and the standard upright position. From these results, it would seem that the aero recumbent is the obvious choice.

Further research revealed that there were power losses and other differences inherent to the different seating positions. We saw that the recumbent designs had a 20-25% loss of power, and a 5-10% difference in the TT position (McCraw). This made analysis complicated, because while the recumbent and HPV required less power to maintain speed, there was less power available for input.

With some initial comparisons between the vehicle configurations, we further investigated the differences via qualitative and quantitative analysis. These analyses are based upon a set of acceptance criteria, and were evaluated in three stages as outlined below.

Acceptance Criteria

The acceptance criteria were partly based on our specifications table as well as team discussion. They are:

- A. Rideability: How easy the vehicle is to operate. Difficulty to maintain balance, maneuver, use controls, switch circuit configurations, etc.
- B. Manufacturability: Closely linked to production time and production cost. How feasible the vehicle is to manufacture. The design should limit special parts or extra design considerations.
- C. Aesthetics: The vehicle is visually appealing and incorporates the hydraulic components efficiently within space constraints.
- D. Weight: How heavy the vehicle is. Heavier vehicles go slower per a given power input.
- E. Aerodynamics: How aerodynamic a vehicle is also affects performance. More aerodynamic vehicles (assuming equal weight) travel faster per a given power input.
- F. Production time: Special components or frame requirements will require more production time, which leaves less resources available for analysis and testing.
- G. Production cost: We have a finite amount of capital for the project.
- H. Drivetrain efficiency: Longer frames/circuits have more head loss and possibly more junctions / fittings, which all equate to less efficiency.

Evaluation 1: Go//No Go

Bicycle Design	Go	No Go
Recumbent	X	
Tricycle	X	
Standard Touring	X	

Aero/HPV		X
TT Bicycle	X	

Figure 6: Go/No Go Matrix.







As seen in Figure 6, the aerodynamic/HPV vehicle design was deemed as “No Go” and therefore eliminated. This decision was largely based on the manufacturability, production time, and production cost. Unfortunately, we do not have a preexisting HPV fuselage available to us. Even if we did, it would require a lot of time and fabrication to retrofit our hydraulic components within the already tight packaging restraints of the inside of an HPV. A poorly made HPV can have comparable drag to a standard bicycle. Consequently, much of our team’s resources would have had to focus on the aerodynamics, rather than the hydraulic circuit and other elements. Creating a new, effective HPV also requires carbon or fiberglass skills and materials, as well as a time and cost intensive mold.



Figure 7: Inside of a typical HPV bicycle.

Due to its aerodynamic design and profile, there is very limited space for a traditional drivetrain, even less for a hydraulic circuit. Image courtesy: recumbentblog.com

Evaluation 2: Pugh Matrix

Concept						
Criteria	Current	Recumbent	Tricycle	Standard Touring	Aero/HPV	TT
Rideability	DATUM	-	+	S	-	-
Manufacturability		-	-	S	-	S
Aesthetics		-	-	+	+	+
Weight		-	-	S	-	S
Aerodynamics		+	+	+	+	+
Production Time		-	-	S	-	S

Production Costs	S	-	S	-	S
Drivetrain Efficiency	-	-	S	-	S

Figure 8: Pugh Matrix of vehicle design candidates, with the 2015-2016 bicycle as the datum reference. A “+” indicates better than datum, “-” indicates worse than datum, “S” indicates same as datum.

Figure 8 is our Pugh Matrix, with the 2016 bike as the datum. The 2016 design is the datum because it is the standard to which we were looking to improve upon going into competition. The 2016 design had done well in recent years, winning first place in 2015 and second place in 2016. We aim to win the competition while also doing better than Cal Poly teams of past.

The recumbent had several negative scores. A recumbent by design is difficult to start from standstill, which hinders its rideability and performance in the sprint competition. Also, based on previous research we also found that the power input from the rider is different on a recumbent due to pedal positioning and the rider’s leg positions. This would affect us because we do not have a recumbent to ride and train on to become more powerful and comfortable in the recumbent position before the competition. It’s more difficult to manufacture with reservations for the hydraulic components based on its frame shape. It also requires more production time because there is little known about touring or heavy loaded recumbents and the frame geometries required. Recumbents are heavier relative to a traditional bicycle due to their larger frames and seats. The only positive is that it is more aerodynamic. See Appendix B for figures and calculations. However, due to the unfamiliarity with the position and inability to train with a recumbent, the power lost from the positioning may outweigh the power savings from the aerodynamics.

The tricycle solves some of the recumbent’s rideability issues, but also increases production costs. Both designs require cranksets at the front of the bike, which would require long hydraulic lines to the drive wheel. These longer lines have more head loss and less efficiency. A closer look at loss analysis can be found in Tubing Analysis (Section 4.A.vi).

The standard touring bicycle was most similar to the current design. However, with the addition of drop bars and different geometry, rideability with the large amount of weight is improved, as well as aerodynamics due to the lower positioning.

The HPV scored higher in aesthetics and aerodynamics, but scored worse in every other category. As mentioned in the Go/No Go comparison, the HPV had several drawbacks.

The TT (time trial) bicycle design scored higher in aerodynamics and aesthetics but sacrificed rideability due to its aerobar positioning. In the aerodynamic position, rider’s arms were close to the centerline of the bicycle. This created unstable steering. In the non-aerodynamic position, rider’s hands are on the outer “bull horns” of the base bars. This was more stable but lost most of the aerodynamic position benefits.

Overall, the vehicles similar to the current design scored better than radical, new design concepts.

Evaluation 3: Weighted Decision Matrix







		Criteria	Rideability	Manufacturability	Aesthetics	Weight	Aerodynamics	Production Time	Production Costs	Drivetrain Efficiency	Overall Satisfaction
Concept	Weight/100		20	10	5	15	15	10	5	20	100
Current	 Raw Score/100	70	70	50	70	50	70	70	70	70	66
	Weighted Score	14	7	2.5	10.5	7.5	7	3.5	14		
Recumbent	 Raw Score/100	50	40	50	60	90	50	70	60	59.5	
	Weighted Score	10	4	2.5	9	13.5	5	3.5	12		
Tricycle	 Raw Score/100	90	40	50	50	90	50	60	60	65.5	
	Weighted Score	18	4	2.5	7.5	13.5	5	3	12		
Standard Touring	 Raw Score/100	80	70	70	70	70	70	70	75	73	
	Weighted Score	16	7	3.5	10.5	10.5	7	3.5	15		
Aero/HPV	 Raw Score/100	40	40	80	50	100	40	40	60	56.5	
	Weighted Score	8	4	4	7.5	15	4	2	12		
TT	 Raw Score/100	60	70	80	65	90	65	65	70	70	
	Weighted Score	12	7	4	9.75	13.5	6.5	3.25	14		

Figure 9: Weighted Decision Matrix.

Figure 9 shows our Weighted Decision Matrix for all of the vehicle designs. We assigned a weight to each of the criteria, and gave each design a raw score for each criteria. The weighted score is the raw score multiplied by the weight of criteria. We also chose to include the current design as the datum reference. We saw that only the standard touring and TT designs score higher, whereas the recumbent designs were all scored less.

Chainz then decided to pursue a traditional bicycle design with the standard touring configuration. We felt that it best compromised performance with rideability and manufacturability. This was affirmed by our quantitative analysis as well as our 3 evaluations.

4.A.ii Hydraulic Circuit Analysis

Once the general frame design was selected, the next pertinent design decision was the hydraulic circuit. A hydraulic circuit is a combination of hydraulic components that together perform a function while keeping the fluid in a closed system. We began the design process by researching as many circuits as we could from previous competitions and testing some out at the previous 2016 Chainless Challenge competition. From this we brainstormed new circuits that could feasibly accomplish our goals. What follows is the evaluation process for determining the hydraulic circuit that would be ideal for our requirements, beginning with a basis from which to judge each design.

Acceptance Criteria:

- A. Circuit Weight – Overall weight of circuit, based on number of required components to achieve functions.
- B. Complexity – Based upon the number of required components and custom parts.

- C. Efficiency – How proficient the design would be in the efficiency challenge, based upon the formula given by the Challenge. This analysis assumes that the accumulator volume and pre-charge are the same between circuits.
- D. Sprint – How proficient the design would be in the sprint challenge. Based upon ability to store pressure in the hydraulic accumulator.
- E. Time Trial – Based on rideability due to weight distribution, ability to coast, and ability to store energy while riding.
- F. Production Cost – Based on the number of components required, the nature of the components, and the amount of time for implementation.
- G. Energy Storage – The ability of the circuit to store energy, dependent on maximum energy obtainable and the ability to store energy while riding. If a design has regenerative braking it is assumed to be able to reach maximum calculated pressure as shown in Appendix G.

Evaluation 1 – Go/No Go:

Circuit Design	Go	No Go
Regenerative Braking	x	
Pedal Generation	x	
Pedal + Regen	x	
Parallel Motor and Regen	x	
Free Wheel Crank	x	
Single Pump System	x	
Centrifugal Pump		x

Figure 10: Go – No Go Matrix Evaluation.

The only idea that is outside the realm of feasibility was the centrifugal pump and rudder system. The reason being that it was a very inefficient method to transfer force through fluid power, using a rudder (or turbine) was only usually beneficial when there is a continually moving source of fluid to harness energy from (e.g. a river).

Evaluation 2 – Pugh Matrix:

An initial Pugh Matrix was created in order to evaluate relatively how each circuit satisfies the criteria and how the characteristics relate. The purely regenerative braking concept was used as the datum as it was the same type of circuit as the previous Cal Poly entry. To explain the other concepts further, the pedal circuit types had the ability to charge the accumulator using the pedal cranks. The single pump system used one pump as both pump and motor, however this design cannot do direct drive. The free wheel crank system had a free wheel mechanism in the crank on top of regenerative braking.

Concept	Only Brake Regen	Only Pedal Gen	Pedal + Brake Regen	Parallel Regen and Motor Circuits	Free Wheel Crank w/ Regen	Single Pump System	Front Wheel Regen
Criteria							
Circuit Weight	D A T U M	+	-	-	-	+	S
Complexity		-	+	-	+	-	-
Efficiency		-	S	-	S	-	S
Sprint		-	-	+	S	-	S
Time Trial		+	+	+	+	S	S
Production Cost		+	-	+	-	+	S
Energy Storage		-	+	S	+	S	+
Σ^-		4	2	3	2	3	1
Σ^+		3	4	3	3	2	1
Σ		0	-1	1	0	1	-1

Figure 11: Initial Pugh Matrix Evaluating Against 2016 Circuit Design.

The result of this initial Pugh Matrix was that the leading design based on these criteria is the hydraulic circuit that had regenerative braking and pedal charging. Through the Pugh Matrix we saw how Energy Storage and Weight were positively correlated to the ability to achieve competition requirements. On designs that did not have regenerative braking, the inability to achieve high pressures (i.e. energy) outweighed the fact that the design was lighter in weight. The difference in energy storage ability can be seen in Pump/Motor Analysis (Section 4.A.iv).

Concept	Only Brake Regen	Only Pedal Gen	Pedal + Brake Regen	Parallel Regen and Motor Circuits	Free Wheel Crank w/ Regen	Single Pump System	Front Wheel Regen
Criteria							
Circuit Weight	+	+	D A T U M	+	+	+	+
Complexity	+	+		+	-	+	-
Efficiency	S	-		-	+	-	-
Sprint	S	-		-	S	S	S
Time Trial	-	S		-	+	-	-
Production Cost	+	+		+	-	+	+
Energy Storage	-	-		-	-	-	+
Σ^-	2	3		4	3	3	3
Σ^+	3	3		3	3	3	3
Σ	1	0		0	-1	0	0

Figure 12: Secondary Pugh Matrix Evaluating Against Previous Outcome.

The result of this Pugh Matrix was that the design that met the most criteria was the purely regenerative braking design. Although it cannot pedal-to-charge, that was a feature that could or could not be helpful depending on the competition course. Though the pedal-to-charge would add energy to the system while riding if combined with a free-wheel mechanism, the maximum amount of pressure we could produce from the pedals was 260 psi and not significant when compared to the initial charge pressure as shown in Max Pressure Analysis (Section 4.A.iii). From these first evaluations we were able to see the configurations that would be most feasible for meeting our requirements, to better visualize these circuits we created diagrams showing the flow directions for each mode. These diagrams can be found in Appendix E.

Evaluation 3 – Weighted Decision

This evaluation is meant to show how important each criteria was in obtaining a satisfactory design that met the problem requirements. Through group discussion we found a balance that be was conducive to achieving our and our Sponsor's design goals. The criteria weights were justified as follows:

- Circuit Weight - 25%
 - Important for rideability at low speeds.
 - A simpler, lighter circuit will increase reliability and safety.
 - Better power to weight ratio (assuming same Energy Storage)
 - Gives more leeway for added weight in other systems.
- Energy Storage – 25%
 - Positively correlated to all competition criteria
 - From past competitions, the winning designs were either able to store a large amount of energy or able to efficiently use energy while riding.
- Sprint – 15%
 - Positively correlated to storing more energy in accumulator.
 - If Sprint requirement is accomplished, the Efficiency requirement is likely to be achieved.
- Efficiency – 12%
 - Less human input for more fluid power. Increases rideability
 - Important competition requirement that validates design.
- Time Trial – 12%
 - Important competition requirement that validates design.
 - If circuit supports natural cadence and/or has a freewheel, allows for increased human work.
- Complexity – 5%
 - Although complexity would most likely decrease reliability, we did not want it to unjustly dissuade designs.
- Production Cost – 5%
 - Although the budget is not unlimited, conservative cost estimates are still within our range for all designs.

Design Criteria	Circuit Weight	Complexity	Efficiency	Sprint	Time Trial	Production Cost	Energy Storage	Overall Satisfaction
Weighting Factor	0.25	0.05	0.12	0.15	0.12	0.05	0.25	1
Alternatives								
Only Braking Regen	75	75	90	90	75	75	90	82.05
Only Pedal Gen	90	90	50	50	75	90	50	66.5
Pedal + Braking Regen	50	50	75	75	75	50	100	71.75
Parallel Regen and Motor Circuits	90	75	50	90	90	75	90	82.8
Free Wheel Crank w/ Regen	50	50	90	75	90	50	100	75.35
Single Pump System	100	75	75	75	25	75	50	68.25
Front Wheel Regen	75	50	90	90	50	75	90	77.8

Figure 13: Detailed Decision Matrix with Weighting Factors

Results:

From the weighted decision matrix, we saw that the circuit designs that were best suited in meeting the problem requirements were the purely regenerative braking circuit, the parallel regenerative braking, and direct-drive motor circuits. The configurations for these circuits can be seen in the following figures. To see the flow directions for each operational mode, see Appendix E.

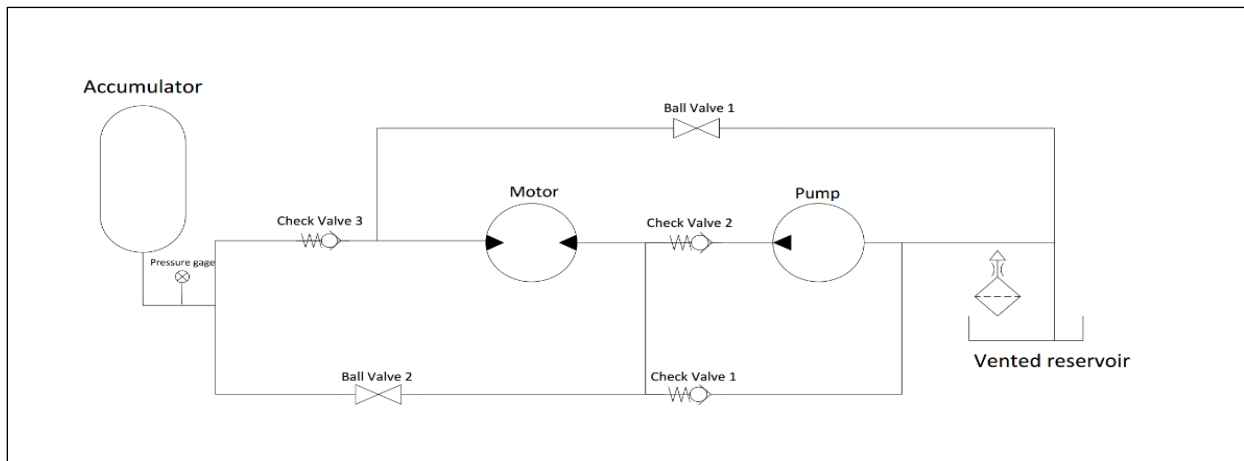


Figure 14: Schematic for Regenerative Braking Circuit.

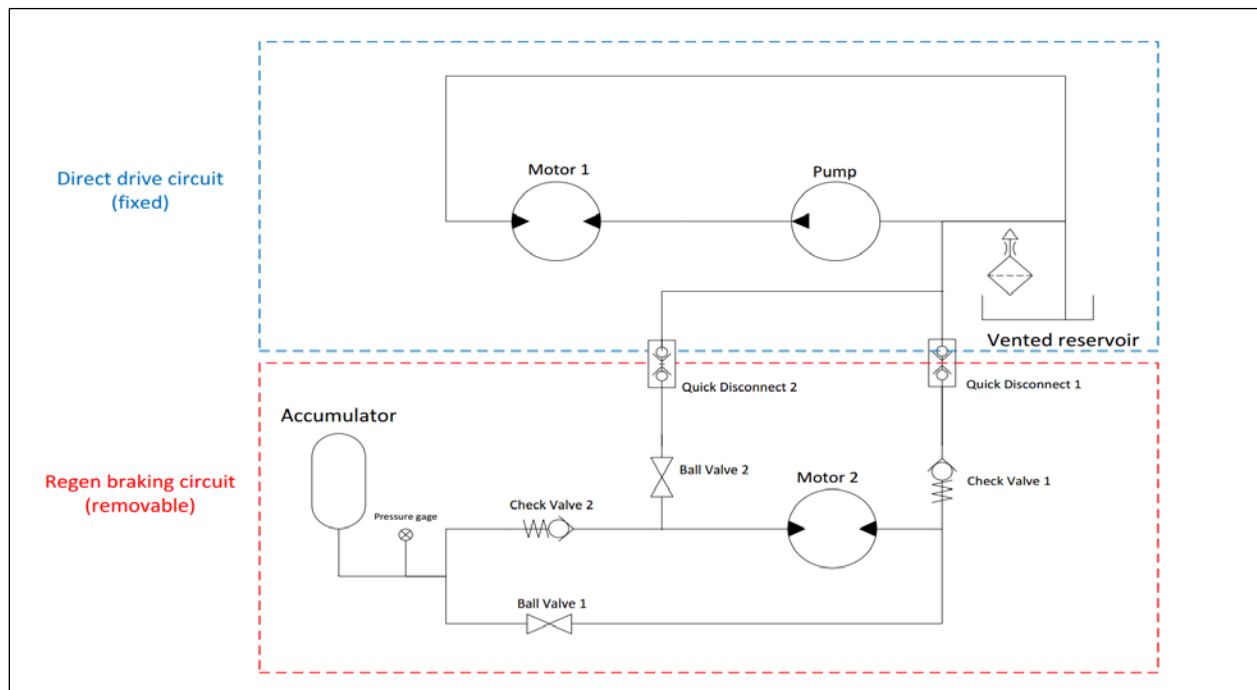


Figure 15: Schematic for Parallel Direct Drive and Regenerative Braking Circuits.

After considering these two circuit designs, we found that while the ability to drop part of the circuit for the Time Trial was beneficial in our weight requirement, the ability to disengage the motor was too important. To add a clutch and associated fixture material on top of the extra motor in the Parallel circuit design would bring the system weight far beyond the problem requirements, approximately 35 lbs. over.

For manufacturing and attaching the hydraulic circuit there are specifically designed drop-out steel brackets on the frame to attach the motor and pump. All circuit components are to be connected by stainless steel tubing in order to minimize the basic geometry and head losses as seen in Tubing Analysis (Section 4.A.vi). All welded components will be steel as we are not equipped to heat-treat aluminum.

4.A.iii Max Pressure Analysis

Before selecting individual components to use in our hydraulic circuit, the operating pressure of the circuit needed to be determined. The Challenge rules dictated that teams would be given ten minutes to charge their accumulator and only one team member can be charging the accumulator at a time. From that, it was determined that our physical ability to charge the accumulator should be used to determine the maximum pressure possible.

Our first solution consisted of a rider pedal-charging the accumulator. This would require the bike to be held stationary and upright while the rider pedaled to move fluid through the pump and into the accumulator. A rider input of 21 Nm was assumed at the crankset based on 200 watts at 90 RPM, which was typical for a standard bike and average rider. This torque was then combined with the pump and gear ratio found on the 2016 bike to find a maximum charge pressure of approximately 260 psi (Appendix G). It was noted that the 15:1 gear ratio between the crankset and pump significantly hurt the charge pressure but could be fixed by adding some sort of selectable gearing just for charging. This, however, would over complicate the drivetrain and at a lower RPM, the efficiency of the pump decreased.

The next solution consisted of push charging the bike. Push charging can be achieved by putting the circuit into regeneration mode and pushing the bike. It used the rear motor as a pump and charged the accumulator without adding any complexity to the drivetrain. This analysis assumed a 27.25-inch wheel, a 225 N pushing force, and a 2.7:1 gear ratio at the rear axle. The 27.25-inch wheel and the 2.7:1 gear ratio was based on the 2016 bike. The 225 N pushing force came from Canadian Centre for Occupational Health and Safety and represents the “standing pushing force that should not be exceeded” by an employee utilizing "full body involvement." The resulting torque at the rear axle was determined to be approximately 78 Nm. It was then assumed what 30% of the pushing force would be required to keep the rear wheel from slipping which then produced an adjusted torque of 56 Nm and a maximum charge of approximately 4,000 psi (Appendix G).

Based on this analysis, we decided to utilize push charging in our design and require all of our hydraulic components to be rated for 4,000 psi unless we decide to run the bike at a lower pressure to save weight.

4.A.iv Pump/Motor Analysis

In hydraulic systems, pumps and motors are comprised of essentially the same technology. Functionally, the only difference between the two is that each one is designed to be slightly more efficient for its respective purpose (either as a pump or motor). Thus, in the forthcoming analysis we will consider pumps and motors as one and the same. We compared gear, inline axial, radial, and bent axis pumps. The major factors used to compare pumps were: overall efficiency, pressure limit, rideability, and weight. O Chainz did not want to reduce the bike’s efficiency from previous years, but also has recognized the need to reduce the overall weight of the bike. It is also important to note that overall efficiency is the product of a pump’s volumetric and mechanical efficiency. The efficiency values presented in this section were published by Bosch Rexroth USA (Machinery Lubrication). Components were researched and compared assuming a 5 cc/rev fixed displacement (or similar) in order to compare weight and pressure to the current components on the bike. Rideability refers to how smooth a rider can pedal at the crank and was determined using information obtained from previous competitions. Parker was frequently used as a baseline to simulate what configurations would typically be found on the market.

The 2016 bike utilized two F11-5 bent axis Parker models, one as the pump and the other as the motor. In general, bent axis piston pumps offer the highest overall efficiency at 92%. The previously-used F11-5 offers 4.9 cc/rev with a max pressure of 6000 psi and weighs 11 pounds. Bent axis piston pumps are also considered to provide the most rideable experience of all the piston pumps. It is doubtful that the accumulator can actually be charged to 6000 psi so finding a pump with a lower rating should help reduce weight.

Gear pumps work by utilizing two rotating gears, which create a vacuum as they unmesh on the inlet side of the pump. Fluid is transferred along the outside of the pump housing between the gear teeth to the outlet side where the gears mesh (Viking Pumps). Gear pumps suffer from a relatively low overall efficiency of 85% for external gear and 90% for internal gear models. A model like Parker’s PG503 setup with a 4.8 cc/rev can operate at a pressure of 3300 psi and weighs about 3 pounds. This would save a considerable amount of weight (16 pounds pump/motor combined) but limit our max pressure and hurt rideability.

An inline axial piston pump uses a fixed-angle swashplate with pistons attached to it on a piston plate. The pistons rest in the cylinder block and are pulled out of their bores as the swashplate turns with the drive shaft. Removing a piston from its bore a vacuum is created at the inlet port and fluid fills the bore. As the swashplate continues to turn, the piston is forced back into its bore and the fluid discharges through the outlet. Inline axial piston pumps are well known for their compact design and low cost but are typically used for larger displacements (Hydraulics and Pneumatics). Axial piston pumps boast an overall

efficiency of 91%, which is the second best behind bent axis pumps. The problem with inline axial pumps, however, is that they are typically made for commercial purposes and models small enough for our application are hard to find. The smallest made by Parker for example have a displacement of 18 cc/rev and weigh close to 30 pounds, which is not an option for this project.

Lastly, radial piston pumps were researched as a possible solution. What we found was that they had a comparable overall efficiency of 90%. Radial pumps, however, are typically designed for 9000 psi operation which makes them bigger and heavier than we need. Much like inline axial piston pumps, they were not feasible on our scale.

The results of our pump and motor research can be seen graphically in Figure 16 below.

		Criteria	Rideability	Overall Efficiency	Weight	Cost	Overall Satisfaction
Weight/100			40	30	25	5	100
Concept							
Bent Axis		Raw Score/100	90	92	40	100	78.6
		Weighted Score	36	27.6	10	5	
Gear Pump		Raw Score/100	50	85	100	40	72.5
		Weighted Score	20	25.5	25	2	
Inline Piston		Raw Score/100	50	91	0	20	48.3
		Weighted Score	20	27.3	0	1	
Rotary Piston		Raw Score/100	50	90	0	75	50.75
		Weighted Score	20	27	0	3.75	

Figure 16: Pump Type Comparison

The above matrix shows us that if we were able to continue using bent axis pumps while remaining under our max weight specification it would be ideal.

4.A.v Display Analysis

The display is placed in the rider’s view and show performance data in real-time, such as accumulator pressure, pedal cadence and speed.

In choosing a display, an initial 14 candidates, shown below, were put through four iterations of evaluation. In each evaluation, criteria of: feasibility, size, cost, ease of implementation, aesthetics, and display flexibility were considered.

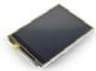

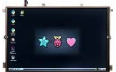











No.	Description	Image
1	3.2" TFT LCD Touch Shield for Arduino Mega	
2	2.4" TFT LCD Shield for Arduino	
3	10.1" TFT LCD Display 1280 x 800 HDMI	
4	Seeedstudio 2.8" TFT Touch Shield	
5	2.2" TFT LCD Shield for Arduino	
6	LCD Keypad Shield for Arduino	
7	3-wire Serial LCD Module	
8	LCD12864 Shield for Arduino	
9	Standard LCD 20x4 + extras – white on blue	
10	4D 4.3" LCD Cape for Beaglebone black	
11	7" Nextion HMI LCD Touch Display	
12	4.3" TFT LCD Intelligent Display	
13	Arduino 3.2" LCD-TFT Display with Resistive Touch Kit	
14	10.4" LCD Touch Screen Monitor	

Figure 17: 14 Initial Candidates for Display Selection.

The first two evaluations consisted of a “go/no go” decision and a series of Pugh matrices. These evaluations narrowed the candidate pool from the original 14 options to 6. For the next evaluation, a weighted decision matrix was constructed for these final 6 candidates. In the weighted decision matrix, the criteria of “feasibility” and “ease of implementation” were weighted the highest, while the criteria of cost and aesthetics did not carry much weight. The results from this decision matrix are shown below in Figure 18.



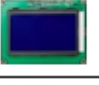


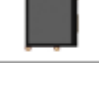
		Criteria						Overall Satisfaction
		A	B	C	D	E	F	
Concept		Weighting Factor						
		0.30	0.10	0.05	0.05	0.30	0.20	1.00
	1	100 30	80 8	100 5	80 4	90 27	70 14	88
	4	80 24	70 7	60 3	85 4.25	80 24	75 15	77.25
	7	100 30	70 7	100 5	70 3.5	100 30	40 8	83.5
	10	20 6	90 9	65 3.75	90 4.5	20 6	100 20	49.25
	11	80 24	60 6	50 2.5	90 4.5	90 27	90 18	82
	12	40 12	80 8	40 2	90 4.5	40 12	90 18	56.5

Figure 18: Weighted Decision Matrix for the remaining LCD candidates

From weighted decision matrix, the strongest candidates were '3.2" TFT LCD Touch Shield for Arduino Mega' (candidate 1), '3-wire Serial LCD Module' (candidate 7), '7" Nextion HMI LCD Touch Display' (candidate 11), and, arguably, 'Seedstudio 2.8" TFT Touch Shield' (candidate 4). To determine which of these candidates would be chosen, their feasibility and performance was analyzed in the final evaluation.

In the final evaluation, we considered the results from the prior three evaluations and the individual specifications of each LCD. From these results, we originally decided to further pursue candidates 1, 4, and 11. In this pursuit, we discovered that we inherited candidate 2: '2.4" TFT LCD Shield for Arduino' from the 2015-2016 Chainless Challenge team. Although the inherited LCD was not one of our final contenders from the LCD selection process above, field testing confirmed that it performed well with respect to all of our acceptance criteria. Thus, *we used the '2.4" TFT LCD Shield for Arduino' in our final design.*

Additionally, in testing the inherited LCD, we discovered a new criterion that was not addressed in the foregoing analysis: The LCD screen needed to be readable while riding the bicycle in sunlight. Through testing the '2.4" TFT LCD Shield for Arduino' for this criterion, we found that the screen was readable in most scenarios, but was unreadable when exposed to direct sunlight. To combat this, the display has a flexible positioning so that one can move it out of direct sunlight, and has a 3D printed shading attachment. A model of the LCD and accompanying hardware is shown below in Figure 19.

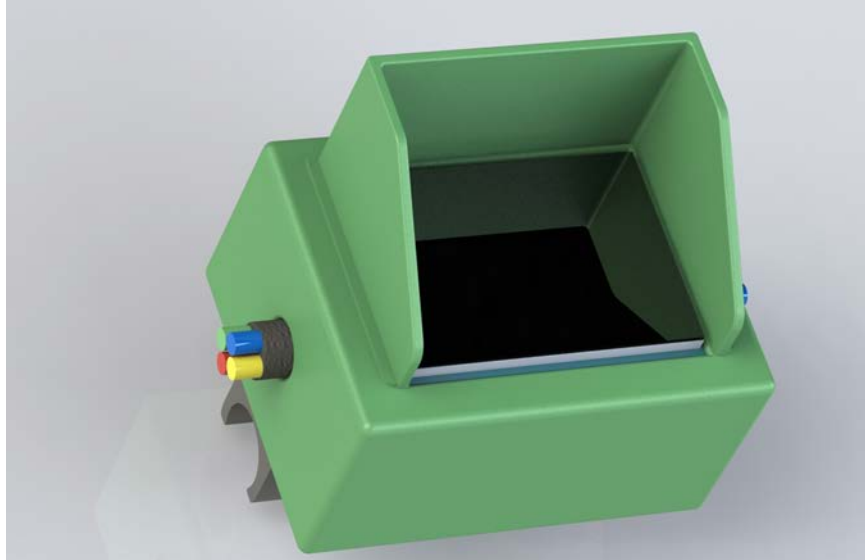


Figure 19: Rendering of the LCD with accompanying hardware.

4.A.vi Tubing Analysis

The previous Cal Poly bike used reinforced wire hosing to connect the hydraulic components on the bike. This year, in order to increase the efficiency of the hydraulic circuit, the benefits of switching to drawn tubing were explored. Drawn tubing has a lower friction factor than reinforced hosing, which decreased the pressure loss as fluid moved through the circuit. The premise of this analysis was that drawn tubing had a much lower absolute roughness (0.0025mm) than reinforced hose (0.35mm). First the major and minor losses based on a six-foot long tube (assumed total length of the circuit) were calculated to determine their effect on the system. The major loss represented the loss from friction and minor loss represented loss due to the change in velocity from bends and fittings. From that comparison, we determined that the minor losses were one order of magnitude smaller than the major losses and were therefore neglected in further analysis. It also reasoned that while the drawn tubing introduced more bends into the system, it also resulted in less fittings being used and effectively canceled out any changes.

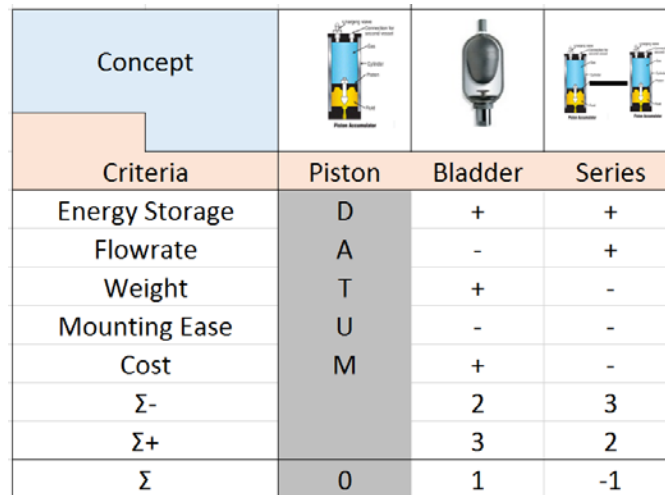
Pressure loss was then estimated using Darcy-Weisbach equation for pressure losses in conduits. The first situation considered was flow caused by pedal input. A rider input of 90 rev/min was assumed to represent an upper limit of what the system could experience. The assumed cadence was transmitted from the pedals through the gearing and to the pump where the fluid displacement of the pump was used to calculate a flow rate. Flow rate lead to fluid velocity using an inside pipe diameter of 0.37in (based on the current bike). Having fluid velocity calculated, we could find the Reynolds number (turbulent flow occurs when $Re > 2000$). At 90 rev/min, the Reynolds number was calculated to be approximately 415, which indicated that the flow was laminar (Appendix I). According to the Darcy-Weisbach equation, however, roughness does not affect laminar flow but only turbulent flow. This meant that drawn tubing did not offer any efficiency increase while pedaling the bike.

The next situation that was analyzed was if flow could become turbulent when the accumulator was dumped. To model this complex process, a speed was first assumed at the rear wheel. This speed was then transferred to the pump as before to calculate a Reynolds number. After ranging the input speed of the rear wheel, it was determined that the circuit does not experience turbulent flow until the bike is going 30 mph. The drawn tubing has 40% less pressure loss than the reinforced hose at that point (Appendix I).

Due to the structure of the competition and the limitations of our design, it is not practical to expect the bike to be going 30 mph. If it does reach a top speed of 30 mph or higher while discharging the accumulator, it will not be maintained for very long and therefore drawn tubing would not add much to the efficiency of the bike. Through this analysis, however, we were able to determine through rearranging the Darcy-Weisbach equation that the diameter of the tubing greatly affects the pressure drop (to the 5th power). Increasing the diameter would decrease the pressure drop. It would be much more beneficial to increase the size of the diameter instead of worrying about the roughness of the circuit (Table 3, Appendix I).

4.A.vii Accumulator Analysis

Another aspect that needed to be considered was the accumulator pressure, volume, and geometry. As explained previously, a hydraulic accumulator is a device that stores fluid power. Typically, accumulators use a compressible fluid such as nitrogen gas to store energy. This stored energy is what pushes the relatively incompressible system fluid and gives the circuit power. In our research of accumulators as well as previous Chainless Challenge teams' hydraulic circuits, we found that for our application there are really only two types of hydraulic accumulators; those that use a piston to separate the fluid and gas, and those that use an elastic "balloon" that is filled with gas. This gave us a variety of options that were evaluated as three: a single piston accumulator, a single bladder accumulator, or a combination of the two in series. Using these we performed an evaluation using a Pugh Matrix as seen in Figure 20.



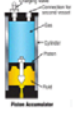

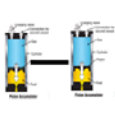
Concept			
Criteria	Piston	Bladder	Series
Energy Storage	D	+	+
Flowrate	A	-	+
Weight	T	+	-
Mounting Ease	U	-	-
Cost	M	+	-
Σ^-		2	3
Σ^+		3	2
Σ	0	1	-1

Figure 20: Pugh Matrix for different accumulator options.

From the evaluation coinciding with the Pugh Matrix we found that a bladder type hydraulic accumulator is more beneficial for the primary reasons of weight savings and better power delivery at low pressures. Although piston accumulators have a higher flow rate capacity, we calculated our expected direct-drive flow rate to be approximately 4.5 GPM. Since this flow rate is two percent of the capacity of bladder style accumulators we decided that it is not actually a concern, further cementing the decision to use a bladder style accumulator.

We then sought to find the total stored energy of the accumulator. We have developed a calculator that allows us to get an idea of the ideal pre-charge for the nitrogen gas stored in the accumulator. This calculator uses the accumulator reservoir geometry as well as the bore geometry in order to calculate the pre-charge based on required work. A sample output is shown below in Figure 21. The full code can be found in Appendix E.

```

23 %set up system of nonlinear equations
24 %solve using fsolve
25 x = fsolve(@myprecharge_fxn, guess);
26
27 Po = x(1); %Precharge pressure
28 Xmin = x(2); %Minimum accumulator displacement
29
30 %display result to console
31 fprintf('\nPrecharge estimation: %d psi\n',Po);
32
33

```

Command Window

New to MATLAB? See resources for [Getting Started](#).

[Equation solved.](#)

fsolve completed because the vector of function values is near zero as measured by the default value of the [function tolerance](#), and the [problem appears regular](#) as measured by the gradient.

[<stopping criteria details>](#)

Precharge estimation: 2.757814e+02 psi

f_x >>

Figure 21: Screenshot of pre-charge calculator for bladder accumulator.

Additionally, if we ignore differences in flow characteristics the bladder style is the clear option due to weight savings. Through comparisons of accumulators of similar capacity in the Parker catalog we found that the bladder style accumulators are usually 20-30% lighter. This gives a much needed weight savings when there is so little opportunity to do so with these heavy carbon steel and cast iron hydraulic components. The bladder style is the best option in this regard when compared to using multiple accumulators in order to achieve the desired volume. When using two bladder style accumulators to achieve our desired 1 Liter fluid volume the weight is increased by 15% when factoring the added fittings. This is not to mention the added complexity and cost of another pressure transducer and valves.

4.A.viii Clutch Analysis

The 2016 bike used a clutch to enable the bike to freewheel. The problem with the current configuration was that the clutch began to slip at higher pressures, and effectively limited the amount the accumulator could be charged to approximately 2,200 psi.

A different approach that 0 Chainz explored to allow the bike to freewheel was adding an internally geared hub to the rear axle. The problem, however, was that these hubs were designed for human inputs and we failed to find one that could handle the 78 Nm torque produced by charging the accumulator to 4,000 psi. We then refocused our attention to improving the clutch.

The clutch is used to disengage the drive motor from the rear wheel, allowing the bicycle to freewheel, or roll without moving fluid through the hydraulic circuit. The clutch is engaged when the pump is driving the rear wheel, either via accumulator discharge or direct drive depending on the circuit configuration. However, it also is engaged when the bicycle hydraulic circuit is recharging the accumulator. The current clutch “slips” or loses engagement in the current design when charging to pressures higher than about 2,200 psi. Additional technical information about the clutch can be found in Appendix L. To analyze the clutch, the following relationships were used to determine clutch clamping force and torque capacity:

$$\text{Clamp Force, } P=6 \text{ } k * X$$

$$\text{Torque Capacity, } T=P * \mu * N * r_{\text{clutch avg.}}$$

Where μ is the coefficient of friction and N is number of friction surfaces (2). After consulting the Parker F11 manual, pressure change is:

$$\text{Pressure Change, } \Delta P = T * 63\mu * D$$

Where P is in bar, T is torque in Nm, μ is efficiency, and D is pump displacement in cc/rev. Unit conversions were made to suit.

Our initial assumption was that the normal clamping force of the clutch would need to be higher to prevent slipping due to larger torque required to charge the accumulator to higher pressure. This could be achieved with either different clutch discs or stiffer, more powerful springs. It was determined that the pressure capacity would scale linearly with the increase in normal force. We began by finding new springs that would fit our clutch and have a clamping force necessary to reach 4,000 psi.

First, we measured the existing springs in the clutch. Diameters, coil thicknesses, and hole diameters were measured. A spring constant was determined experimentally using a scale, arbor press, and a pair of calipers. After consulting McMaster, the metric springs were listed in lbs./mm, which coincided well with our pounds scale and metric calipers. We measured 3 of the 6 springs and found an average spring constant of 7 lbs./mm. This meant an existing clamp force of 208 pounds.

McMaster had a spring that would be suitable dimensions but only 10.47 lbs./mm spring constant. This is 1.5 times the existing spring rate, but our calculations show that this would only yield approximately 3,000 psi max pressure. We consulted with Professor Fabijanic and determined that custom springs would be needed. We then ordered custom springs made by Pohl Springs that are 350 lbs./in or 13.78 lbs./mm which almost 2 times the existing spring rate which would yield a 4,000 psi accumulator charge to test with.

There are some potential problems that needed to be investigated further in this design solution. First, it was possible that the new clamp force would require an unreasonable amount of pulling force at the lever, which would yield it inoperable. Second, if the lever force was not too high to operate, the cable would now be under higher stress and could potentially yield or stretch. Lastly, the clutch shell could flex under the higher loads from its internal springs.

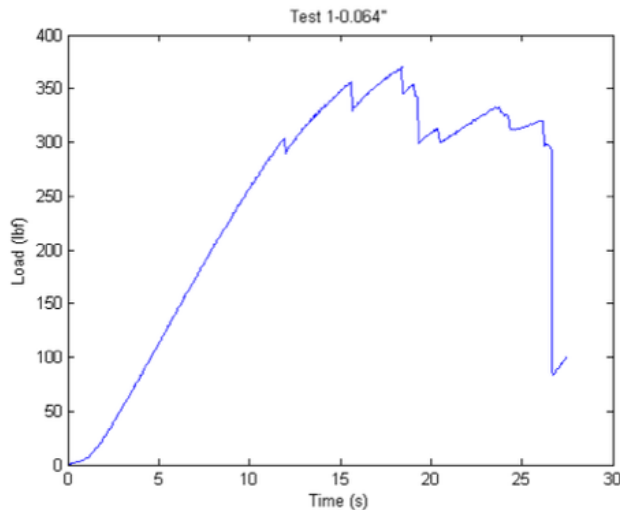


Figure 22: Results from tensile test with bicycle brake cable.

Our clutch uses a bicycle standard brake cable that is 1.6mm or 0.064'' in diameter. An outside tensile test revealed that the cable yields at around 300 pounds of load. We approximated the tension in the cable as the clamp force of the clutch (413 lbf), this study revealed that our clutch cable would fail.



Figure 23: Dual cable pull brake lever.

One solution would be to use a dual cable pull lever, as seen above in Figure 23. This would allow us to use 2 cables to engage the clutch, and splits the loads evenly into the safe region. Our team was not satisfied with this solution and decided to look into further.

During our spring analysis we also realized that pressure capacity scales linearly with the coefficient of friction of the clutch discs. After consulting the original manufacturer, they suggested switching to a higher friction disc. Their recommendation was an aluminum-steel friction surface rather than steel-steel that is currently in use. Preliminary research showed that steel-steel has a coefficient, μ , of approximately 0.25 whereas aluminum-steel was near 0.61. This would enable more than a doubling of accumulator pressure and allow us to attain our 4,000 psi goal.



Figure 24: Clutch discs from a motorcycle clutch.

Figure 24 shows a typical clutch disc that would be replaced by aluminum discs. To ensure that aluminum discs would be able to handle the loading conditions in the clutch, a basic shearing analysis was conducted. Using properties for 6061-T6 Aluminum and making relatively large assumptions about loading conditions, the factor of safety for shearing in the clutch teeth was found to be 25.8, and the factor of safety for shearing on the clutch face was found to be 432. These results are tabulated below in Figure 25a and 25b. The full spreadsheets, including all assumptions used, can be found in Appendix O.

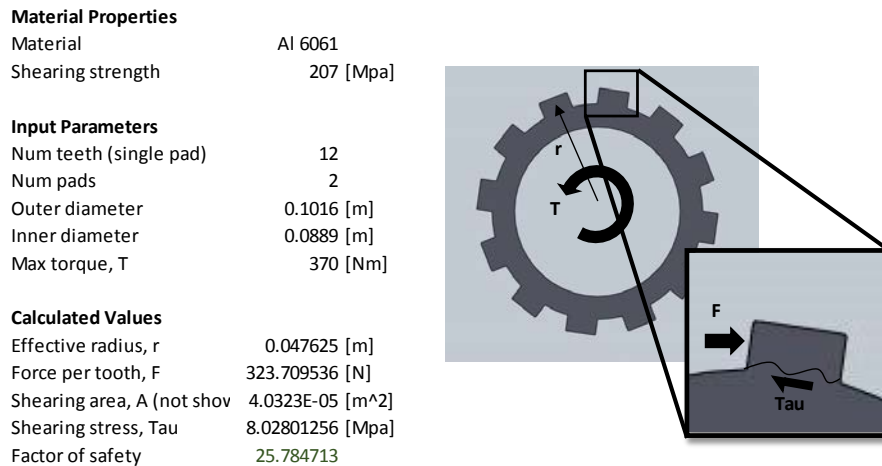


Figure 25a: Tooth shearing calculations for Al 6061-T6 clutch disc.

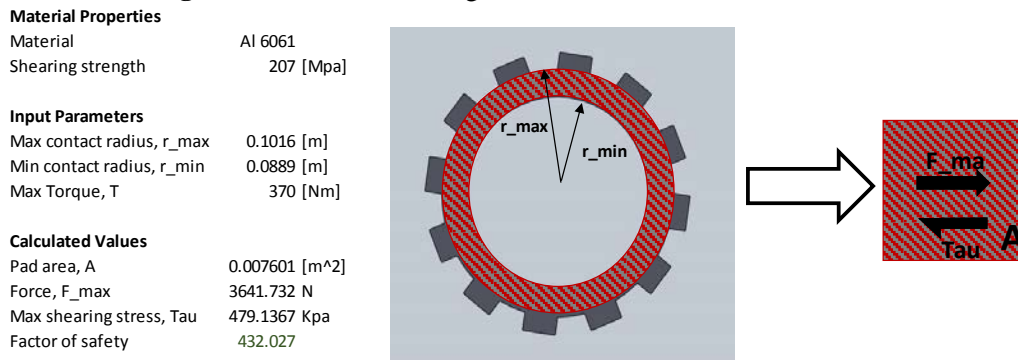


Figure 25b: Surface shear calculations for Al 6061-T6 clutch disc.

One of the main assumptions used in the shearing analysis was that the clutch discs undergo static loading as the accumulator is discharged. Since accumulator discharging is time variant, the loading conditions seen by the clutch disc are largely dynamic, and static loading is a “poor” approximation. That being said, given our high factors of safety derived from our static analysis, we are confident that the clutch discs will hold under real-world dynamic conditions. To gain further insight on the actual clutch loading conditions, we conducted a finite element analysis on a single clutch disc. This process, along with our results, are outlined in the next subsection.

4.A.ix Clutch Disc FEA

We conducted a finite element analysis of one aluminum clutch disc using the SolidWorks Simulation add-in. In the analysis, we assumed an equally distributed load, statically applied to each of the disc teeth.

For simplicity and a large safety factor, this load was a net torque of 200 Nm about the central axis. This value was derived by determining the torque required to accelerate the bike at 5 m/s² from a standstill (see Appendix B for spreadsheet used). For our first simulation, both sides of the clutch disc were assumed to be fixed. These loading conditions are shown below in Figure 26.

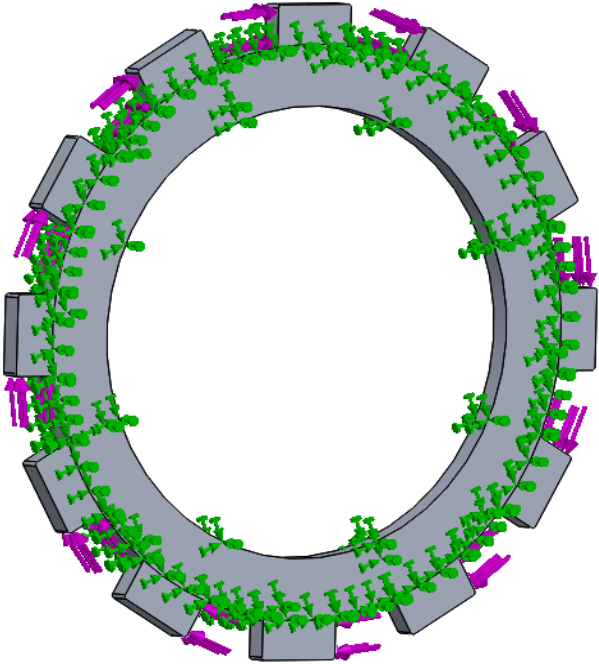


Figure 26: Loading conditions for first simulation of AL 6061-T6 clutch disc.

Using the above loading conditions, a mesh convergence study was performed. As shown below in Figure 27, convergence was achieved using a mesh of around 50,000 elements. Since it was not very computationally expensive, a mesh of 220,000 elements was used in our main analyses.

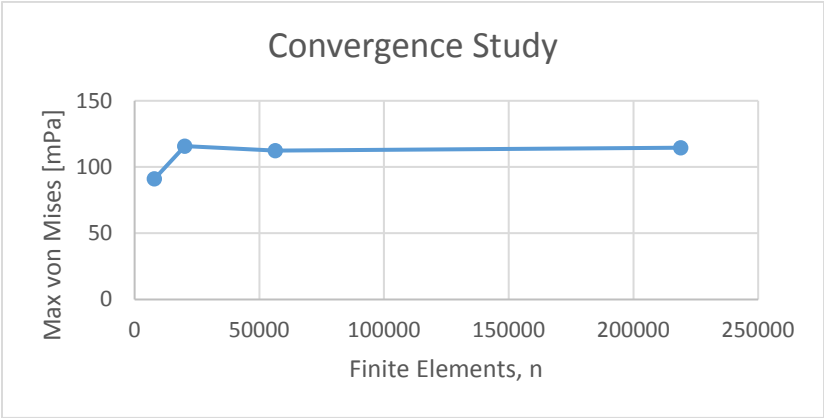


Figure 27: Mesh convergence plot for clutch disc finite element analysis. Maximum von Mises stress plateaus before a mesh of 50,000 elements.

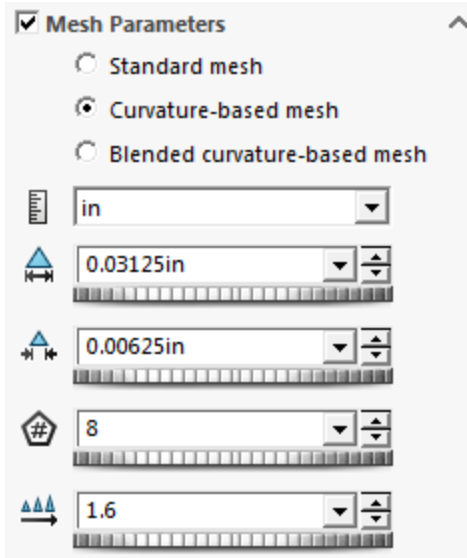


Figure 28: Mesh parameters used in finite element analysis of the clutch disc.

Examining the results of the first simulation, we noticed stress concentrations at the tooth radii where the loads were applied. A visualization of this phenomenon is shown below in Figure 29. The resulting stress distribution is sensible because radii are known to produce stress concentrations, and one would expect larger stresses near where a load is applied. To reinforce the analysis, a second simulation was performed only holding one side of the disc fixed. As expected, this resulted in a similar stress distribution as the first simulation, with a higher stress concentration near the fixed side. A visualization of the second simulation is shown below in Figure 30.

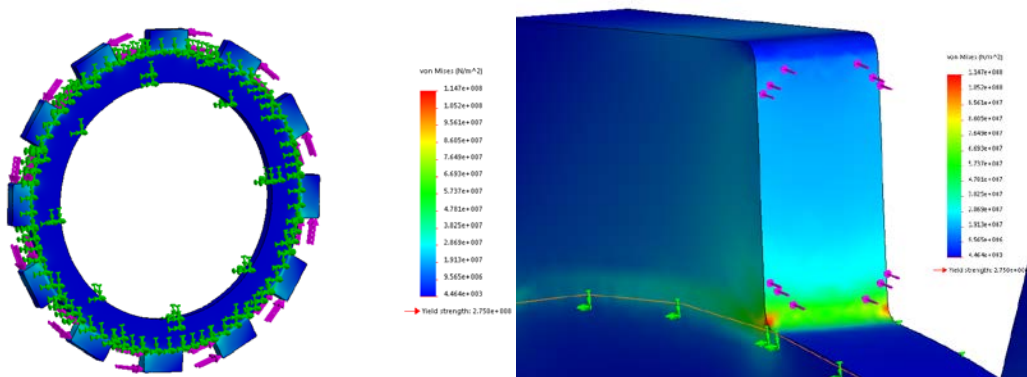


Figure 29: Visualization of von Mises stress on clutch disc subject to 200 Nm torque. Note the stress concentrations at the radii adjacent to the loaded faces.

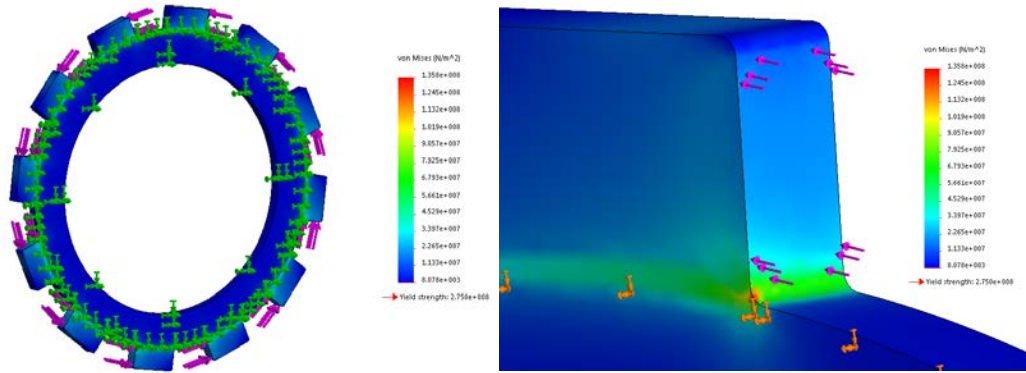


Figure 30: Visualization of a clutch disc subjected to 200 Nm torque, with only one face fixed. Note that the stress concentration is only present on the radii adjacent to the fixed face, and is slightly higher in magnitude than the first case.

Given the assortment of assumptions used in both simulations, we cannot use these analyses to draw accurate conclusions about the magnitude of the real-world stresses. In reality, both sides of the clutch discs will have some degree of partial contact, uneven loading applied to the teeth, and will experience non-static loading conditions. We can, however, use our model as a general approximation of real-world conditions, and gain insight from the observed stress distributions. From these analyses, we learned that the largest stresses occur near the radii on the loaded teeth, and that fixing only one face of the clutch disc slightly increases maximum stress. Additionally, since we used an excessive torque for our simulation and still achieved a large (>2) factor of safety for our expected stresses, it is likely that we will be significantly below the yielding stress for Al 6061-T6 with our real-world loading.

4.A.x Tire Analysis

There are several component selections related to the bicycle that still need to be made, designed, or specified. These range from standard bicycle components, to considerations for the hydraulic circuit.

Firstly, 0 Chainz plans on improving the actual, physical bicycle over the previous design. This comes by way of some simpler decisions, such as utilizing different road tires instead of the "knobby" tires that are currently on the bike. Bicyclerollingresistance.com has done extensive testing of road tires comparing their rolling resistances. The tires are tested on a rolling resistance test machine consisting of a drum, electric motor, and spun to approximately 18mph. More information regarding their tests can be found on their site. We looked to the touring bicycle tire category, as our bike will be heavily loaded.

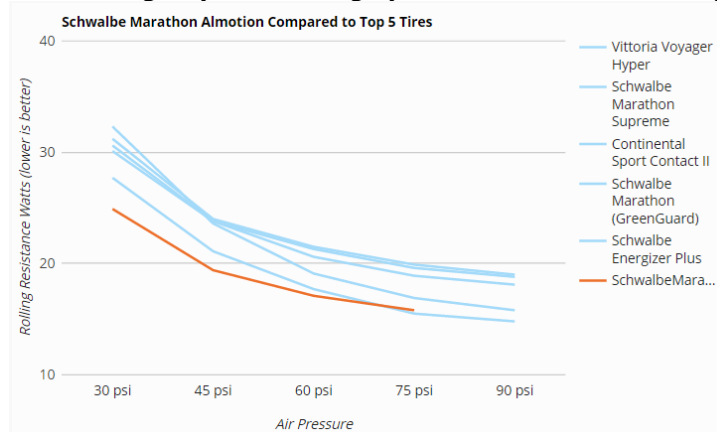


Figure 31: Comparison of various tires and rolling resistance vs. inflation pressure.

Figure 31 above shows the results from the touring tire testing. There was a clear winner, the Schwalbe Marathon Almotion. This tire produced 15.8 watts of rolling resistance compared to the worst tire tested at 29.6 watts. The tires currently on the bike are certainly even worse, as they were not even considered for testing and the knobs surely increase rolling resistance. Our bicycle's actual savings will likely vary from the laboratory testing results, but the test results serve as a useful decision making tool.

4.A.xi Aerodynamic Analysis

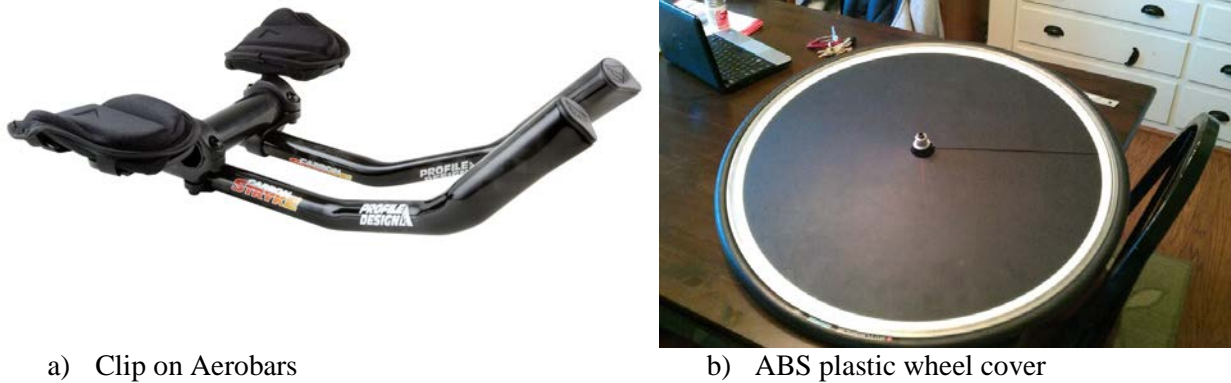


Figure 32: Aerodynamic considerations for the bicycle.

Another consideration was to make the bicycle more aerodynamic. By utilizing drop bars instead of flat handlebars, the rider positioning is much lower. This reduces the frontal area and the aerodynamic drag. We also have aerodynamic clip on handlebars that would further reduce our aero resistance, as seen in Figure 32 a). While it was mentioned that the TT bicycle or position is more unstable, it's sufficiently stable for straight sections of the time trial event, and the drop bars should have no trouble negotiating the cornering sections. Another TT component that we previously considered is aerodynamic wheels. Typical aero wheels are cost prohibitive for our purposes, and many have a rider and bike weight limit that is lower than our system. Instead, 0 Chainz we looked into manufacturing ABS plastic wheel covers to go onto the existing wheels that we have, such as in Figure 32 b). This change would improve aerodynamics with negligible increase in weight, at a low cost.

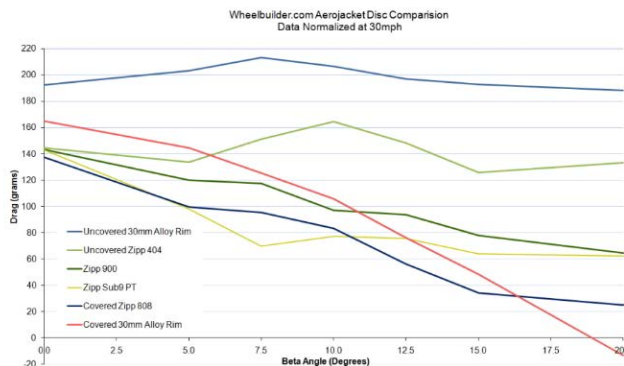


Figure 33: Data from wheelbuilder.com study on the aerodynamic drag of various wheels and covers.

Wheelbuilder.com makes abs wheel covers for multiple makes and models. We looked at the results of their study, and the results were mixed as seen in Figure 33. Yaw (or beta) is the effective wind angle, taking into consideration the rider's velocity and drag and the angle and velocity of meteorological wind.

At 0 degrees of yaw from the wind velocity, there is approximately 30 grams of drag saved by going with an aero wheel cover. 30 grams of drag at our intended operating speed of 18 miles per hour equates to just over 2 watts saved per wheel. These savings are much greater, however, as yaw increases. At 15 degrees of yaw, there are approximately 140 grams of drag saved and an 11 watt saving per wheel. However, the issue with increasing yaw is that our wheels effectively become a large "sail" to the wind, and the bicycle's stability is compromised. At this time, it is not considered to be a high priority item but is still up for consideration provided all other subsystems are built and validated before the competition date.

5. Final Design Considerations

5.A Bike Geometry

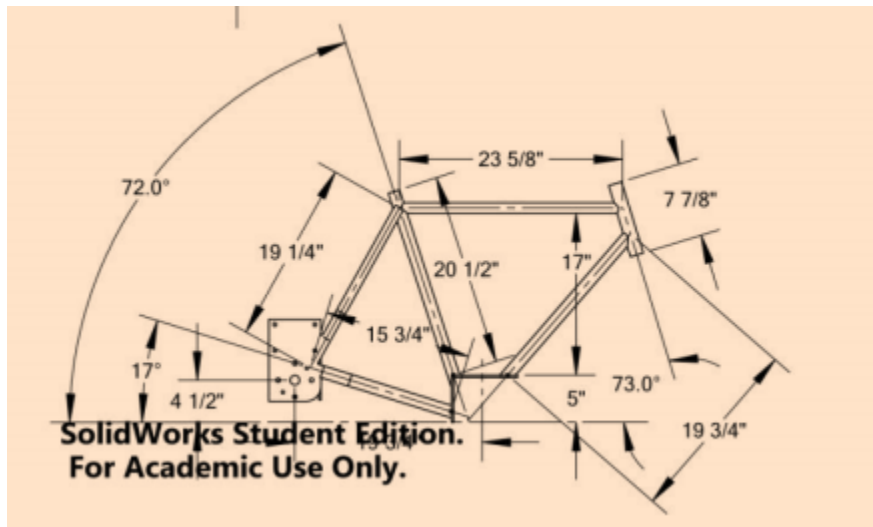


Figure 34: The previous Cal Poly chainless frame design.

The previous Cal Poly Chainless Challenge teams have done well in the past two years, earning a first and second place in 2015 and 2016, respectively. However, their bicycle design was not optimized. There were certain areas such as the knobby tire selection and upright, wide handlebar that hindered performance. The knobby tires had more rolling resistance and the upright positioning was not aerodynamic.

Riding the current bicycle as a team affirmed our preliminary analysis. The bicycle was awkward to maneuver, especially at lower speeds. This is a hindrance in the time trial event's slalom and course turns. The bike is also very tall with a flat top tube, as seen in Figure 34, which makes it difficult to fit four riders of various heights.

0 Chainz began this project with the idea that our circuit design and other changes would necessitate a new bicycle frame. The previous bicycle frame had some design flaws that we recognized; primarily, these were related to the fit, weight, and geometry of the bicycle.

However, as our team made more and more design decisions, we realized that the lead times and costs of a new frame would be significant. We met with the Cal Poly Framebuilders club on campus to discuss manufacturing a new frame. Loren Sunding, who previously built our existing frame, quoted 40 shop hours at \$15 per hour. The tubesets, cablestops, and other frame accessories would put the total cost well over a thousand dollars. More importantly, the frame would not be ready until Winter quarter. This long

lead time would put an extra burden on our team by restricting our time available for testing of our mechatronic components and final layout.

One of the team goals for this project was project completion well before the competition date in order to allow significant testing and iteration of our components. Our solution was to modify the existing frame. O Chainz talked with Professor Fabijanic and received bicycle design and handling literature and an excel spreadsheet tool. The excel spreadsheet tool is based on research done by Dr. Davol, Dr. Owen, and Professor Fabijanic where they utilized a bicycle handling qualities model referred to as the Patterson Control Model, PCM (Davol et al.). The model describes multiple variables that affect a bicycle's handling, or how it responds to inputs. After gaining an understanding of bicycle handling and how we can alter it, we began to generate solutions such as moving our bicycle's center of mass and using a fork with a different offset and mechanical trail. We met with George Leone to discuss our options and he agreed that given our timeline that it would be the most level-headed approach to improving our bicycle's handling.

The bicycle design tools require several measurements of the bicycle. Most of these are measured statically, but we also utilized a large mechanical swing to find the bicycle's radius of gyration by timing the swing's oscillations. We measured the bicycle and rider system with and without the hydraulic components for comparison and a control for our later designs.

To extend the use of the PCM spreadsheet to hypothetical bicycle configurations, an additional "radius of gyration calculator" spreadsheet was constructed. Using concepts from statics and dynamics, this spreadsheet approximated the new mass and radius of gyration of the bike that resulted from different hydraulic component locations. The new mass and radius of gyration were then re-input into the PCM spreadsheet, and handling curves were generated. Two screenshots from the "radius of gyration calculator" are shown below in Figure 35. The full spreadsheets used for this analysis can be found in Appendix P.

Component Name	Mass [kg]	Coordinates [cm] (see note 2)		Distance from cg [cm]		(distance from x_cg) ² [m ²]	I_xcg [kg*m ²]
		y	z	y	z		
Frame + wheels + Anthc	100.24383	0	101.2698	0.302	11.2843093	0.012742662	11.6264612
Accumulator	8.4368112	13.5	55.5	13.802	-34.4854907	0.137973429	1.164055769
Pump	5.1709488	-1	61	-0.698	-28.9854907	0.084064638	0.43469394
Motor	5.1709488	-22	44	-21.698	-45.9854907	0.258548426	1.336940675
Planetary gearbox	1.814368	0	49	0.302	-40.9854907	0.167990144	0.304795941
Crank + bevel assembly	5.6245408	-4	30	-3.698	-59.9854907	0.361193698	2.031548691
Clutch housing	0.907184	-12	45	-11.698	-44.9854907	0.216054605	0.19600128

Results							
Total mass =	127.369	kg					
Center of gravity =	(XXX,		-0.302,		89.985	cm
ROG about x_cg (kx) =	0.366	m					

Figure 35: Screenshots from "radius of gyration calculator" that extends use of the PCM spreadsheet to hypothetical bike configurations.

By adding the Parker F-11 pump, motor, and accumulator locations to the spreadsheet, we can verify that our calculator works by comparing the calculated values to empirical data. We have verified our tools and have accuracy within 5%. This allows our team to update the hydraulic components with our new selections and locations and modify the CG location. We can iterate with different circuit configurations as well as rider positions with handlebar changes, and see their respective changes in the bicycle handling spreadsheet. Figure 36 below visually defines terms that will be mentioned throughout this analysis.

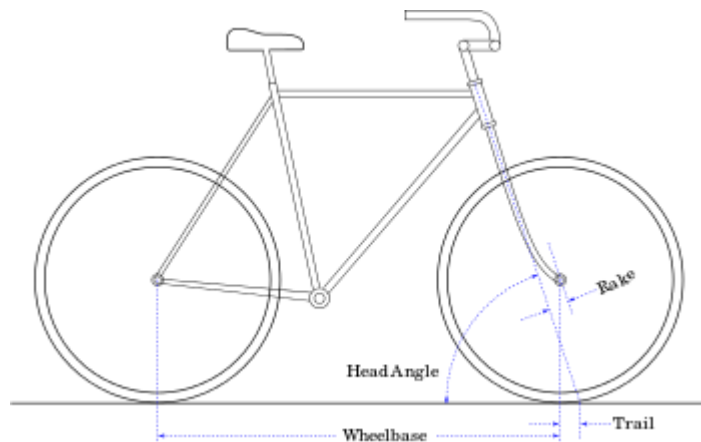


Figure 36: Basic front end bicycle geometry.

Changing the bicycle's fork changes the bicycle's handling significantly. Bicycle forks are designed for a particular wheel size and come in varying amounts of rake depending on the application. The rake is the distance between a parallel line from the middle of the headtube and the wheel axle. Extending this headtube line down, and a vertical line downwards from the axle, is the trail of the bicycle. Trail is the distance between the steering axis and the wheel's point of contact. Mechanical trail affects the wheel's turning moment and its steering tendencies.

One of the more critical findings with our current bicycle was its control sensitivity or control authority. A bicycle that is *under controlled* responds slowly to rider inputs. An *over controlled* bicycle responds too quickly to inputs and can be "twitchy" to ride. The PCM defines the inputs as a torque applied at the steering axis. Control authority is the roll rate divided by the rider intention. Intention is force and displacement of the rider input. More detailed explanation can be found in the original literature, *Model of a Bicycle from Handling Qualities* by Dr. Davol et. All. The PCM defines as a general case that an over controlled bicycle has 0.0745 degrees per second of frame roll rate for every foot of motion. It also suggests a control sensitivity for a touring bike, similar to our heavily loaded hydraulic bike, of 0.0638 [deg/s/ft.].



Figure 37: The Trek FX 3 that was used as our control bicycle.

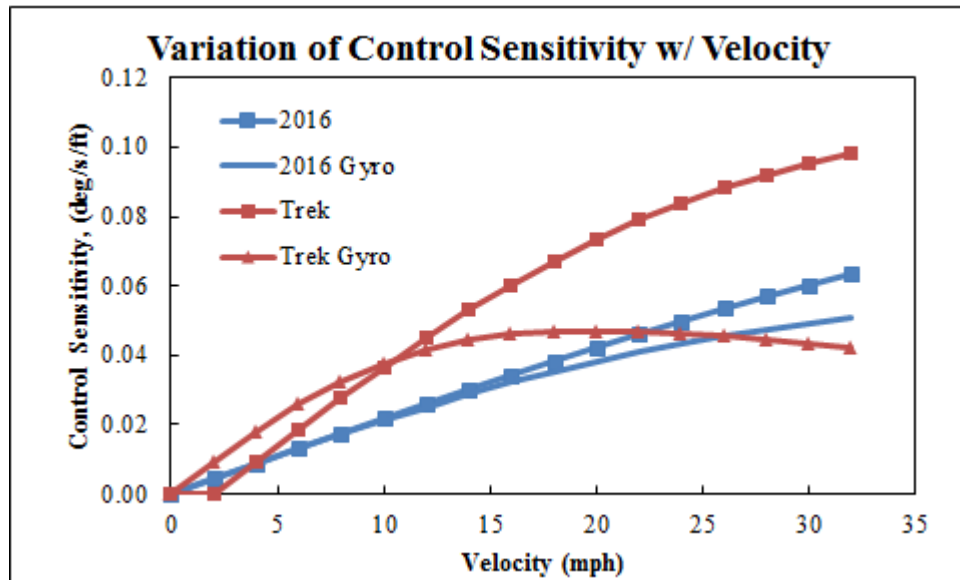


Figure 38: Variation of Control Sensitivity with Velocity for the 2016 bicycle and a Trek FX 3 as comparison. Each bike has a curve with and without gyroscopic considerations.

Figure 38 above shows the variation of control sensitivity with velocity for our current bike and a flat bar hybrid bicycle as comparison. The flat bar hybrid, a Trek FX 3 (Figure 37) was provided by Foothill Cyclery. Each member of the team test rode it and found its ride qualities agreeable, and a starting goal for our handling. Our analysis confirmed our initial impressions when we rode the bicycle; that it was awkward and difficult to maneuver, and its control authority is well below the suggested values.

For competition, our single speed bicycle is designed for approximately 16-18 miles per hour based on cadence. This region is largely in the 0.03 and 0.4 [deg/s/ft.] region, very far below the suggested 0.06 [deg/s/ft.]. Our team decided to focus on raising the control authority of the bicycle for better rideability.

We are using our tools developed to optimize both CG location and fork rake through different iteration. Forks are also relatively inexpensive, and come in various rakes as previously mentioned. We purchased multiple forks to test with the final bicycle to further validate our handling models and qualitatively assess the bicycle based on rider feedback.



Figure 39: Solidworks assembly of our bicycle.

Figure 39 above shows the current Solidworks model of our bicycle. This model aided us in varying component location feasibility, as well as hardline configuration and solenoid locations. It's also acted as another way for us to confirm our mass centers and their corresponding changes in the PCM. For technical information on components and assemblies see Appendix K.

5.B Hydraulic System

The final selection of major hydraulic system components is outlined below. Additional information about each component can be seen in Appendix M.

5.B.ii Tubing Selection

Converting to drawn tubing would require more planning and consideration as to how the circuit was attached to the frame but adds to the aesthetic appeal and performance of the bike. Our analysis determined that drawn tubing had a minor role in increasing the efficiency of the bike from lower friction factor, but it still is an important part of our design. It was especially significant during the discharge of the accumulator, where the flow becomes turbulent.

The greater benefit to using hard lines for our hydraulic circuit was the increase in inner diameter from 0.25in ID to 0.37in ID which would lower our losses through the system. The previous team had purchased drawn tubing and fittings rated to 4,300 psi which we used in our design.

5.B.iii Accumulator Selection

For the final design, the planned hydraulic accumulator to be used was the Parker UK Series High Pressure Bladder Accumulator in the one-liter form factor, as seen below in Figure 40. The accumulator is rated for 5000 psi, which is above our overall system rating goal of 4000 psi, and weighs roughly 12.5 lbs. This was ultimately our final selection due mainly to the superior ability to store energy over the similar volume bladder accumulators offered by Eaton, which were only rated at 3000 psi. Although this accumulator is quite expensive at \$1600 the ability to store ~30% more energy in the system is justified through increased performance and weight savings. Compared to the current accumulator this selection saves 6 lbs. of weight which translates into a 1% energy savings for human input at top speed. This energy savings per unit weight was derived from the bicycle performance analysis in Appendix B. The small form factor also gave us a more play in mounting location, which allowed us to more finely tune our handling in the PCM referenced in Frame Geometry (Section 5.A).



Figure 40: Parker UK Series High Pressure Bladder Accumulator

In choosing the accumulator, we found that there was difficulty in finding one that checked all the boxes for weight and energy goals as specified in the requirements. This is a problem that we also ran into trying to find a pump and motor combination as there is little need for hydraulic components with such little displacements in industry.

Unfortunately, our team neglected to investigate the precharging resources that we had available to us at the time of assembly. We mistakenly thought that a fitting would be readily available, and were unable to find a BSP charger in time for our testing. Thus, we are using the already-existing 4000 psi capacity accumulator from last year's bike due to our logistical oversight. We hope that later Cal Poly Chainless Challenge teams can capitalize on our investment and use it in the next year's competition.

5.B.iv Pump/Motor Selection

0 Chainz decided to use the Parker F-11-5 as our pump and motor. We were strongly encouraged to continue to use bent axis piston pumps by our advisor, Dr. Widmann, because they offer a smoother pedal cadence in comparison to other style pumps and motors. They are also efficient at our designed input RPM with our existing gear reductions. The Eaton parts catalog supplied by SunSource included gear pumps/motors. Our analysis indicated that bent axis piston pumps were more efficient than gear pumps. While keeping the same F-11 pump/motor did not help us save weight, it was still more efficient than our next best option and met the sponsor's requirement.

5.C Freewheel Mechanism

This year, one of 0 Chainz' focuses was to increase the pressure capacity of our hydraulic vehicle in order to improve our scores in the sprint and efficiency challenge. With the exception of the clutch, all of our components could handle our goal pressure of 4000 psi. For clutch testing, see Section 9.A.

Our team had considered multiple freewheel mechanisms. Freewheeling was a desired characteristic because removing the rear wheel from the circuit would lower the losses in the system during coasting. Some ideas considered were located either in the rear or front drive subsystem. Disconnecting the front drive system was deemed too complex, and we investigated removing the rear wheel from the circuit. We were unable to find an internally geared rear hub that had a rated load high enough for our calculated loads at the maximum charge and discharge design cases. We decided to improve upon the existing clutch.

We originally decided to improve upon our existing clutch primarily through the use of aluminum clutch discs to increase the coefficient of friction and max load before slipping. The discs were water jet cut by Central Coast Creative Cutting in San Luis Obispo. The reason for water jet cutting the Al 6061-T6 clutch discs was to allow us to make accurate cuts while maintaining the heat treatment of the material. Despite expecting a larger coefficient of friction with the aluminum clutch discs, we found that our clutch slipped at an even lower pressure. In the essence of time, we decided to rigidly attach the clutch discs to the rear driveshaft by using a keyway. A photo of the new design is shown below in Figure 41.



Figure 41: Clutch “fix” using keyway. Note that this eliminates freewheeling capabilities, but allows us to attain our goal accumulator pressure.

Now we can comfortably reach our desired pressure of 4000 psi without slipping. Although we can no longer freewheel, the rigid rear wheel assembly had a net positive gain on our performance in the efficiency and spring competition events due to our significantly higher pressure capacity. To make sure that the keyway would not experience mechanical failure, maximum expected stresses on the keyway were calculated, and it was shown to have a factor of safety against yielding of approximately 2. The results of these calculations are found in Appendix Q.

5.D Electromechanical System

Our team implemented a microcontroller-based rider interface to automate and control the hydraulic fluid flow through an electromechanical system. Our mechatronics system displays real-time metrics on an LCD visible to the rider, along with conveniently placed switches that enable the rider to control bike mode and toggle accumulator discharge. A schematic of our electromechanical system is shown below in Figure 42.

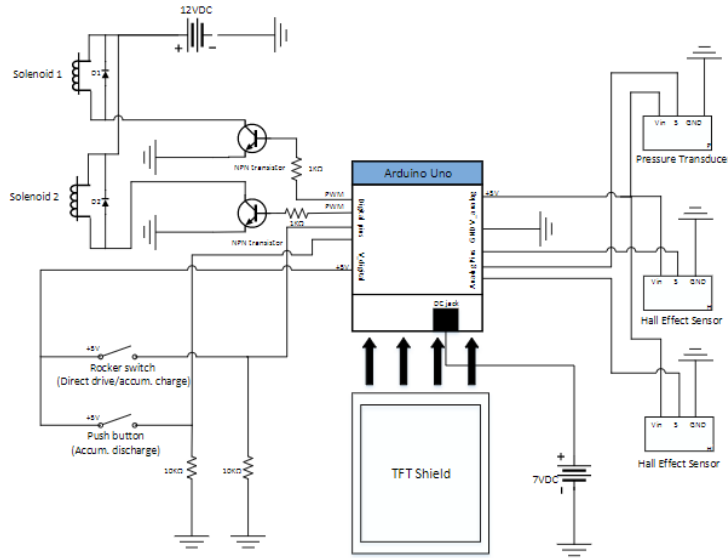


Figure 42: General schematic for the integrated microcontroller system.

5.D.i Components

Major components in the electromechanical system include:

1. One Arduino Uno microcontroller
2. One custom PCB printed by OshPark
3. One ‘2.4” TFT LCD Shield for Arduino’
4. Two hall effect sensors to measure pedal cadence and bike speed
5. Two switch inputs to control bike mode and toggle accumulator discharge
6. Two solenoids valves to charge bike mode
7. One analog pressure transducer to measure gage pressure in the accumulator
8. One battery to power both the analog and digital components using a switching regulator

Note that the Arduino Uno, display shield, and two solenoid valves were inherited from the 2016 Chainless Challenge team, and most of the remaining components were selected based on price and convenience. Specific models for all electromechanical components can be found in the “Mechatronics BOM” in Appendix J. One aspect that warranted special attention was battery selection.

Due to unique power demands, a separate battery was originally going to be used to power the solenoid valves from the rest of the system. To size the batteries, the power, current and voltage requirements due to all components in each system were tabulated (see Appendix N). A summary of these requirements are shown below for the solenoid power supply in Table 2a and for the power supply to the rest of the components in Table 2b.

Table 2a: Power requirements for solenoid power. Note that in this case, maximum current must be considered since it is of large magnitude.

Solenoid power supply	
Voltage	12 V
Expected Current	0.683 A
Max Current	4.66 A
Power	8.196 W
Ideal continuous operating time	8 hrs
Power needed	5.464 Ah

Table 2b: Power requirements for the rest of the electromechanical system.

Everything else power supply	
Voltage	7 V
Current	0.177 A
Power	0.782 W
Ideal continuous operating time	48 hrs
Power needed	5.36 Ah

Later in the design process we realized that we could arrange our system such that only one solenoid was powered at one time, with both solenoids being powered off in ‘direct-drive’ mode. This significantly reduced our power requirements, and allowed us to ditch the secondary 1.5V alkaline batteries and run solely off of the 12V lithium-ion rechargeable battery. To make this possible, a switching regulator, or “buck converter” was used to step down the 12V power to the 5V level needed to power the digital logic.

5.D.ii Layout

In choosing the layout for the electromechanical components on the bike, the main design considerations were user-friendliness, accessibility, and aesthetics. To obtain user friendliness, the display unit was placed on the center of the handlebars in direct view of the rider, and the control switches were placed near the handlebars. This also improved accessibility by allowing the user to see the performance data at all times and avoided awkward positioning when the user pressed the switches to change drive mode. Proper wire management, discrete battery storage, and a sleek display contributed to overall the aesthetics of the bike. Figure 43 below, shows the general placement of the display assembly, handlebar switches and battery box.

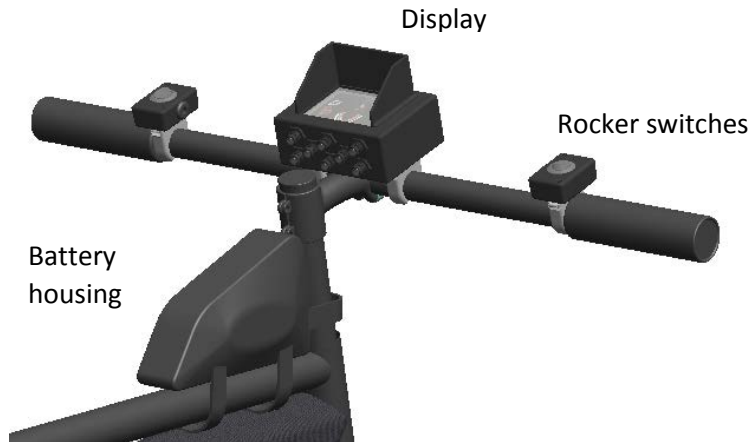


Figure 43: Locations of frontal electromechanical components. Note that wires have been omitted.

For the rear assembly, we needed to find a sleek and cost effective way to mount the solenoid valves. This was accomplished by welding a 1” x 1” hollow steel tube to the rear of the bike and milling out mounting holes for solenoid placement. By mounting the solenoid valves in the rear, the length of both hydraulic tubing and electronics cables was minimized. The resulting solenoid placement is shown below in Figure 44.

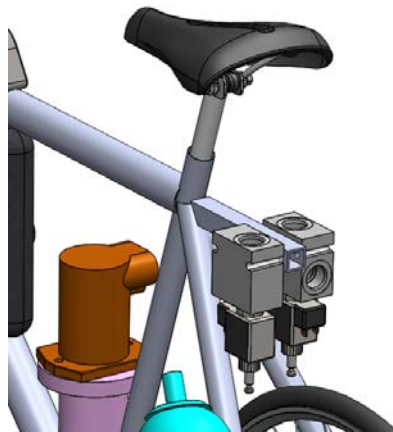


Figure 44: Rear mounting locations for solenoid valves.

To measure pedal cadence, a hall effect sensor and magnet were attached to the main bevel gear inside the gearbox connected to the crankset. This placement allowed for minimal interference with the rider’s pedaling, and promoted reliable cadence measurement. To measure bike speed, another hall effect sensor and magnet combo was assembled on the rear wheel. The magnet was attached to the rear wheel spokes using a Specialized spokes magnet, while the hall effect sensor was mounted to an elongated bolt connected to the clutch housing. This configuration allowed for ease of assembly, and reliable speed measurement. Photos of the mounting locations for both hall effect sensors are shown below in Figures 45a and 45b.



Figure 45a: Placement of hall effect sensor used for cadence measurement (red circle). The hall effect sensor is placed inside of the crank housing and allows for minimal invasiveness while the rider is pedaling.



Figure 45b: Hall effect sensor mounting for vehicle speed measurement (red circle). The hall effect sensor mounted to the rear motor housing and takes advantage of a pre-existing bolt location for minimal additional hardware.

Drawings for mechatronics system assemblies can be found in Appendix K. Additional photos of the mechatronics system can be found in *Electromechanical Circuit Fabrication* in section 8.B.

After the general layout was determined, we needed to verify that there would not be significant power losses across the wires. To accomplish this, a simple voltage drop analysis was performed. Assuming “worst case” conditions of an input voltage and current of 12V and 4A on ten feet of 16AWG wire, the resulting power loss was less than 0.01%. Summarized on Table 3 below, these results confirm that any reasonable wiring configuration used on our bike will not have significant power losses.

Table 3: Wire power losses due to “worst case” conditions.

Input Parameters		
Voltage	12	V
Current	4	A
Wire thickness	0.0508	in
Wire length	10	ft
Table Values		
Wire resistance	5.51E-08	Ω ft
Calculated Values		
Wire cross-sectional area	0.001108	ft ²
Voltage drop	0.001989	V
%Power loss	0.016578	%

5.D.iii Printed Circuit Board Design

A custom PCB was designed to interface the microcontroller with all of the electromechanical components in a low-profile and low-clutter design. This PCB was designed as a shield to mount in-between the display shield and Arduino, inside of the display housing. On the PCB, we placed the necessary transistors, resistors, and diodes to connect all of the external hardware to exposed screw terminals. The result was a space-efficient design that took some ingenuity to fit inside the limited real-estate of the display housing. The Eagle board file for our custom shield is shown below in Figure 46.

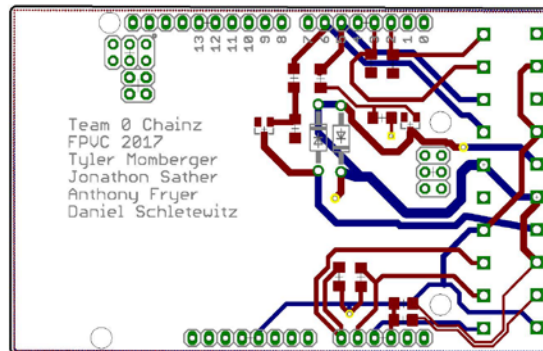


Figure 46: Eagle board image of our custom PCB

We sent this schematic to OshPark to print a two-layer PCB to support our project. This PCB (with soldered on components) is shown assembled below in Figure 47. The full Eagle .sch and .brd files for the circuit board are included in Appendix R.



Figure 47: Assembled custom PCB in our display housing. The heatshrink package sitting on top is the buck converter, which steps down the 12V power to the 5V power used for the logic circuit.

5.E Cost Analysis

To see the full cost analysis and bill of materials, see Appendix J. From this we found that our team costs were within our budget of \$8000 and had a full prototype cost in the range of the entries of the 2016 Chainless Challenge. These costs can be seen in Table 4.

Table 4: Total Prototype Costs and 2017 Incurred Costs

<u>Cost of This Year's Bicycle:</u>	<u>\$5,549.85</u>
<u>Cost of Complete/Updated Bicycle:</u>	<u>\$20,899.02</u>

There were several components with this year's bicycle that were inherited from previous teams due to their perceived performance and for ease of manufacturing. This allowed our team to focus on other areas of the vehicle, circuit, and mechatronics system design and manufacturing.

Obviously, the prototype vehicle costs were significant due to the amount of manufacturing required. With a projected 500 units per year, there are several manufacturing considerations that would need to be made in order to make it economically viable. For instance, with our drivetrain components, we would likely utilize casting methods rather than expensive CNC. This would drive the costs down, but is a manufacturing process that is only feasible for large scale manufacturing. Additionally, our hardline manufacturing took an approximate 20 hours to complete, whereas a large scale manufacturing process would either be automated or streamlined for factory production. This applies to the frameset as well. The frame was one of our more expensive items, but there are several factories with manufacturing and tooling capabilities to produce our frames on a large scale for a fraction of the cost. Our mechatronics R&D was very time intensive, and is included in our prototype costs. However, the actual cost of the mechatronics components is relatively small and adds a significant amount of functionality to the bicycle.

6. Management Plan

The management procedure for the detailed design and manufacture of this design adheres to the structure and intended timeline of the Cal Poly Mechanical Engineering Senior Project. This process will also adhere to the rules and guidelines set by the National Fluid Power Association for the 2017 Fluid Power Vehicle Challenge. All records of responsibilities and important deadlines are to be recorded and updated in the Gantt chart as the process develops. The general structure of management and individual responsibility will be as follows, with all deadlines and tasks shown in Appendix D.

- Jim Widmann (Sponsor/Advisor) – Dr. Widmann is to serve as the final stamp of approval to any design in order to verify its feasibility and safety. He is also to approve any Safety Procedures required for working with our system. All purchases are to be finalized by Dr. Widmann in order to be eligible for reimbursement.
- George Leone (Advisor) – Serves as an advisor for any manufacturing processes that are to be performed in the production of the vehicle. Also has the power to verify the safety of the design as well as the safety procedure. To specifically oversee the manufacture of aero attachments.
- Jonathon Sather (Main Point of Contact) – To be the primary contact between the team and the sponsor. Required to schedule all meetings with sponsor as well as any contact with Parker-Hannifin and the NFPA. To regularly review and verify Gantt chart tasks, timelines, and associated responsibilities. Jonathon is also one of the two team members tasked with the design, manufacture, and verification of the mechatronic system. Is to also be a primary team member in the design and implementation of the gearing systems at the pump/crank and motor/wheel.
- Tyler Momberger (Team Safety Officer) – It is the responsibility of the safety officer to evaluate all potential risks through the Hazard Identification Checklists then subsequently plan, execute, and record the corrective actions that are taken to mitigate risk. Is to be present on all major build days to verify that all procedures are being followed. Tyler is also to be the other main team member tasked with design, manufacture, and verification of the mechatronic system. Tyler is also to be in charge with specifying and implementation of the hydraulic accumulator, as well as a lead in the implementation of the hydraulic circuit.
- Daniel Schletewitz (Team Secretary) – Primarily tasked with maintaining and verifying that all major decisions and meetings are well documented for future use and justifications. Is to also be the primary organizer for meetings within the team. Daniel is also to be a lead on the detail design, implementation, and verification of the hydraulic circuit. In charge of specifying the pump and motor to be used within the circuit.
- Anthony Fryer (Team Treasurer) – To be in charge of all purchases that are made by the team as well as to maintain a record of all expenditures. To receive the final approval by Dr. Widmann for any purchase coming from the team budget. Anthony is to be the team lead on the detail design and manufacture of the bicycle frame, and to be a primary member in the design and implementation of the gearing between crank/pump and motor/wheel.

6.A Construction and Validation Timeline

As we progressed through the project, we realized that we were not on time for many of the deadlines that we originally planned. The immediate consequence of this is that we did not get to accomplish all of our stretch goals, such as implementing a new clutch, and we did not get to do as thorough testing as we would have liked. However, the biggest takeaway was that we learned the value of detailed planning and setting a realistic timeline around a critical path. A snippet of our Gantt chart used through the duration of

the project is shown below in Figure 48. The full timeline, including detailed individual tasks, can be found in Appendix D.

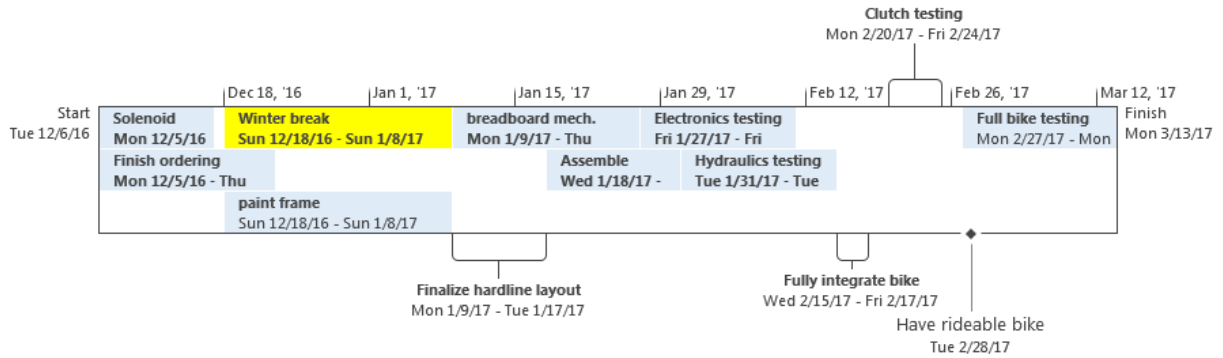


Figure 48: Snippet of timeline used to plan tasks and set deadlines

7. Concept Hazard Identification Checklist

In order to identify the potential risks and hazards associated with the manufacturing and use of the proposed design, we used the Concept Hazard Identification Checklist provided to all Cal Poly Senior Project teams. The filled out checklist can be found in Appendix S, and the associated table of corrective actions for the identified hazards is shown below in Table 5. Note that the hazards are only present when the manufacturing and use begins, so a planned manufacturing date was set for all corrective actions.

Table 5: Concept Hazard Identification Table in response to checklist. The filled out checklist is found in Appendix S.

Description of Hazard	Corrective Actions to Be Taken	Planned Completion Date	Actual Completion Date
There will be exposed gears that create a pinch point	Design housings/shields that block user from accidentally touching pinch point	11.15.16	
Gear train could lock causing bicycle to crash at cruising speed	All critical components properly contained and shielded	11.15.16	
Bike could fall over onto somebody while stationary or while riding.	While stationary bike will always be on bike stand. All pressure to be discharged if stationary for longer than 15 minutes. Rider must always wear helmet	11.15.16	
Will be using pressurized fluids	Validation of circuit by Sponsor and Leone, Ensure all fittings are correct size and that installment guides are followed by manufacturer. Use cardboard to check for leaks	11.15.16	
Will be using a battery	Ensure proper voltage, verify circuit on breadboard. All wires to have proper insulation. Battery to not be exposed to high heat	11.15.16	
Fluid can kill cells if penetrates the skin	Ensure no leaks in circuit, use cardboard to check for leaks	11.15.16	

8. Manufacturing

The manufacturing of the bike focused primarily on the hydraulic and electromechanical circuits. Standard bike components such as the brakes, cables, and pedals were also fixed or updated as necessary.

8.A Hydraulic Circuit Fabrication

The hydraulic circuit was made by first using Solidworks' Routing add in to layout the placement of the tubing as seen below in Figure 49. In our situation, our frame already defined the location of our pump and motor and our calculations determined the best location of the accumulator would be opposite of the motor. With this information we decided to locate the solenoids behind the rider's seat above the wheel because it allowed for the easiest tube routing.

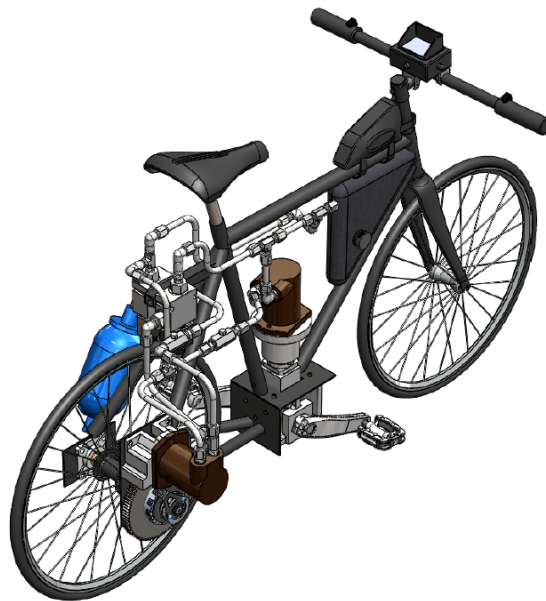


Figure 49: Solidworks Model with tubing

The limiting factors when using rigid tubing is the minimum bend radius and straight length at either end, which is dictated by the bending and flaring tools being used. These quantities will be expanded upon later in *Bending Hard Lines* (8.A.i) but it is important to note that it was crucial that the Solidworks model accurately reflected these numbers. This model also allowed us to determine what fittings would be required to construct the circuit.

8.A.i Bending Hard Lines

Engineering drawings were made using the Solidworks model of each segment of the hydraulic circuit to be used as reference when making the lines. An example drawing can be seen below in Figure 50.

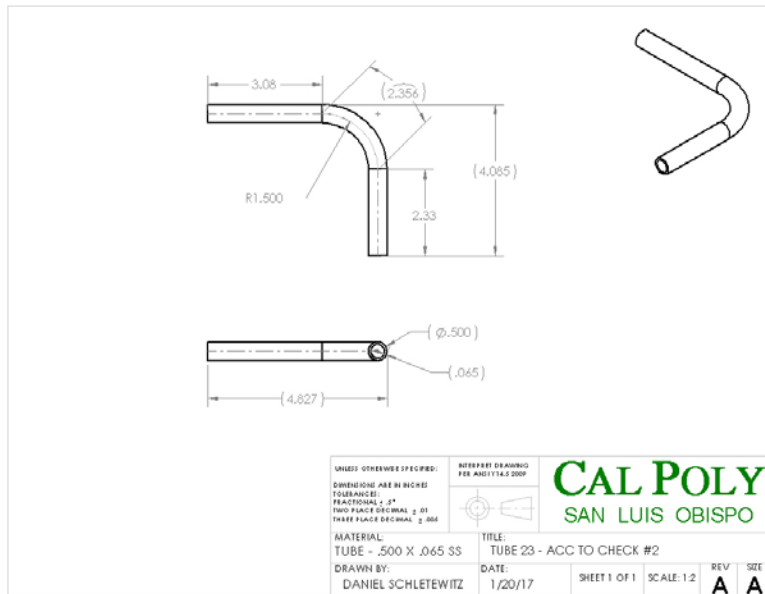


Figure 50: Tube Segment Drawing

In order to make it easier on ourselves, we attempted to limit the number of bends in each segment to one whenever possible. We also used swivel fittings where necessary to give ourselves another degree of freedom to ensure fittings would point the right direction once they were tightened down.

We reached out to the BioResource & Agriculture Engineering (BRAE) Department and they graciously allowed us the use of their bending and flaring equipment. For our 0.5 in. OD tubing, the department had a 1.5" in. radius bending die as seen in Figure 51. Because the wall thickness on the tubing was so thick (0.065 in.), we were unable to use a yoke style flaring tool. We instead used a hammer style flaring tool which required 2.625 in. between the end of the bend and the tube to flare to accommodate the form and sleeve. This method presented some challenges because the tube would often slide down through the form instead of flaring and required multiple setups to make a single flare. As time went on we got better and better at preventing this. The flaring setup can be seen below in Figure 51. Our goal was for the flare to engage two thirds of the fitting so we marked a line on an old fitting and used it as a reference.

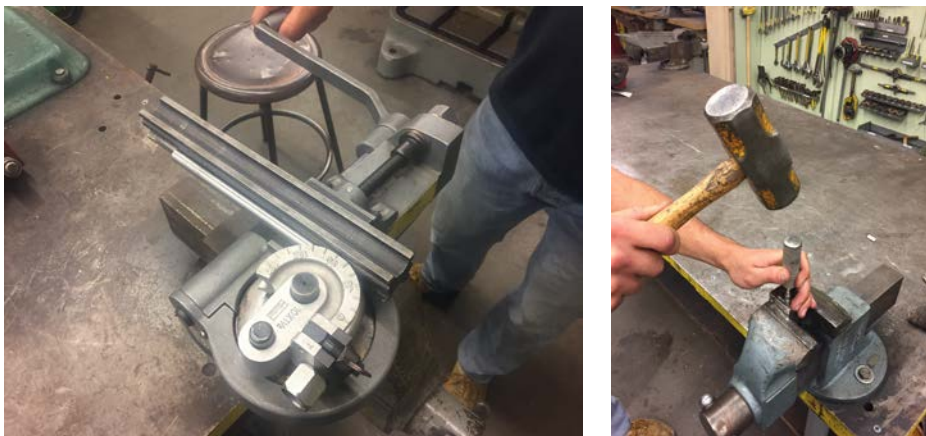


Figure 51: Tube Flaring Setup

In some situations, we were able to flare one end of the tube and slide on a sleeve before bending the tube. This shortened the required straight length to 2 in. but could only be done to one side of a segment. In areas where the minimum straight length was not a problem, segments were cut long to leave an extra 0.25 in. on either side of the bend. This allowed us to mark the segment in place and cut the extra off both ends to ensure a good fit.

8.A.ii Hydraulic Circuit Assembly

Once all the segments were made, the circuit was deconstructed and each flare was checked to ensure that it had proper engagement and had been deburred and cleaned. To ensure that the circuit did not leak, we purchased brass conical seals, which go on the end of the fittings and deform as the tube is tightened against it. Each segment was placed hand tight until the whole circuit had been constructed and then everything was tightened down with a wrench. Teflon tape or Loctite was used on the appropriate fittings where needed.

8.B Electromechanical Circuit Fabrication

To fit our electromechanical circuit into a clean and compact package, we constructed a custom circuit board to that mounted to our microcontroller board. This circuit board contained the necessary electrical components for actuating the hydraulic circuit and sensing the measured quantities. As mentioned in *Electromechanical System* in section 5.D, the circuit was constructed using Eagle software, and then sent to OshPark for fabrication. Once the board was received, all that remained to do was solder all the components onto the board.

After the PCB was assembled, the next step was to put together the display assemblies. This involved stacking the Arduino, custom PCB, and display shield, and placing it inside of the display housing. The specific procedure for these constructions is straightforward, and can be inferred from the assembly drawings in Appendix K. In addition to the display construction, switch assemblies were also created using SPST panel mount switches into a small project box by Hammond Manufacturing. The resulting switch and display modules are shown below in Figure 52.



Figure 52: Display and switch assemblies mounted on the 2017 bike.

On the rear of the bike, the construction was more straightforward. As described in *Electromechanical System* in section 5.D, hall effect sensors and magnets were mounted to the crank and rear wheel, which allowed for calculations of rider cadence and bike speed. The mounting locations of these sensors was designed to use minimal additional hardware and incur minimal rider interference.

Additionally, a pressure transducer was mounted on the accumulator node, so that accumulator pressure could be monitored by the rider. This pressure transducer, manufactured by Gems, was fastened into a tee fitting facing the rear of the vehicle. Figure 53 shows the mounted pressure sensor integrated into the fully-constructed rear end of the bike.



Figure 53: Rear view of assembled bike showing the location and mounting of pressure sensor (circled in red).

9. Testing

The details for the system and subsystem-level tests are laid out below, with detailed tabulations in Appendix H. The systems for testing are categorized as hydraulic system tests, electronic system tests, and integrated system tests. Due to limited time requirements, the originally planned hydraulic system tests were not performed on the isolated hydraulic system. Instead, we performed integrated system tests that incorporated the desired metrics from the proposed isolated tests. The downside to performing the hydraulic tests at the system level is that the tests are “higher risk” due to them being performed in a later (and more permanent) stage of development.

9.A Clutch Tests

Our initial clutch test was to verify the maximum charging pressure the previous, existing system could achieve. Before the clutch could be tested the hydraulic circuit was checked for leaks using the procedure described in the first part of *Flow and Leak Testing* (9.B.i) below.

To verify the maximum pressure that the clutch could hold, the clutch was assembled and all fasteners were torqued to the manufacturer's specification. All hydraulic safety procedures were followed to reduce the risk of injury. The bike was then put into regeneration mode and pushed to charge the accumulator to

the target pressure. The test showed the highest pressure before the clutch slipped was 2000 psi. This procedure was repeated ten times to verify the reliability of the clutch.

We researched using stiffer springs and different clutch discs, as mentioned in *Freewheel Mechanism* in section 5.C. However, after consulting the clutch manufacturer, we discovered that the bearings were not rated for the axial loads that the stiffer springs would provide for the required increase in normal force. Instead, we tried using aluminum clutch discs at the advice of the clutch manufacturer, as they claimed it would increase the coefficient of friction by a factor of two. We repeated our clutch tests with the new discs, and found that the clutch still slipped at pressures ranging from 1800-2200 psi. Consequently, we decided the clutch ineffective for our design goals.

Due to the results of this test with the original and modified clutch discs, we decided to pursue a fixed gear design to get a higher maximum system pressure. With the rear wheel locked in place we were easily able to reach a system pressure of 4000 psi. The addition of the direct drive rear wheel meant that our system would have more losses due to the rear motor still pushing fluid through the circuit. However, our efficiency testing found that our overall score was much higher due to the increase in accumulator pressure than it would be if we had the lower pressure and the clutch disengaging capabilities. It was deemed an appropriate decision to eliminate the clutch from our system.

9.B Hydraulic System Tests

We originally planned to test the hydraulic system in isolation prior to integrating it with the rest of the bike. Testing the hydraulic system by itself would be a low risk way of detecting any problems before complicating the system with other components. Unfortunately, due to a longer-than-expected time for assembly, the tests on the isolated hydraulic system were not performed, and instead higher-risk tests were conducted on the fully assembled system. These tests are found in *Integrated System Tests* in section 9.D.

9.C Electronic System Tests

9.C.i Solenoid Power Testing

One solenoid valve (part number: DSH121NTSPD012D-12T) was connected to a 12V, variable current power supply. Current was monitored as it was brought up from zero to 2.33A, and it was noted how much current it took to operate the solenoid valve. Once the valve was engaged, the current was slowly lowered, and we noted how much current it took to keep the valve open. This test was used to get the exact current requirements for our solenoid valves, with the idea that we could save power by only giving the valves the current they need to operate. From our tests we found that the solenoids required 1.1 V to actuate and held all the way down to 0.62 V.

Note that after these tests were performed, there was a change in the electromechanical circuit configuration. As a result, we achieved a lower power requirement in our system, and no longer need to throttle the solenoid duty cycles. Additionally, we recognized that the measurements obtained from this test were taken at atmospheric pressure, and thus likely do not reflect the solenoid power demands under operating conditions. Taking all of this into consideration, we are operating the solenoid valves at full duty cycle to ensure reliability.

9.C.ii Logic Testing

The entire electromechanical circuit was temporarily assembled using a breadboard and connected to a 12V power supply. In this test, the microcontroller logic and the functionality of the components was tested. This involved making sure that all of the sensors read properly and that the solenoid valves responded appropriately to button inputs. The purpose of this test was to make sure that the electromechanical system operated as expected once it was integrated on the bike. An image of the assembled breadboard used for testing is shown below in Figure 54.

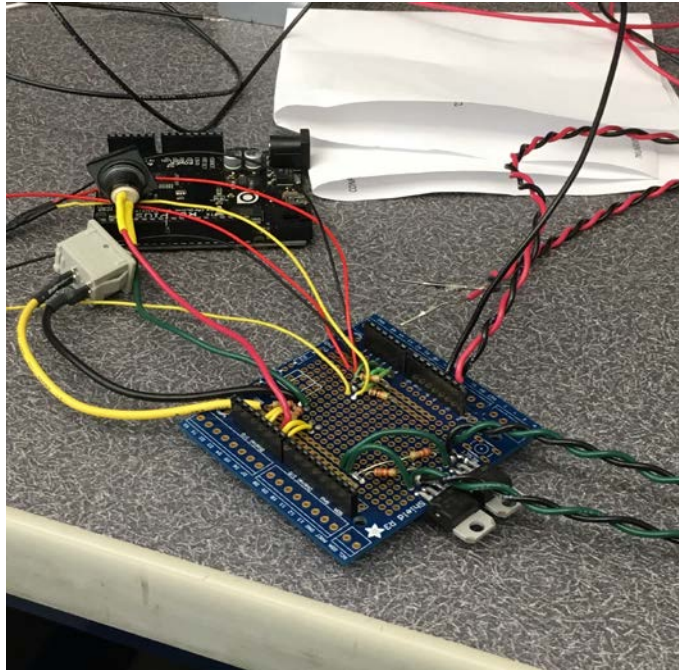


Figure 54: Prototyping board used for logic testing the system.

From the logic tests we made a few important observations. First, we found that the timing requirements for our RPM calculations using the hall effect sensors were not strict enough, resulting in data losses and inaccurate results. To improve this functionality, we changed our sensors to trigger external interrupts in hardware, which improved our RPM measurements drastically. Second, we discovered that the Gems pressure transducer could not measure pressure without being submerged in hydraulic fluid. This caused an initial scare when we noticed that the sensor did not appear to be operating correctly in air, consistently reading 0 psi. Thankfully, when we integrated the sensor into the hydraulic system, this “error” ceased to exist. The remaining logic tests met all the requirements, and gave us confidence to take our design to the next step of development.

9.D Integrated System Tests

9.D.i Flow and Leak Testing

The hydraulic circuit was assembled using Loctite 545 Hydraulic Thread Sealant or Teflon tape on all necessary fittings. Conical connections also had a softer, copper conical crush seal for improved seals between fittings. The pedals were then slowly turned by hand while a piece of cardboard was used to check for leaks at all connections.

The fully assembled circuit was then driven with the bicycle on a repair stand. There were some immediate leaks that were sorted with tightening the fittings. We continued pumping fluid through the system until all initial leaks were rectified.

During our testing, we brought the system to maximum pressure (~4000 psi) multiple times to check for leaks. We also would leave the system pressurized overnight to check for leaks. Thankfully, our system held without failure throughout the majority of our testing. The singular incident of failure was during a regenerative charging of the accumulator. The regenerative mode seems to pulse. This pulse is experienced by way of a vibration and an audible noise. We predict that this pulsing response creates dynamic system pressures higher than the standard maximum operating pressure. Consequently, there was an incident where the system leaked through a fitting during the regenerative mode at very high pressures. However, the system holds pressure when reconfigured to direct drive, and held pressure for a later discharge. Therefore, we consider our system to be a success.

9.D.ii Competition-Specific Performance Testing

The fully integrated bike system was assembled and tested against competition metrics. Team members rode the bike for a 200m sprint, an “efficiency challenge”, and performed endurance testing. The results from the sprint and efficiency testing are summarized below in Table 6.

Table 6: Summary of results from performance events.

Event	Metric	Result
Sprint	Fastest time	29.8s
Efficiency	Best score	84.25

Based on previous years’ results, our sprint time of 29.8 would likely put us in the top 3 for the sprint event. Unfortunately, this result does not meet our original goal of sub-29s, but there is still a chance that we will meet our goal in competition. Our efficiency score of 84.5 is nearly twice that of last year’s, which easily meets our goal of a 10% improvement. We did not directly perform an endurance event, but instead performed reliability testing to ensure safe and consistent operation over many miles.

9.D.iii Reliability Testing

The duration of our testing was an approximate 10-15 miles of usage. Throughout our testing, there was an isolated incident of hydraulic circuit failure and some initial troubleshooting with the mechatronics system. After correcting for this early mishaps, we now believe that all of our subsystems and components will perform well at competition.

9.D.iii Other Metrics

In addition to the above performance testing, we also tested for other useful metrics such as maximum velocity in various modes of operation, assessment of regenerative braking, and assessment of discharging strategies. The results from these tests can be found in Appendix H.

9.E Bike Layout Analysis

A quantitative comparison of several different vehicle designs was used before selecting our vehicle layout. The former Cal Poly entries have been two wheeled bicycles, although the rules allow for vehicles with more than 2 wheels. Our analysis compared different vehicle configurations and we decided to pursue the traditional bicycle design. The previous entry rode very poorly, especially at low speeds.

Consequently, we decided to optimize the existing frame to improve the handling. Changes to the handling include wider handlebars, different component locations, and a new fork with a reduced offset.

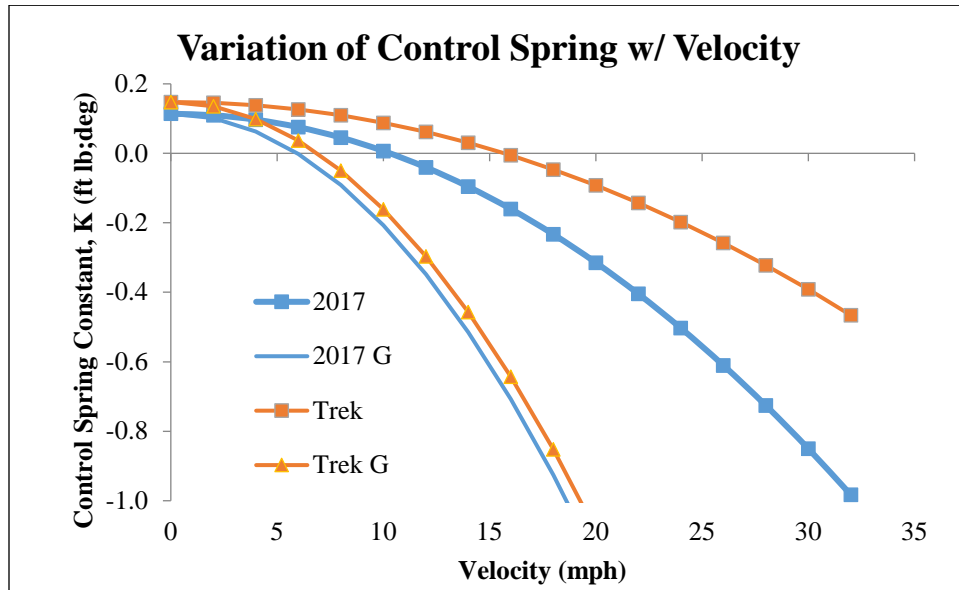


Figure 55: Variation of control spring with velocity.

Control spring is the torsional moment felt at the handlebar by the rider. A positive control spring value is considered unstable. A positive control spring means that the handlebars continue to travel in the direction of rider input. This means that the rider must initiate an input, and then immediately counter their own input. The critical speed is the speed at which the control spring is equal to 0, and becomes stable. The critical speed was reduced from 6.4 to 6.0 mph with the old and new bicycle designs, respectively. The lowering of the critical speed was a design target for the efficiency challenge. With a lower critical speed, we can theoretically go further in the efficiency challenge while maintaining control.

The control spring is defined by the set of equations:

Control Spring

$$\Delta Q = K \Delta \delta$$

Q – Control Torque

δ - Steering Angle

K – Effective Spring Constant

$$K = (K_1 - K_2 v^2)$$

v – Bike Velocity

$$K_1 = mg \frac{B}{A} T \cos(\beta) \left[\sin(\beta) - hT \frac{B}{A(h^2 + k_x^2)} \right]$$

m – Mass of Bike and Rider

g – acceleration of Gravity

k_x – Radius of Gyration About C.G.

$$K_2 = T \cos^2(\beta) m \frac{B}{A^2} \left[\frac{k_x^2}{(h^2 + k_x^2)} \right]$$

By changing the fork and lowering fork offset, we increased the trail, T. The addition of hard lines and the solenoids, and mechatronic components also raised the CG height, h, while decreasing the distance of the center of gravity from the rear wheel, B. Through our changes the control spring more closely matches the Trek reference bike.

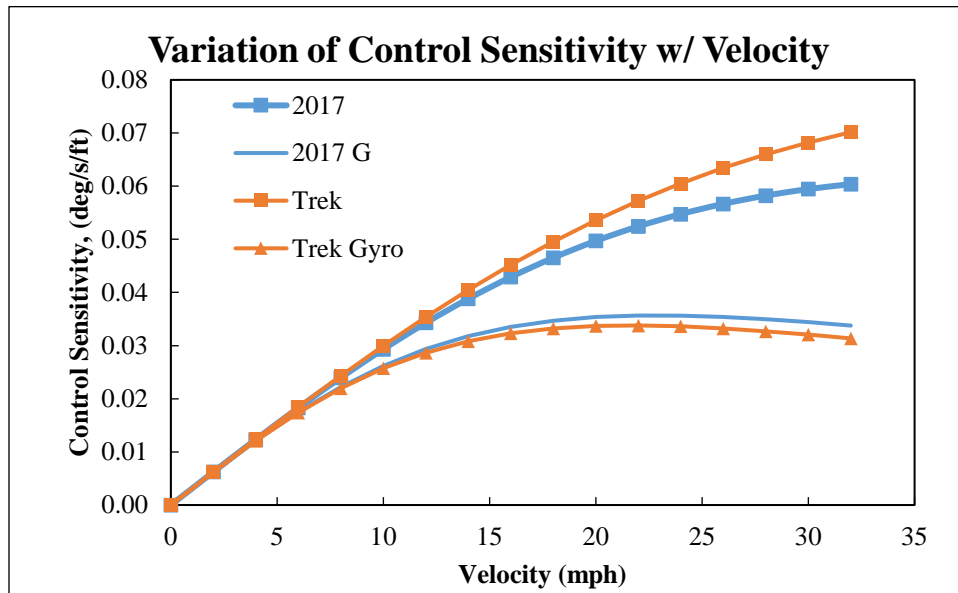


Figure 56: Variation of control sensitivity with velocity.

Control sensitivity is the roll velocity as a function of rider intention. Controlling the roll of a bicycle is important as it is the primary means of maneuvering a singletrack vehicle. Control sensitivity is defined by the set of equations:

Control Sensitivity

$$\frac{\dot{\theta}}{Int} = \frac{K_4 v}{\left[R_h + \frac{K_3}{R_h} (-K_1 + K_2 v^2) \right]}$$

$$K_4 = \frac{B}{hA} \cos(\beta)$$

$$K_3 = \frac{1}{1500} \text{ m/N constant}$$

Int – Intension of Rider

One of the most significant factors is the handlebar radius, which was increased with the wider handlebars. The geometry and component / center of mass changes previously mentioned also positively impacted our control sensitivity.

We immediately noticed improved bicycle handling during our testing. The bicycle was easier to maneuver at low and high speeds, while also offering improved ergonomics with the new cockpit. The other component changes, such as headset and tires, also improved the overall ride quality of the bicycle as well. With the competition now held in a new location, we predict that the handling will be of greater importance this year.

10. Conclusions

It has been a tumultuous past year with our team, and we have learned a lot about hydraulics, project management, system integration, controls, vehicle dynamics, and ourselves over the course of this project. One of our first roadblocks was our limited hydraulic experience, with all of us being relatively inexperienced in the field save for a few interactions with hydraulic automotive and bicycle components. Consequently, there were several mistakes made throughout the project with regards to the hydraulic system.

Firstly, we misestimated the time and skill required to manufacture the hydraulic hard lines. We also purchased several fittings that were unnecessary or inappropriate for the application at hand. We also under researched the various types of fittings, which led to our eventual abandoning of the new accumulator that we purchased. We recommend that next year's team do more preemptive research before the design and build phases of the project. Also, while the Cal Poly ME department is an invaluable resource, we received much of our hydraulic circuit advice from the Cal Poly BRAE department. As a result, we realized that consulting different departments and using their knowledge base is beneficial for any project's success.

Secondly, there were scheduling conflicts that arose from our troubleshooting phases. This began with the mechatronics system after the breadboard validation phases. We now understand that this can arise during the assembly due to loose connections, etc. These troubleshooting delays extended into other areas of our project. We should have padded our project timeline to include more time for troubleshooting and repair. Additionally, we should have either included more time for assembly and

manufacturing or invested more time earlier on to leave ourselves with more time at the end for testing and validation of our vehicle and its subsystems.

Thirdly, we feel that the a more fulfilling and perhaps better performing option for this project would have been to start from scratch or go in a unique direction. We feel that through our refinements, the performance of this current bicycle configuration is near a maximum. We went into the project knowing that the previous year's design earned a second place, and sought to refine and improve upon it. Along the way, we encountered design issues or features that we did not like or would have done differently, which is expected when inheriting a design. Such items included the clutch. We would recommend that next year's team go in different design directions, especially if the rules change to allow for a hybrid drivetrain configuration or other drastic vehicle changes.

Additionally, our team prioritized vehicle performance and rider ergonomics and control over the user experience and manufacturability of our design. This is a decision that we felt was justified, but after viewing other teams' blogs we would recommend that the next year's team also look into improving the overall user experience and manufacturability.

Lastly, we all agreed that this project was both fulfilling and invaluable to our experience and knowledge as engineers. It challenged our problem solving abilities while incorporating elements of controls, vehicle dynamics, fluid dynamics, and manufacturing. We look forward to competing in this year's NFPA Fluid Power Vehicle Challenge.

Appendices

Appendix A: Works Cited

Appendix B: Comparison Plots

Appendix C: QFD House of Quality

Appendix D: Gantt Chart

Appendix E: Hydraulic circuit configurations (with flow directions)

Appendix F: Precharge and Work Calculators (Matlab Code)

Appendix G: Maximum Charge Pressure Calculations

Appendix H: Integrated System Tests

Appendix I: Tubing Friction Analysis

Appendix J: Cost Analysis and BOMs

Appendix K: Solidworks Models

Appendix L: Clutch Diagram

Appendix M: Hydraulic Components

Appendix N: Mechatronics Power Supply

Appendix O: Clutch Analysis

Appendix P: Patterson Control Model

Appendix Q: Keyway Analysis

Appendix R: Eagle Schematic and Board for Custom PCB

Appendix S: Concept Design Hazard ID Checklist

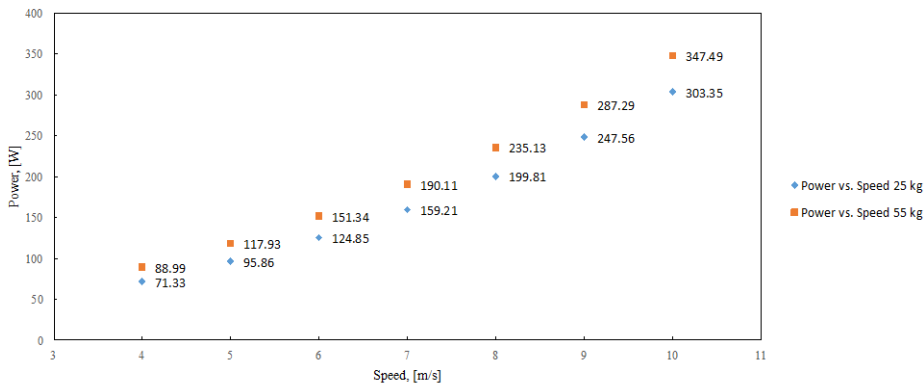
Appendix A: Works Cited

- "Aero Covers." Wheelbuilder.com. Wheelbuilder.com, n.d. Web. 22 Oct. 2016.
- "Cycling Aerodynamics & CdA - A Primer." *Cycling Power Lab*. N.p., n.d. Web. 17 Apr. 2016.
- Beek, Anton Van. "Calculator for Designing Shaft Keys." Calculator for Designing Shaft Keys. N.p., n.d. Web. 04 Mar. 2017.
- Bike Under Pressure. "Parker Hannifin Chainless Challenge 2014-15 Senior Design Project" Apr. 2015 Web. 2016.
- Davol, Andrew, Dr., Frank Owen, Dr., and John Fabijanac. Model of a Bicycle from Handling Qualities Consideration. Handling Qualities Model of a Bicycle. N.p., n.d. Web.
- Hydraulics and Pneumatics. "*Chapter 8: Air and Hydraulic Pumps.*" Web. 28 May 2016
<http://hydraulicspneumatics.com>
- Machinery Lubrication. "Hydraulic Pumps and Motors: Considering Efficiency." Web. 28 May 2016.
<http://machinerylubrication.com>
- McCraw, Dave. "Recumbent Position Power Loss." *Dave McCraw*. N.p., 20 Apr. 2013. Web. 16 Apr. 2016.
- "Road and Mountain Bike Rolling Resistance Data, Charts and Reviews." Bicycle Rolling Resistance. .p., n.d. Web. 22 Oct. 2016.
- Viking Pumps. "*The Ultimate Solution For High Pressure Pumping.*" Web. 28 May 2016.
<http://vikingpump.com>

TT Position

Force and Power based on speed	25 kg bike	30 kg bike	35 kg bike	40 kg bike	45 kg bike	50 kg bike	55 kg bike
Net Force [N], assuming constant velocity, 0 acceleration at 4 m/s	17.83	18.57	19.30	20.04	20.78	21.51	22.25
Net Power [W], assuming constant velocity, 0 acceleration at 4 m/s	71.33	74.27	77.21	80.16	83.10	86.04	88.99
Net Force [N], assuming constant velocity, 0 acceleration at 5 m/s	19.17	19.91	20.64	21.38	22.11	22.85	23.59
Net Power [W], assuming constant velocity, 0 acceleration at 5 m/s	95.86	99.54	103.22	106.89	110.57	114.25	117.93
Net Force [N], assuming constant velocity, 0 acceleration at 6 m/s	20.81	21.54	22.28	23.02	23.75	24.49	25.22
Net Power [W], assuming constant velocity, 0 acceleration at 6 m/s	124.85	129.27	133.68	138.10	142.51	146.93	151.34
Net Force [N], assuming constant velocity, 0 acceleration at 7 m/s	22.74	23.48	24.22	24.95	25.69	26.42	27.16
Net Power [W], assuming constant velocity, 0 acceleration at 7 m/s	159.21	164.36	169.51	174.66	179.81	184.96	190.11
Net Force [N], assuming constant velocity, 0 acceleration at 8 m/s	24.98	25.71	26.45	27.18	27.92	28.66	29.39
Net Power [W], assuming constant velocity, 0 acceleration at 8 m/s	199.81	205.70	211.58	217.47	223.35	229.24	235.13
Net Force [N], assuming constant velocity, 0 acceleration at 9 m/s	27.51	28.24	28.98	29.71	30.45	31.19	31.92
Net Power [W], assuming constant velocity, 0 acceleration at 9 m/s	247.56	254.18	260.80	267.42	274.05	280.67	287.29
Net Force [N], assuming constant velocity, 0 acceleration at 10 m/s	30.33	31.07	31.81	32.54	33.28	34.01	34.75
Net Power [W], assuming constant velocity, 0 acceleration at 10 m/s	303.35	310.70	318.06	325.42	332.78	340.13	347.49

Power vs. Speed for Different Weights: TT Bike

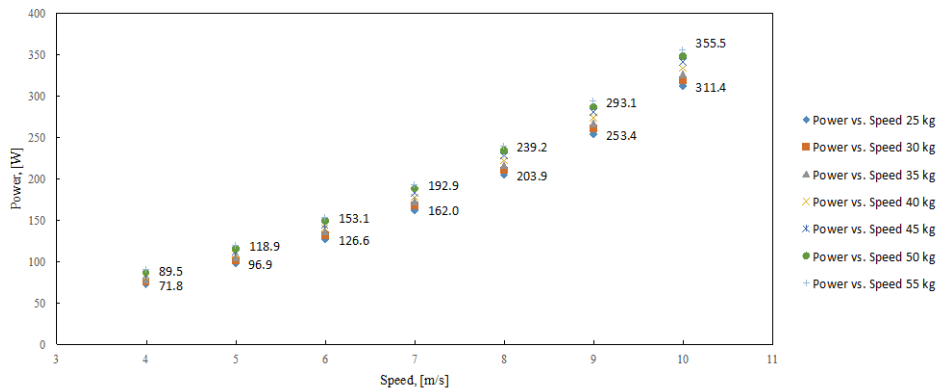


<http://www.cyclingpowerlab.com/CyclingAerodynamics.aspx>
<http://mccraw.co.uk/recumbent-position-power-loss/>

Recumbent

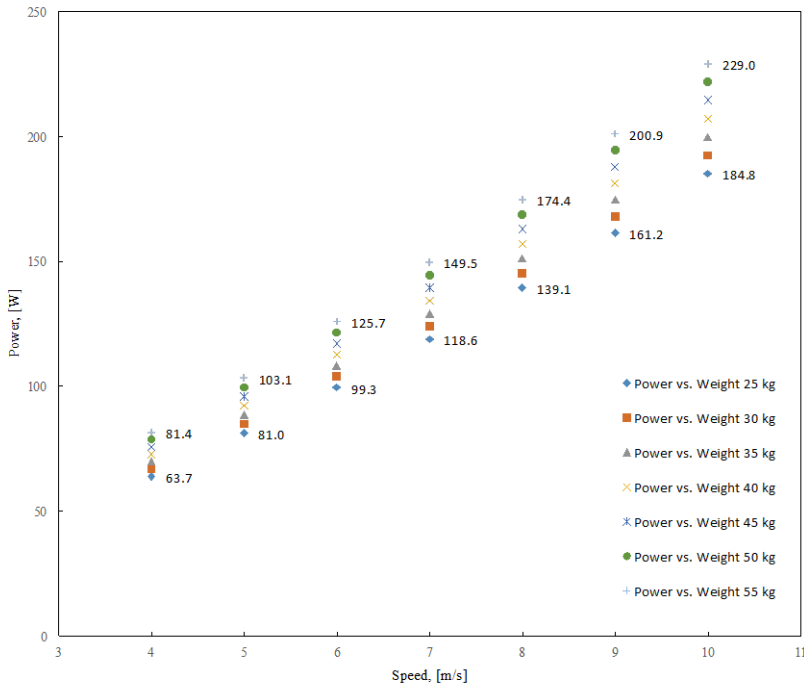
Net Force [N], assuming constant velocity, 0 acceleration at 5 m/s	19.37	20.11	20.84	21.58	22.32	23.05	23.79
Net Power [W], assuming constant velocity, 0 acceleration at 5 m/s	96.86	100.54	104.22	107.90	111.58	115.26	118.93
Net Force [N], assuming constant velocity, 0 acceleration at 6 m/s	21.10	21.83	22.57	23.31	24.04	24.78	25.51
Net Power [W], assuming constant velocity, 0 acceleration at 6 m/s	126.59	131.00	135.42	139.83	144.24	148.66	153.07
Net Force [N], assuming constant velocity, 0 acceleration at 7 m/s	23.14	23.87	24.61	25.34	26.08	26.82	27.55
Net Power [W], assuming constant velocity, 0 acceleration at 7 m/s	161.96	167.11	172.26	177.41	182.56	187.71	192.86
Net Force [N], assuming constant velocity, 0 acceleration at 8 m/s	25.49	26.23	26.96	27.70	28.43	29.17	29.90
Net Power [W], assuming constant velocity, 0 acceleration at 8 m/s	203.92	209.81	215.69	221.58	227.46	233.35	239.24
Net Force [N], assuming constant velocity, 0 acceleration at 9 m/s	28.16	28.89	29.63	30.36	31.10	31.84	32.57
Net Power [W], assuming constant velocity, 0 acceleration at 9 m/s	253.41	260.03	266.65	273.27	279.90	286.52	293.14
Net Force [N], assuming constant velocity, 0 acceleration at 10 m/s	31.14	31.87	32.61	33.34	34.08	34.82	35.55
Net Power [W], assuming constant velocity, 0 acceleration at 10 m/s	311.37	318.73	326.08	333.44	340.80	348.16	355.51

Power vs. Speed for Different Weights: Recumbent



Aero Recumbent

Force and Power based on speed	25 kg bike	30 kg bike	35 kg bike	40 kg bike	45 kg bike	50 kg bike	55 kg bike
Net Force [N], assuming constant velocity, 0 acceleration at 4 m/s	15.94	16.67	17.41	18.14	18.88	19.61	20.35
Net Power [W], assuming constant velocity, 0 acceleration at 4 m/s	63.74	66.69	69.63	72.57	75.52	78.46	81.40
Net Force [N], assuming constant velocity, 0 acceleration at 5 m/s	16.21	16.94	17.68	18.42	19.15	19.89	20.62
Net Power [W], assuming constant velocity, 0 acceleration at 5 m/s	81.04	84.72	88.40	92.08	95.76	99.44	103.12
Net Force [N], assuming constant velocity, 0 acceleration at 6 m/s	16.54	17.28	18.01	18.75	19.49	20.22	20.96
Net Power [W], assuming constant velocity, 0 acceleration at 6 m/s	99.25	103.67	108.08	112.50	116.91	121.33	125.74
Net Force [N], assuming constant velocity, 0 acceleration at 7 m/s	16.94	17.67	18.41	19.14	19.88	20.62	21.35
Net Power [W], assuming constant velocity, 0 acceleration at 7 m/s	118.55	123.70	128.86	134.01	139.16	144.31	149.46
Net Force [N], assuming constant velocity, 0 acceleration at 8 m/s	17.39	18.13	18.86	19.60	20.33	21.07	21.81
Net Power [W], assuming constant velocity, 0 acceleration at 8 m/s	139.13	145.02	150.90	156.79	162.67	168.56	174.45
Net Force [N], assuming constant velocity, 0 acceleration at 9 m/s	17.91	18.64	19.38	20.11	20.85	21.59	22.32
Net Power [W], assuming constant velocity, 0 acceleration at 9 m/s	161.16	167.78	174.40	181.02	187.65	194.27	200.89
Net Force [N], assuming constant velocity, 0 acceleration at 10 m/s	18.48	19.22	19.95	20.69	21.43	22.16	22.90
Net Power [W], assuming constant velocity, 0 acceleration at 10 m/s	184.83	192.18	199.54	206.90	214.26	221.61	228.97

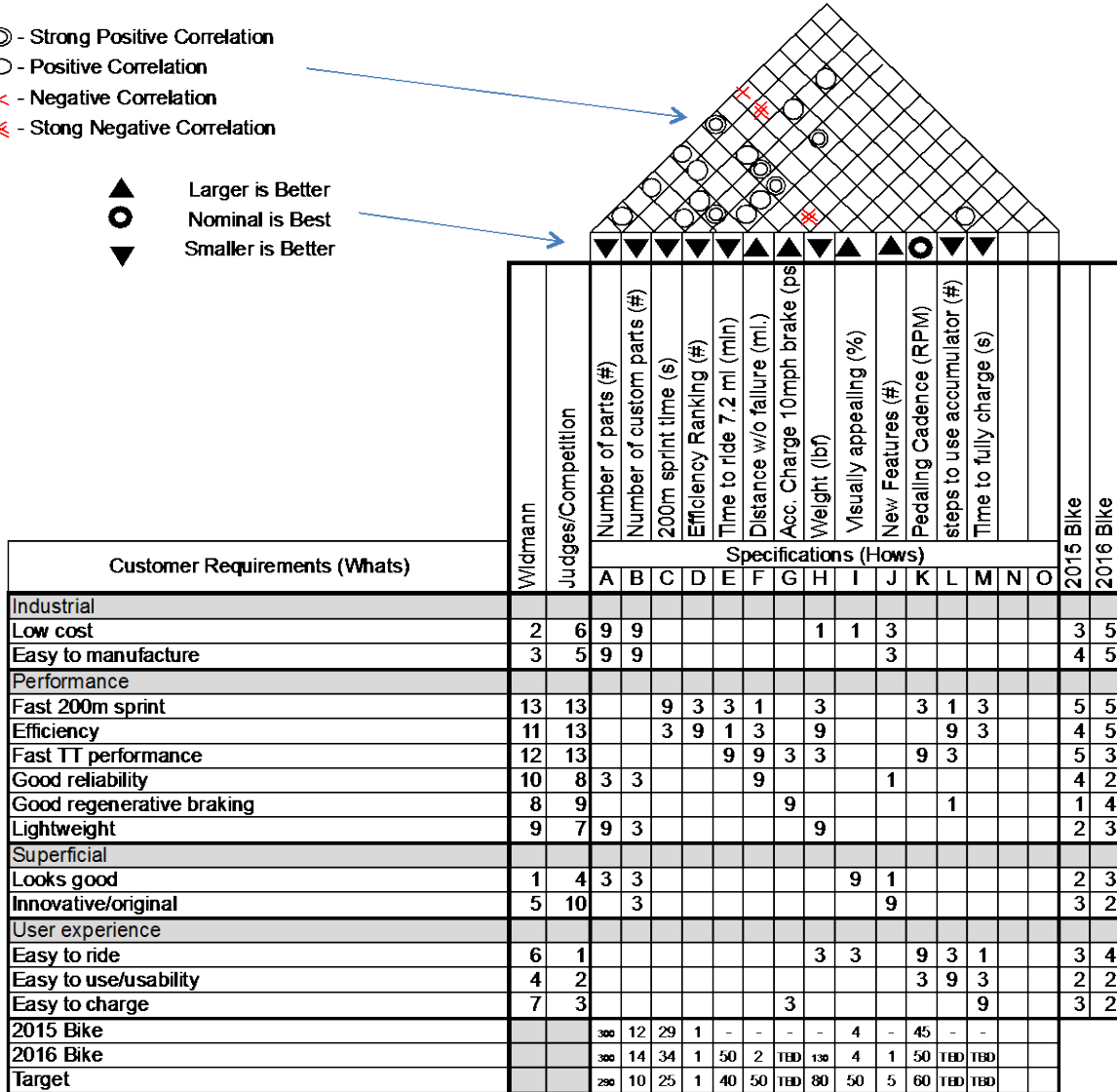


Power vs. Speed for Different Weights: Aero Recumbent
 0.0000

Appendix C: QFD House of Quality

- ⊙ - Strong Positive Correlation
- - Positive Correlation
- ✕ - Negative Correlation
- ⊗ - Strong Negative Correlation

- ▲ Larger is Better
- Nominal is Best
- ▼ Smaller is Better



Appendix D: Current Gantt Chart

ID	Task Mode	Task Name	Duration	Start	Finish	Predecessors	Resource Names	pr '16	3	10	17
1	✓	Overall QFD	5 days	Fri 4/15/16	Thu 4/21/16						
2	✓	Project Proposal	11 days	Tue 4/12/16	Tue 4/26/16						
3	✓	Project Proposal Due	0 days	Tue 4/26/16	Tue 4/26/16						
4	✓	Determine vehicle style to use in competition	9 days	Mon 4/25/16	Thu 5/5/16						
5	✓	Have general vehicle shape decided	0 days	Fri 5/6/16	Fri 5/6/16	4					
6	✓	Beef up old report	4 days	Mon 5/23/16	Thu 5/26/16		Daniel				
7	✓	4 evaluations on pump	11 days	Tue 5/17/16	Tue 5/31/16		Daniel				
8	✗	Evaluations on clutch	11 days	Tue 5/17/16	Tue 5/31/16		Anthony				
9	✗	Evaluations on accumulator	8 days	Tue 5/17/16	Thu 5/26/16		Tyler				
10	✓	4 evaluations on display	6 days	Tue 5/17/16	Tue 5/24/16		Jonathon				
11	✓	Get lost solenoid valves	25 days	Tue 4/19/16	Mon 5/23/16						
12	✓	First 3 evaluations for hydraulic circuit	4 days	Mon 5/23/16	Thu 5/26/16		Tyler				
13	✓	Make a few hydraulic circuit models in Viso	4 days	Mon 5/23/16	Thu 5/26/16		Jonathon				
14	✓	First 3 evaluations for bike form	4 days	Mon 5/23/16	Thu 5/26/16		Anthony				
15	✗	Create Solid Model of bike frame	106 days	Mon 5/23/16	Mon 10/17/16	11,12	Anthony				
16	✓	Preliminary plans for construction/validation	4 days	Mon 5/23/16	Thu 5/26/16		Jonathon				

Project: CC 2017 Project Timeline Date: Fri 10/28/16	Task		Inactive Summary		External Tasks
	Split		Manual Task		External Milestone
	Milestone		Duration-only		Deadline
	Summary		Manual Summary Rollup		Progress
	Project Summary		Manual Summary		Manual Progress
	Inactive Task		Start-only		
	Inactive Milestone		Finish-only		

ID	Task Mode	Task Name	Duration	Start	Finish	Predecessors	Resource Names	pr '16	3	10	17
17	✓	Concept design Hazard identification checklist	4 days	Mon 5/23/16	Thu 5/26/16		Tyler				
18	✓	Update presentation for PDR	3 days	Thu 5/26/16	Sun 5/29/16						
19	✓	PDR written	11 days	Fri 5/27/16	Fri 6/10/16	6,9,10,12,13					
20	✓	Have system pressure rating decided	1 day	Mon 5/9/16	Mon 5/9/16						
21		Analyze subsystems	110 days	Fri 5/6/16	Thu 10/6/16	4					
22	✓	Understand last year's bike	10 days	Mon 4/18/16	Fri 4/29/16						
23	✓	Preliminary Design Report	0 days	Tue 5/24/16	Tue 5/24/16	2,7,8,9,10					
24	✓	Safety FMEA	21 days	Wed 4/27/16	Wed 5/25/16						
25		Present concept models/ decision methodology	0 days	Tue 5/17/16	Tue 5/17/16						
26	✓	Preliminary Design Report Due	9 days	Tue 5/31/16	Fri 6/10/16	23,24					
27	✓	PDR Presentation	0 days	Tue 5/31/16	Tue 5/31/16						
28		Touch up PDR for sponsor	6 days	Tue 5/31/16	Tue 6/7/16	26					
29	✓	Schedule PDR with sponsor	0 days	Tue 5/24/16	Tue 5/24/16						
30		PDR with sponsor	0 days	Fri 6/10/16	Fri 6/10/16	29					
31		Have long lead time parts ordered	0 days	Tue 10/4/16	Tue 10/4/16	21					
32		Schedule CDR with sponsor	0 days	Wed 10/19/16	Wed 10/19/16						
33		CDR with sponsor	0 days	Thu 10/20/16	Thu 10/20/16	32					
34		CDR written	18 days	Sat 10/1/16	Tue 10/25/16						
35		CDR due	0 days	Wed 10/26/16	Wed 10/26/16	34					
36		CDR presentations	0 days	Tue 10/25/16	Tue 10/25/16						

Project: CC 2017 Project Timeline
Date: Fri 10/28/16

Task		Inactive Summary		External Tasks	
Split		Manual Task		External Milestone	
Milestone		Duration-only		Deadline	
Summary		Manual Summary Rollup		Progress	
Project Summary		Manual Summary		Manual Progress	
Inactive Task		Start-only			
Inactive Milestone		Finish-only			

ID	Task Mode	Task Name	Duration	Start	Finish	Predecessors	Resource Names	pr 16	3	10	17
37		Manufacturing and test review	35 days	Fri 10/21/16	Thu 12/8/16						
38		Senior design expo	0 days	Tue 11/29/16	Tue 11/29/16						
39		Final report written	16 days	Sun 2/26/17	Fri 3/17/17						
40		Final report due	0 days	Mon 3/20/17	Mon 3/20/17	39					
41		Chainless Challenge 2017 Comp	3 days	Wed 4/5/17	Fri 4/7/17						
42		Feasibility test for pedal-charging-accumulator	6 days	Mon 9/19/16	Mon 9/26/16						
43		Dyno testing on 2016 bike	6 days	Mon 9/19/16	Mon 9/26/16						
44		Design/order new bike frame	35 days	Mon 9/19/16	Fri 11/4/16						
45		Bike frame lead time	14 days	Mon 11/7/16	Thu 11/24/16	44					
46		Order hydraulic components	35 days	Mon 9/19/16	Fri 11/4/16						
47		Select clutch	7 days	Sat 10/1/16	Mon 10/10/16						
48		Design supporting components for clutch	14 days	Tue 10/11/16	Fri 10/28/16	47					
49		Hydraulic components lead time	14 days	Mon 11/7/16	Thu 11/24/16	46					
50		Select electromechanical circuit components	7 days	Fri 9/30/16	Sat 10/8/16						
51		Design/select mounting for LCD	16 days	Mon 10/10/16	Mon 10/31/16	50					
52		Final Design Report Due	0 days	Thu 10/27/16	Thu 10/27/16						
53		Order electromechanical circuit components	21 days	Mon 10/10/16	Mon 11/7/16	50					
54		Electronics load testing	24 days	Mon 10/10/16	Thu 11/10/16						
55		Chemical compatibility assessment	13 days	Tue 10/25/16	Thu 11/10/16						
56		Order remaining components	9 days	Tue 10/25/16	Fri 11/4/16						

Project: CC 2017 Project Timelin
Date: Fri 10/28/16

Task	Inactive Summary	External Tasks
Split	Manual Task	External Milestone
Milestone	Duration-only	Deadline
Summary	Manual Summary Rollup	Progress
Project Summary	Manual Summary	Manual Progress
Inactive Task	Start-only	
Inactive Milestone	Finish-only	

ID	Task Mode	Task Name	Duration	Start	Finish	Predecessors	Resource Names	pr 16	3	10	17
57		System testing- test clutch pressure	5 days	Mon 10/31/16	Fri 11/4/16						
58		Finish component placement, CG and trail	9 days	Tue 10/25/16	Fri 11/4/16						
59		Make mock electronic circuit and test functionality (Breadboard)	14 days	Thu 10/27/16	Tue 11/15/16	54					
60		Define mounting method for all components	11 days	Thu 10/27/16	Thu 11/10/16						
61		Order mounting fixtures	5 days	Fri 11/11/16	Thu 11/17/16	60					
62		Finish Welding cable management/ mounts	26 days	Fri 11/11/16	Fri 12/16/16						
63		Paint Frame	17 days	Sun 12/18/16	Sun 1/8/17						
64		Assemble hydraulic circuit	7 days	Mon 1/9/17	Tue 1/17/17						
65		Leak tests on hydraulic circuit	7 days	Mon 1/9/17	Tue 1/17/17						
66		Integrate electromechanical circuit with hydraulic components	10 days	Mon 1/16/17	Fri 1/27/17						
67		Pressure tests on hydraulic circuit	7 days	Fri 1/27/17	Mon 2/6/17						
68		Flow tests on hydraulic circuit	7 days	Fri 1/27/17	Mon 2/6/17						
69		Continuous use tests on hydraulic circuit	7 days	Fri 1/27/17	Mon 2/6/17						
70		System testing- competition requirements	14 days	Mon 2/6/17	Thu 2/23/17	66					
71		System testing- log lots of miles	14 days	Mon 2/6/17	Thu 2/23/17	66					

Project: CC 2017 Project Timelin
Date: Fri 10/28/16

Task		Inactive Summary		External Tasks	
Split		Manual Task		External Milestone	
Milestone		Duration-only		Deadline	
Summary		Manual Summary Rollup		Progress	
Project Summary		Manual Summary		Manual Progress	
Inactive Task		Start-only			
Inactive Milestone		Finish-only			

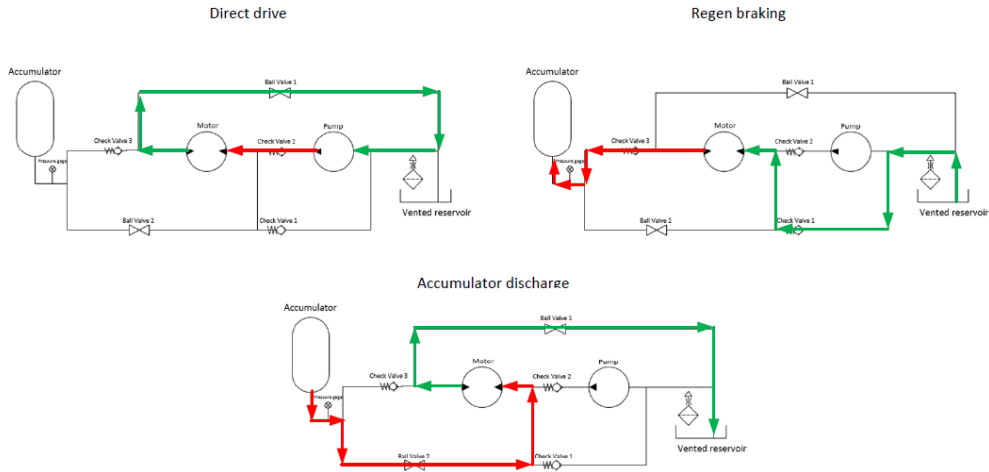
Appendix E: Hydraulic Circuit Configurations (With Flow Directions)

Last updated: May 24, 2016 by Jonathon Sather

CONFIDENTIAL

Hydraulic Circuit

Brake Regeneration



CONFIDENTIAL

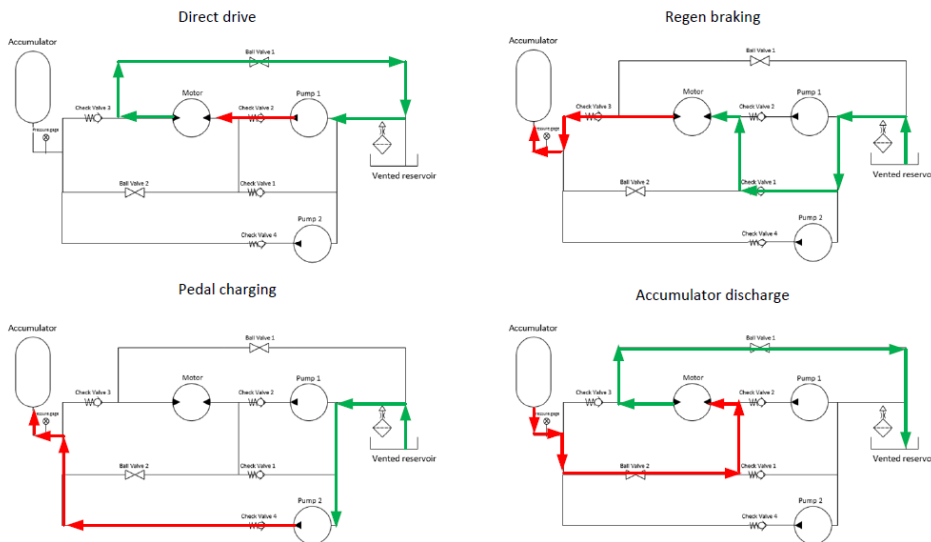


Last updated: May 24, 2016 by Jonathon Sather

CONFIDENTIAL

Hydraulic Circuit

Pedal and brake regeneration (two pumps configuration)

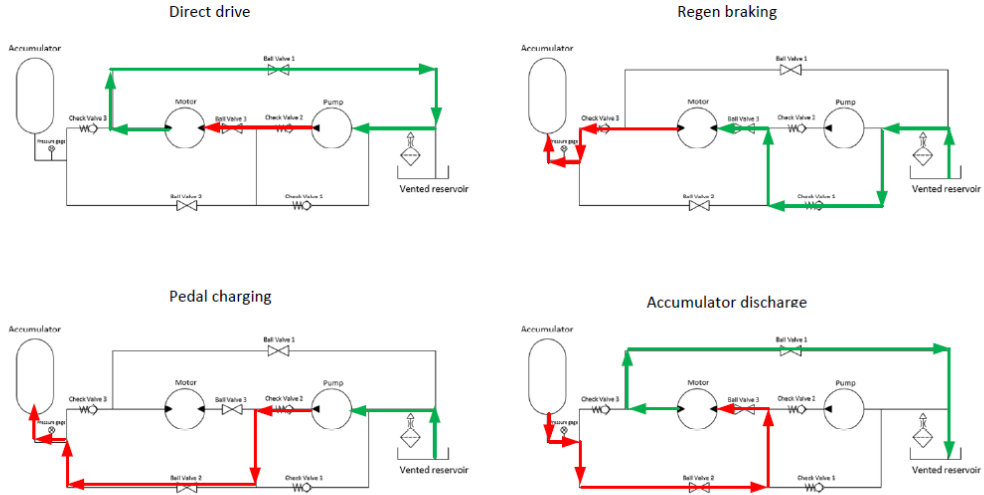


CONFIDENTIAL



Hydraulic Circuit

Pedal and brake regeneration (one pump configuration)



CONFIDENTIAL

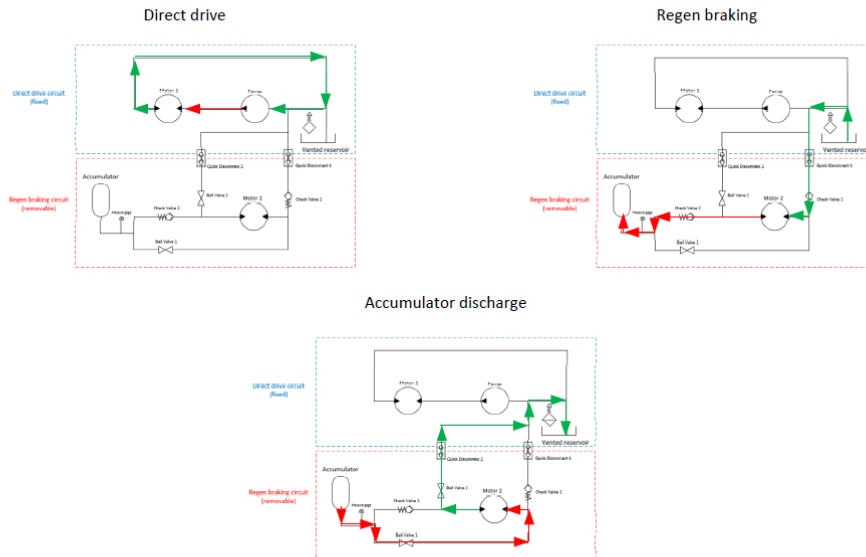


Last updated: May 24, 2016 by Jonathon Sather

CONFIDENTIAL

Hydraulic Circuit

Parallel direct drive/regenerative braking



CONFIDENTIAL



Appendix F: Precharge and Work Calculators (Matlab Code)

Precharge Calculator

Main:

```
%clean slate
clc;
clear all;

%define variables
global W Pmax A n Xmax
W = 6000; %[J] Energy stored
Pmax = 4000; %[psi] Max pressure
A = 6; %[in^2] Cross-sectional area
n = 1; %Polytropic process coefficient
Xmax = 12; %[in] Max displacement of piston
guess = [200 1]; %[psi in] Guesses for precharge pressure and minimum
%          accumulator displacement

%convert to freedom units
W = W/1.35582*12; %[in-lbf]

%set up system of nonlinear equations
%solve using fsolve
x = fsolve(@myprecharge_fxn, guess);

Po = x(1); %Precharge pressure
Xmin = x(2); %Minimum accumulator displacement

%display result to console
fprintf('\nPrecharge estimation: %d psi\n',Po);
```

Precharge function:

```
function precharge_fxn = myprecharge_fxn(x)
%Function holds precharge equations in terms of Po
%and Xmin
%x(1) == Po
%x(2) == Xmin

global W Pmax A n Xmax

precharge_fxn = [W/(A*Xmax^n*(log(Xmax/x(2))))-x(1);
    Pmax*(x(2)/Xmax)^n - x(1)];

end
```

Work Calculator

Main:

```
%Work calculator for bladder accumulator
%By Jonathon Sather

%derivations for formulas used can be found Jon's log book

%clean slate
clc;
clear all;

%define variables
global Po Pmax A n Xmax
Pmax = 5000; %[psi] Max pressure
Po = Pmax/3; %[psi] Precharge pressure
A = 7.07; %[in^2] Cross-sectional area
n = 1.1; %Polytropic process coefficient
Xmax = 8.205; %[in] Max displacement of piston
guess = [300 1]; %[in-lbf in] Guesses for energy storage and minimum
%          accumulator displacement

options = optimset('MaxFunEvals',1000);

%set up system of nonlinear equations
%solve using fsolve
x = fsolve(@mywork_fxn, guess, options);

W = x(1)*1.35582/12; %[J] Energy storage
Xmin = x(2); %[in] Minimum accumulator displacement

%display result to console
fprintf('\nWork estimation: %d J\n',W);

Work function:

function work_fxn = mywork_fxn(x)
%Function holds precharge equations in terms of Po
%and Xmin
%x(1) == W
%x(2) == Xmin

global Po Pmax A n Xmax

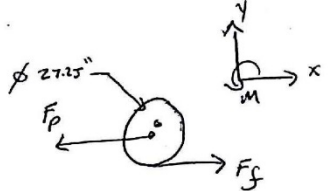
work_fxn = [x(1)/(A*Xmax^n*(log(Xmax/x(2))))- Po;
           Pmax*(x(2)/Xmax)^n - Po];

end
```


Appendix G

(2)

PUSH CHARGING



ASSUMPTIONS:

$F_s = F_p$ (NO SLIP) ← BEST CASE SCENARIO

$F_p = 225 \text{ N}$ (COHS.CA) ← ALLOWABLE FULL BODY PUSH EFFECT

$$T_o = \left(\frac{27.25 \text{ in}}{2} \right) \left(\frac{0.0254 \text{ m}}{1 \text{ in}} \right) 225 \text{ N}$$

= 77.86 Nm



2.7:1 GEAR RATIO

$\Delta P = \frac{(23.84 \text{ Nm}) 63}{(4.9 \frac{\text{cc}}{\text{rev}}) (1)} [\text{bar}]$ ← EQ FROM PARKER PUMP CATALOGUE

= 370.8 bar

= 5378 psi

≠

ASSUME SOME OF F_p GOES TO PREVENT SLIP (~30%)

$\Delta P = 4,000 \text{ psi}$

Appendix H: Integrated System Tests

Integrated System Testing Results

Max Speed (Continuous discharge)

Trial	Max Speed (mph)	Max Pressure (psi)
1	16.5	4000
2	16.3	4000
3	16.5	4200

Max Speed (Rider pedaling only)

Trial	Max Speed (mph)	Rider
1	18.5	Tyler
2	20.54	Jon
3	17.5	Tyler

Discharge Distance + Efficiency

Trial	Distance (in)	Pressure (psi)	Precharge (psi)	Method	Efficiency	Notes
1	4330.711	3950	500	All at once	43.30711	Slight downhill
2	4921.2625	4200	500	All at once	49.212625	Slight downhill
3	n/a	4000	500	All at once	n/a	Leak in reservoir tubing mid-run.
4	3543.309	4000	500	All at once	35.43309	Slight uphill
5	7795.2798	4000	500	Bursts	77.952798	
6	8425.2014	4100	500	Bursts	84.252014	
7	7677.1695	4000	500	Bursts	76.771695	

Pressure Test

Trial	Leaks?	Duration (min)	Pressure (psi)
1	No	1	4000
2	No	1	4000
3	No	15	4000

Endurance Test

Distance (mi)	Notes
10	Runs fine. Exhausting going up hills.

Sprint Test

Trial	Distance	Time (s)	Rider	Notes
1	200m	31.63	Anthony	Slight downhill
2	200m	43.76	Anthony	Slight uphill. Fumble at start
3	200m	29.8s	Anthony	Slight downhill.
4	200m	n/a	Jonathon	Leak while regenerative braking. Conclude testing.

Goal Checklist

Goal: Less than \$7500

Result: Total cost less than \$4500

Goal: Less than 5 custom parts

Result: Not met (especially considering the mechatronics). In hindsight, not a realistic goal.

Goal: No permanent joints onto frame.

Result: Not met. Met, if don't include the glue for the hall effect sensors.

Goal: Less than 5 seconds to reach top speed.

Result: Met with precharge 500psi. Unknown with higher precharge.

Goal: 200m sprint in less than 29 seconds.

Result: Not met with precharge 500psi. Likely possible with higher precharge.

Goal: 10% more efficient than last year's bike

Result: Met. Approx. 100% more efficient on one of our practice runs.

Goal: Bike weight less than 150lb

Result: Met. Weight: 115lb (wet)

Goal: 50 miles without mechanical failure.

Result: Indeterminate. Went 5 miles before reservoir tubing split open. Went another 5 miles before leak in hardlines. Should be good now for *at least* another 5 miles.

Goal: Capable of regenerative braking.

Result: Met. Can charge upward of 500 psi in one brake.

Goal: Streamlined look with quality surface finish.

Result: Met.

Goal: Electromechanical system implemented.

Result: Met. Works great.

Goal: 80-100 RPM (on flat ground)

Result:	cadence (RPM)	80	90	100
	reached?	yes	yes	yes

Goal: Useable controls without looking

Result: Met.

Goal: Charge accumulator in 10 min to max pressure.

Result: Met. Can charge in under 3min.

Appendix I: Tubing Friction Analysis

File:\tscient\SP UFD U3\Pressure Drop Analysis.EES

10/27/2016 10:33:04 PM Page 1

EES Ver. 10.096: #0552: for use only by students and faculty, Mechanical Engineering, Dept. Cal Poly State University

Pressure Drop

0 Chainz

10/18/2016

Inputs

$$D_{\text{inch}} = 0.37 \text{ [in]} \quad \textit{Inside diameter of tubing = 0.37in}$$

$$D = D_{\text{inch}} \cdot \left| 0.0254 \cdot \frac{\text{m}}{\text{in}} \right| \quad \textit{Inside diameter of tubing in m}$$

$$L_{\text{feet}} = 6 \text{ [ft]} \quad \textit{Total curcuit length, ft}$$

$$L = L_{\text{feet}} \cdot \left| 0.3048 \cdot \frac{\text{m}}{\text{ft}} \right| \quad \textit{Total length of tubing}$$

$$D_{\text{sp}} = 5 \text{ [cm}^3\text{/rev]} \quad \textit{Pump/motor displacement}$$

$$\omega = 90 \text{ [rev/min]} \quad \textit{Assumed cadence}$$

$$\nu = 0.00003678 \text{ [m}^2\text{/s]} \quad \textit{Assume Mobil EAL 224H at 10C}$$

$$\rho = 921 \text{ [kg/m}^3\text{]} \quad \textit{Density from Specific Gravity @ 15° C/15° C, ASTM D 1298}$$

$$\mu = \rho \cdot \nu$$

$$\text{gear}_{\text{front}} = 15 \text{ [-]}$$

Calaculate Re for pedaling

$$Q = D_{\text{sp}} \cdot \omega \cdot \text{gear}_{\text{front}} \cdot 0.01667 \text{ [min/sec]} \cdot \left[\left| 0.01 \cdot \frac{\text{m}}{\text{cm}} \right| \right]^3 \quad \textit{Flowrate with 15:1 speed increaser at pedals}$$

$$V = \frac{4 \cdot Q}{\pi \cdot D^2} \quad \textit{Fluid Velocity}$$

$$\text{Re} = \frac{V \cdot D}{\nu} \quad \textit{Reynold's number}$$

Calculate Relative Roughness

$$\epsilon_{\text{drawn}} = 0.0025 \text{ [mm]} \cdot \left| 0.001 \cdot \frac{\text{m}}{\text{mm}} \right| \quad \textit{Absolute Roughness of drawn tubing}$$

$$\epsilon_{\text{hose}} = 0.35 \text{ [mm]} \cdot \left| 0.001 \cdot \frac{\text{m}}{\text{mm}} \right| \quad \textit{Absolute Roughness of Flexible Rubber Tubing - Wire Reinforced}$$

$$\epsilon_{\text{rel,drawn}} = \frac{\epsilon_{\text{drawn}}}{D} \quad \textit{Relavice roughness drawn tubing}$$

$$\epsilon_{\text{rel,hose}} = \frac{\epsilon_{\text{hose}}}{D} \quad \textit{Relative Roughness hose}$$

Calculate Friction Factor

$$f_{\text{laminar}} = \frac{64}{\text{Re}} \quad \text{Laminar Flow}$$

$$f_{\text{turb,smooth}} = \frac{0.316}{\text{Re}^{0.25}} \quad \text{Turbulent Flow, Smooth Pipes}$$

$$f_{\text{turb,rough,pipe}} = \frac{0.25}{\log^2 \left[\frac{1}{3.7} \cdot \varepsilon_{\text{rel,drawn}} + \frac{5.74}{\text{Re}_{\text{acc}}^{0.9}} \right]} \quad \text{Turbulent Flow, Rough Pipes}$$

$$f_{\text{turb,rough,hose}} = \frac{0.25}{\log^2 \left[\frac{1}{3.7} \cdot \varepsilon_{\text{rel,hose}} + \frac{5.74}{\text{Re}_{\text{acc}}^{0.9}} \right]} \quad \text{Turbulent Flow, Rough Hose}$$

Major Head Loss in a Single Pipe

$$g = 9.81 \quad [\text{m/s}^2] \quad \text{Gravity}$$

$$h_{\text{major,loss}} = f_{\text{turb,rough,hose}} \cdot \frac{L}{D} \cdot \frac{V^2}{2 \cdot g} \quad \text{Major losses with turbulent flow in a rough hose}$$

Major Head Loss in a Single Pipe

$$k_{\text{elbow}} = 1.5 \quad [-]$$

Elbow, Threaded Regular 90degrees. Represents worst case we would use.

$$h_{\text{minor,loss}} = \frac{k_{\text{elbow}} \cdot V^2}{2 \cdot g} \quad \text{Minor losses with turbulent flow in a rough hose}$$

Compare Major and Minor Losses and notice the difference in magnitude and neglect minor losses going forward.

Use Darcy-Weisbach equation for pressure losses in conduits as a means of comparison.

Find Pressure Drops

$$\Delta P_{\text{laminar}} = f_{\text{laminar}} \cdot \frac{\rho \cdot L \cdot V^2}{2 \cdot D} \cdot \left| 0.000145038 \cdot \frac{\text{psi}}{\text{Pa}} \right| \quad \text{Laminar conditions}$$

$$\Delta P_{\text{turb,smooth}} = f_{\text{turb,smooth}} \cdot \frac{\rho \cdot L \cdot V^2}{2 \cdot D} \cdot \left| 0.000145038 \cdot \frac{\text{psi}}{\text{Pa}} \right|$$

Look at top speed to determine if turbulent flow occurs

$$\text{MPH} = 45 \quad [\text{miles/hr}]$$

$$\text{gear}_{\text{rear}} = 5.5 \quad [-]$$

$$D_{\text{wheel}} = 27.24 \quad [\text{in/rev}]$$

$$\omega_{\text{accumulator}} = \text{MPH} \cdot \left| 63360 \cdot \frac{\text{in}}{\text{miles}} \right| \cdot \frac{1}{D_{\text{wheel}}} \cdot \left| 0.016666667 \cdot \frac{\text{hr}}{\text{min}} \right|$$

Calculate Re for accumulator dump

$$Q_{acc} = D_{sp} \cdot \epsilon_{accumulator} \cdot gear_{rear} \cdot 0.01667 \text{ [min/sec]} \cdot \left[\left| 0.01 \cdot \frac{m}{cm} \right| \right]^3$$

Flowrate with 5.5:1 speed increaser at rear axle

$$V_{acc} = \frac{4 \cdot Q_{acc}}{\pi \cdot D^2} \text{ Fluid Velocity}$$

$$Re_{acc} = \frac{V_{acc} \cdot D}{\nu} \text{ Reynold's number}$$

$$\Delta P_{turb,pipe,acc} = f_{turb,rough,pipe} \cdot \frac{\rho \cdot L \cdot V_{acc}^2}{2 \cdot D} \cdot \left| 0.000145038 \cdot \frac{psi}{Pa} \right| \text{ Pressure loss in planned system}$$

$$\Delta P_{turb,hose,acc} = f_{turb,rough,hose} \cdot \frac{\rho \cdot L \cdot V_{acc}^2}{2 \cdot D} \cdot \left| 0.000145038 \cdot \frac{psi}{Pa} \right| \text{ Pressure loss in current system}$$

Percent Difference

$$DIFF_{turb,hose} = \left[\frac{|\Delta P_{turb,hose,acc} - \Delta P_{turb,pipe,acc}|}{0.5 \cdot (\Delta P_{turb,hose,acc} + \Delta P_{turb,pipe,acc})} \right] \cdot 100$$

SOLUTION**Unit Settings: SI C kPa kJ mass deg**

$$D = 0.009398 \text{ [m]}$$

$$\Delta P_{tammar} = 5.281 \text{ [psi]}$$

$$\Delta P_{turb,hose,acc} = 127.3 \text{ [psi]}$$

$$\Delta P_{turb,pipe,acc} = 77.79 \text{ [psi]}$$

$$\Delta P_{turb,smooth} = 2.395 \text{ [psi]}$$

$$DIFF_{turb,hose} = 48.3$$

$$D_{sp} = 5 \text{ [cm}^3\text{/rev]}$$

$$D_{inch} = 0.37 \text{ [in]}$$

$$D_{wheel} = 27.24 \text{ [in/rev]}$$

$$\epsilon_{drawn} = 0.0000025 \text{ [m]}$$

$$\epsilon_{hose} = 0.00035 \text{ [m]}$$

$$\epsilon_{rel,drawn} = 0.000266 \text{ [-]}$$

$$\epsilon_{rel,hose} = 0.03724 \text{ [-]}$$

$$f_{laminar} = 0.1544 \text{ [-]}$$

$$f_{turb,rough,hose} = 0.0737 \text{ [-]}$$

$$f_{turb,rough,pipe} = 0.04503 \text{ [-]}$$

$$f_{turb,smooth} = 0.07003 \text{ [-]}$$

$$g = 9.81 \text{ [m/s}^2\text{]}$$

$$gear_{front} = 15 \text{ [-]}$$

$$gear_{rear} = 5.5 \text{ [-]}$$

$$h_{major,loss} = 1.923 \text{ [m]}$$

$$h_{minor,loss} = 0.2012 \text{ [m]}$$

$$kelbow = 1.5 \text{ [-]}$$

$$L = 1.829 \text{ [m]}$$

$L_{\text{feet}} = 6$ [ft]
 $\text{MPH} = 45$ [miles/hr]
 $\mu = 0.03387$ [Pa-s]
 $\nu = 0.00003678$ [m²/s]
 $\omega = 90$ [rev/min]
 $\omega_{\text{accumulator}} = 1744$ [rev/min]
 $Q = 0.0001125$ [m³/s]
 $Q_{\text{acc}} = 0.0007997$ [m³/s]
 $Re = 414.5$ [-]
 $Re_{\text{acc}} = 2946$ [-]
 $\rho = 921$ [kg/m³]
 $V = 1.622$ [m/s]
 $V_{\text{acc}} = 11.53$ [m/s]

No unit problems were detected.

Parametric Table: Table 1

	ω [rev/min]	V [m/s]	Re [-]	$\Delta P_{\text{laminar}}$ [psi]
Run 1	5	0.09012	23.03	0.2934
Run 2	10	0.1802	46.05	0.5867
Run 3	15	0.2704	69.08	0.8801
Run 4	20	0.3605	92.11	1.173
Run 5	25	0.4506	115.1	1.467
Run 6	30	0.5407	138.2	1.76
Run 7	35	0.6308	161.2	2.054
Run 8	40	0.7209	184.2	2.347
Run 9	45	0.8111	207.2	2.64
Run 10	50	0.9012	230.3	2.934
Run 11	55	0.9913	253.3	3.227
Run 12	60	1.081	276.3	3.52
Run 13	65	1.172	299.3	3.814
Run 14	70	1.262	322.4	4.107
Run 15	75	1.352	345.4	4.4
Run 16	80	1.442	368.4	4.694
Run 17	85	1.532	391.5	4.987
Run 18	90	1.622	414.5	5.281
Run 19	95	1.712	437.5	5.574
Run 20	100	1.802	460.5	5.867
Run 21	105	1.892	483.6	6.161
Run 22	110	1.983	506.6	6.454
Run 23	115	2.073	529.6	6.747
Run 24	120	2.163	552.6	7.041
Run 25	125	2.253	575.7	7.334
Run 26	130	2.343	598.7	7.627
Run 27	135	2.433	621.7	7.921
Run 28	140	2.523	644.7	8.214
Run 29	145	2.613	667.8	8.507
Run 30	150	2.704	690.8	8.801

Parametric Table: Table 2

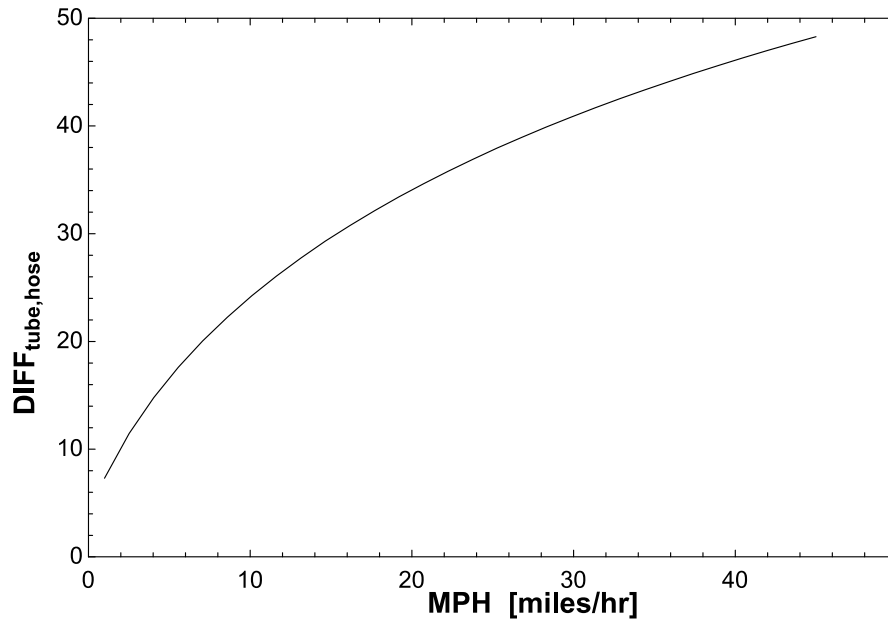
	MPH [miles/hr]	$\omega_{\text{accumulator}}$ [rev/min]	Re_{acc} [-]	$\Delta P_{\text{turb,pipe,acc}}$ [psi]	$\Delta P_{\text{turb,hose,acc}}$ [psi]	$DIFF_{\text{tube,hose}}$
Run 1	1	38.77	65.46	0.2784	0.2995	7.304
Run 2	2.517	97.58	164.8	0.8849	0.9925	11.47
Run 3	4.034	156.4	264.1	1.722	1.997	14.78
Run 4	5.552	215.2	363.4	2.756	3.287	17.59
Run 5	7.069	274	462.7	3.969	4.854	20.05
Run 6	8.586	332.9	562.1	5.35	6.689	22.24
Run 7	10.1	391.7	661.4	6.889	8.789	24.24
Run 8	11.62	450.5	760.7	8.58	11.15	26.06
Run 9	13.14	509.3	860	10.42	13.77	27.74
Run 10	14.66	568.1	959.4	12.4	16.65	29.31
Run 11	16.17	626.9	1059	14.51	19.79	30.77
Run 12	17.69	685.8	1158	16.76	23.18	32.14
Run 13	19.21	744.6	1257	19.14	26.83	33.43
Run 14	20.72	803.4	1357	21.65	30.73	34.64
Run 15	22.24	862.2	1456	24.29	34.88	35.8
Run 16	23.76	921	1555	27.05	39.28	36.9
Run 17	25.28	979.9	1655	29.93	43.94	37.94
Run 18	26.79	1039	1754	32.93	48.85	38.94
Run 19	28.31	1097	1853	36.05	54.01	39.9
Run 20	29.83	1156	1953	39.28	59.43	40.81
Run 21	31.34	1215	2052	42.64	65.09	41.69
Run 22	32.86	1274	2151	46.1	71	42.53
Run 23	34.38	1333	2251	49.68	77.17	43.34
Run 24	35.9	1392	2350	53.37	83.58	44.13
Run 25	37.41	1450	2449	57.17	90.25	44.88
Run 26	38.93	1509	2548	61.08	97.16	45.61
Run 27	40.45	1568	2648	65.09	104.3	46.31
Run 28	41.97	1627	2747	69.22	111.7	47
Run 29	43.48	1686	2846	73.45	119.4	47.66
Run 30	45	1744	2946	77.79	127.3	48.3

Parametric Table: Table 3

	D_{inch} [in]	Re [-]	$\Delta P_{\text{lamimar}}$ [psi]
Run 1	0.25	613.4	25.34
Run 2	0.2931	523.2	13.41
Run 3	0.3362	456.1	7.746
Run 4	0.3793	404.3	4.781
Run 5	0.4224	363	3.108
Run 6	0.4655	329.4	2.107
Run 7	0.5086	301.5	1.479
Run 8	0.5517	278	1.068
Run 9	0.5948	257.8	0.7905
Run 10	0.6379	240.4	0.5976
Run 11	0.681	225.2	0.4601
Run 12	0.7241	211.8	0.3599
Run 13	0.7672	199.9	0.2856
Run 14	0.8103	189.2	0.2295

Parametric Table: Table 3

	D _{inch} [in]	Re [-]	ΔP _{lamimar} [psi]
Run 15	0.8534	179.7	0.1865
Run 16	0.8966	171.1	0.1532
Run 17	0.9397	163.2	0.1269
Run 18	0.9828	156	0.1061
Run 19	1.026	149.5	0.08936
Run 20	1.069	143.5	0.07579
Run 21	1.112	137.9	0.06471
Run 22	1.155	132.8	0.05558
Run 23	1.198	128	0.048
Run 24	1.241	123.5	0.04167
Run 25	1.284	119.4	0.03636
Run 26	1.328	115.5	0.03186
Run 27	1.371	111.9	0.02804
Run 28	1.414	108.5	0.02477
Run 29	1.457	105.3	0.02197
Run 30	1.5	102.2	0.01955



Appendix J: Cost Analysis and BOMs

Bicycle Components BOM

Bicycle BOM							
1	Bicycle tire	Schwalbe	11600593	730	\$75.00	2	\$150.00
2	Bicycle tube	Bontrager	411836	215	\$7.99	2	\$15.98
3	Front brake	Tektro	R540	164	\$79.99	1	\$79.99
4	Rear brake	Tektro	R540	164	\$0.00	1	\$0.00
5	Stem	Bontrager	512322	144	\$64.99	1	\$64.99
6	Handle bar	Bontrager	427218	240	\$89.99	1	\$89.99
7	Brake Levers	Tektro	RL520	272	\$29.99	1	\$29.99
8	Seat	-	-	-	\$24.99	1	\$24.99
9	Fork	Sunlite			\$60.00	1	\$60.00
10	Grips / bar tape	Bontrager	534785	50	\$19.99	1	\$19.99
11	Brake cable	Shimano	SPTFE-P	180	\$20.99	1	\$20.99
12	Cranks	Kalloy			\$19.99	2	\$39.98
13	Spring Preload Bolt	3D Motorsports	-		\$1.25	7	\$8.75
14	PTO Shaft Screw	3D Motorsports	-		\$1.25	1	\$1.25
15	1/4" Bearing Ball	3D Motorsports	-		\$0.99	3	\$2.97
16	Drive Key	3D Motorsports	-		\$1.25	1	\$1.25
Subtotal:							\$611.11

Mechatronics BOM

Mechatronics BOM							
17	Mechatronics R&D	-	-	-	\$60.00	50	\$3,000.00
18	Hall Effect Sensor	OC-MS-001	Sparkfun	COM-09312	\$0.95	5	\$4.75
19	Wheel/Pedal Magnet	OC-MS-002	Specialized	4815-5075	\$5.00	3	\$15.00
20	Pressure sensor	OC-MS-003	GA Wirth	2200RGH500823EA	\$345.00	1	\$345.00
21	Microcontroller	OC-MS-004	Robotshop	RB-Ard-34	\$23.25	1	\$23.39
22	LCD	OC-MS-005	Adafruit	1651	\$34.95	1	\$34.95
23	Buttons	OC-MS-006	Mouser	850-59-211	\$8.02	3	\$24.06
24	Rocker switch	OC-MS-007	Mouser	653-A8MS1162	\$4.76	2	\$9.52
25	Solenoid battery (rechargeable)	OC-MS-008	Super Circuits	-	\$69.18	1	\$69.18
26	Switching regulator	OC-MS-009	Adafruit	1385	\$9.95	2	\$19.90
27	Transistor	OC-MS-010	Mouser	511-TIP120	\$0.60	10	\$6.00
28	Solenoids	OC-MS-011	Parker	DSH121NTSPD012D-12T	\$299.00	2	\$598.00
29	Flyback Diodes	OC-MS-012	Mechatronics Dept.			2	
30	Sunlight shield	OC-MS-013	Cal Poly 3D printing		\$0.00	1	\$0.00
31	Glare screen protector	OC-MS-014	Amazon		\$26.09	1	\$26.09
32	Project box	OC-MS-015	Digikey	HM109-ND	\$6.48	2	\$12.96
33	ABS to ABS adhesive	OC-MS-016	McMaster	75285A72	\$17.96	1	\$17.96
34	Plastic clamp, 1" ID	OC-MS-017	McMaster	2339T12	\$0.80	4	\$3.20
35	Plastic clamp, 1.25" ID	OC-MS-018	McMaster	2339T13	\$1.00	4	\$4.00
36	Standoffs, 0.625"	OC-MS-019	Mouser	534-1894	\$0.48	10	\$4.81
37	Standoff screws	OC-MS-020	Mouser	534-9300	\$0.05	100	\$4.80
38	Screws for clamps - 6-32, 0.5" depth (pack of 25)	OC-MS-021	McMaster	92220A144	\$9.62	1	\$9.62
39	Nuts for clamps- size 6-32, thin lock nuts (pack of 5)	OC-MS-022	McMaster	91581A315	\$6.80	2	\$13.60

40	Washers for clamps-size 6 (pack of 100)	OC-MS-023	McMaster	96765A115	\$3.68	1	\$3.68
41	Straps and cable tie	OC-MS-024	McMaster	1151N2	\$4.08	3	\$12.24
42	Nuts for straps - size 12-24, Pack of 100	OC-MS-025	McMaster	90480A013	\$2.45	1	\$2.45
43	Lezyne Energy Caddy V2 Stem Bag (for battery)	OC-MS-026	Art's Cyclery	-	\$21.99	1	\$21.99
44	Wires	OC-MS-027	Mechatronics Dept.			100	\$0.00
45	Solder	OC-MS-028	Mechatronics Dept.			lots	\$0.00
46	Zip ties	OC-MS-029	Cal Poly Hangar			100	\$0.00
47	Toshiba Mosfet	OC-MS-030	Mouser	757-SSM3K361RLF	\$0.53	2	\$1.06
48	Hollow square steel tube for solenoid bracket (3ft)	OC-MS-031	McMaster	89825K49	\$31.80	1	\$31.80
49	Screws for solenoid mounting = 5/16"-18-2 1/2" long (pack of 10)	OC-MS-032	McMaster	91286A179	\$13.11	1	\$13.11
50	Locknuts for solenoid mount- Grade 8 5/16"-18 (pack of 20)	OC-MS-033	McMaster	97135A220	\$3.68	1	\$3.68
51	Washers for solenoid mount (pack of 50)	OC-MS-034	McMaster	98180A120	\$5.36	1	\$5.36
52	2 Position Connector In-Line Male	OC-MS-035	Digikey	SC1202-ND	\$4.40	6	\$26.40
53	2 Position Connector Panel Mount Female	OC-MS-036	Digikey	SC1207-ND	\$3.98	8	\$31.84
54	3 Position Connector In-Line Male	OC-MS-037	Digikey	SC1204-ND	\$5.09	6	\$30.54
55	3 Position Connector panel Mount Female	OC-MS-038	Digikey	SC1209-ND	\$4.90	12	\$58.80
56	2-3/4" Hex Screw (pack of 10)	OC-MS-039	McMaster	92620A635	\$12.74	1	\$12.74
57	2-1/2" Hex Screw (pack of 5)	OC-MS-040	McMaster	92620A634	\$7.99	1	\$7.99

58	Multipurpose Epoxy	OC-MS-041	McMaster	7541A84	\$10.60	1	\$10.60
59	Neodymium Magnet	OC-MS-042	McMaster	5862K93	\$18.32	1	\$18.32
60	Grommet 7/16" (pack of 100)	OC-MS-043	McMaster	9600K33	\$7.17	1	\$7.17
61	Grommet 13/32" (pack of 100)	OC-MS-044	McMaster	9600K26	\$8.54	1	\$8.54
62	3 Wire Cable (50 feet)	OC-MS-045	McMaster	7422K21	\$30.00	1	\$30.00
63	2 Wire Cable (25 feet)	OC-MS-046	McMaster	7422K2	\$13.00	1	\$13.00
64	Small Plastic Box	OC-MS-047	Digikey	HM376-ND	\$2.34	5	\$11.70
65	Rocker Switch	OC-MS-048	Digikey	EG4776-ND	\$0.99	5	\$4.95
66	Custom PCB Shield	OC-MS-049	Osh Park	N/A	\$30.00	1	\$30.00
67	Polycarbonate sheet	OC-MS-050	Grad lab	N/A	\$0.00	1	\$0.00
68	Smaller Grommet	OC-MS-051	Mechatronics Lab	N/A	\$0.00	1	\$0.00
69	3 Wire Cable	OC-MS-52	Digikey	CE2003SG-100-ND	\$30.88	1	\$30.88
70	Stackable headers	OC-MS-53	Adafruit	85	\$1.95	3	\$5.85
71	50 Ohm Resistor	OC-MS-54	Digikey	764-1183-1-ND	\$1.43	10	\$14.32
Subtotal:							\$4,695.80

Hydraulic Components BOM

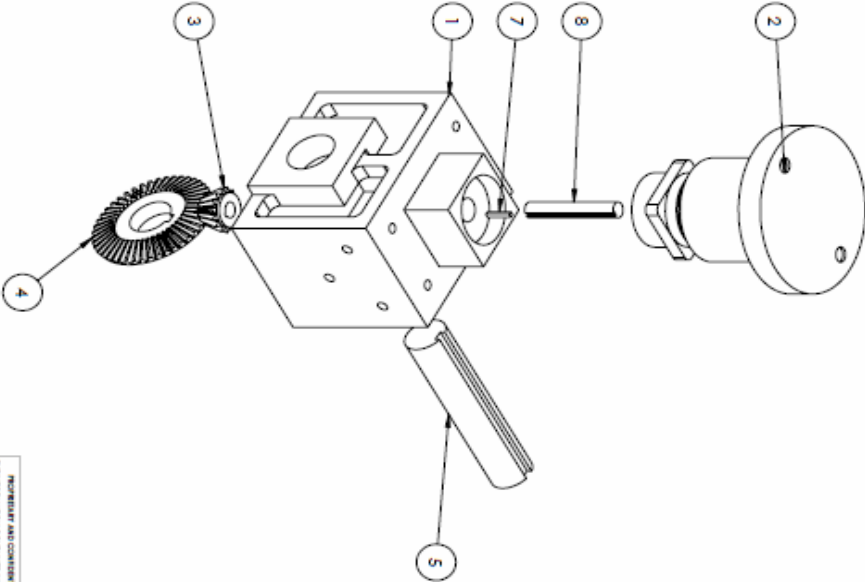
Hydraulics BOM							
71	1/2-1/8 NPT Reducer	48805k265	McMaster		\$29.01	1	\$29.01
72	1/2-1/4 NPT Reducer	48805K75	McMaster		\$28.93	1	\$28.93
73	1/2 NPT BSP Adapter	4092k74	McMaster		\$36.62	1	\$36.62
74	JIC Flare Fittings and Adapters	8 ETX-S	Parker		\$6.27	2	\$12.54
75	JIC Flare Fittings and Adapters	8-8-8 RTX-S	Parker		\$14.28	1	\$14.28
76	Reducer	RI3/4EDX1/2CF	Hose and Fittings Inc.		\$6.36	1	\$6.36
77	Copper Seals	SECO 7C 8	Seco Seals		\$0.91	25	\$22.75
78	Run tee fitting	Parker	8-8-8 RTX-S		\$14.28	1	\$14.28
79	1/2 to 1/8 female adapter	McMaster	48805K265		\$29.01	1	\$29.01
80	1/2 BSPP to NPT	McMaster	4092K74		\$36.62	1	\$36.62
81	90 Degreee flare	Parker	8 ETX-S		\$6.27	2	\$12.54
Subtotal:							\$242.94

Inherited/Manufactured BOM

Inherited / Manufactured Parts							
Item	Description	Manufacturer	Labor Hours	Labor Rate	Part/Material Cost	Quantity	Total Cost
82	Front Drive Unit	Poly	2	\$ 60.00	\$3.00	1	\$123.00
83	Planetary coupler shaft	Poly	11	\$ 60.00	\$0.00	2	\$660.00
84	Planetary coupler insert	Poly	6	\$ 60.00	\$100.34	1	\$460.34
85	Coupler Housing	Poly	23	\$ 60.00	\$152.00	1	\$1,532.00
86	Gearbox Assembly	Poly	4	\$ 60.00	\$5.00	1	\$245.00
87	L-Bracket	Poly	6	\$ 60.00	\$30.93	1	\$390.93
88	Rear dropouts	Poly	15	\$ 60.00	\$95.16	2	\$1,090.32
89	Motor mount	Poly	23	\$ 60.00	\$80.54	1	\$1,460.54
90	Pinion	Poly	5	\$ 60.00	\$28.02	1	\$328.02
91	Gear	Poly	2	\$ 60.00	\$117.02	1	\$237.02
92	Clutch adapter	Poly	25	\$ 60.00	\$12.00	1	\$1,512.00
93	Rear Wheel	Poly	11	\$ 60.00	\$121.23	1	\$781.23
94	Frame	Poly	55	\$ 60.00	\$160.00	1	\$3,460.00
95	Planetary Drive	-	0	\$ 60.00	\$737.00	1	\$737.00
96	Mounting Bearings	-	0	\$ 60.00	\$50.00	2	\$100.00
97	Clutch	-	0	\$ 60.00	\$175.00	1	\$175.00
98	Rear Drive Shaft	Poly	0.5	\$ 60.00	\$26.77	1	\$56.77
99	Parker F11-5 Pump and Motor	Parker	0	\$ 60.00	\$1,000.00	2	\$2,000.00
Subtotal:							\$15,349.17

Cost of This Year's Bicycle:	\$5,549.85
Cost of Complete/Updated Bicycle:	\$20,899.02

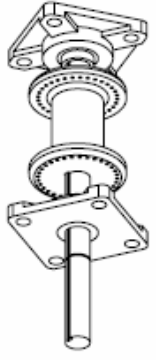
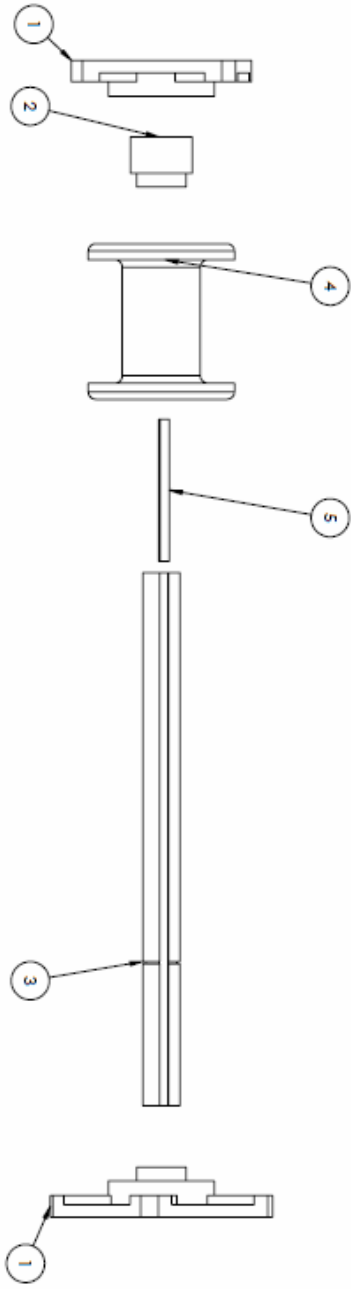
Appendix K: Solidworks Models



ITEM NO.	PART NUMBER	DESCRIPTION	QTY.
1	Crank Enclosure		1
2	Planetary Gear Enclosure		1
3	Inch - Straight bevel pinion 12DP 15PT 45GT 20PA 0.75FW --- 15O1.5H12.0MD0.5R1		1
4	Inch - Straight bevel gear 12DP 45GT 15PT 20PA 0.75FW --- 45O1.5H1MD1.3125R1		1
5	Front Drive Bevel Shaft		1
6	Key 817.1 0.3125x0.3125x.55		1
7	Key 817.1 0.125x0.125x.82		1
8	Front Drive Coupler Shaft		1

PROPERTIES AND COMMENTS:
 THIS DRAWING IS THE PROPERTY OF THE COMPANY. IT IS TO BE KEPT IN CONFIDENCE AND NOT TO BE REPRODUCED OR TRANSMITTED IN ANY FORM OR BY ANY MEANS, ELECTRONIC OR MECHANICAL, INCLUDING PHOTOCOPYING, RECORDING, OR BY ANY INFORMATION STORAGE AND RETRIEVAL SYSTEM. ANY UNAUTHORIZED USE OF THIS DRAWING IS PROHIBITED.

REV	DATE	BY	CHKD	APP'D	TITLE	SCALE	WEIGHT	SHEET	OF
1					Front Drive Assembly	B		1	1



ITEM NO.	PART NUMBER	DESCRIPTION	QTY.
1	Rear_Axle_Bearing_Ho		2
2	6338K433		1
3	Rear_Axle		1
4	Rear_Hub		1
5	Axle_Key		1

UNLESS OTHERWISE SPECIFIED:

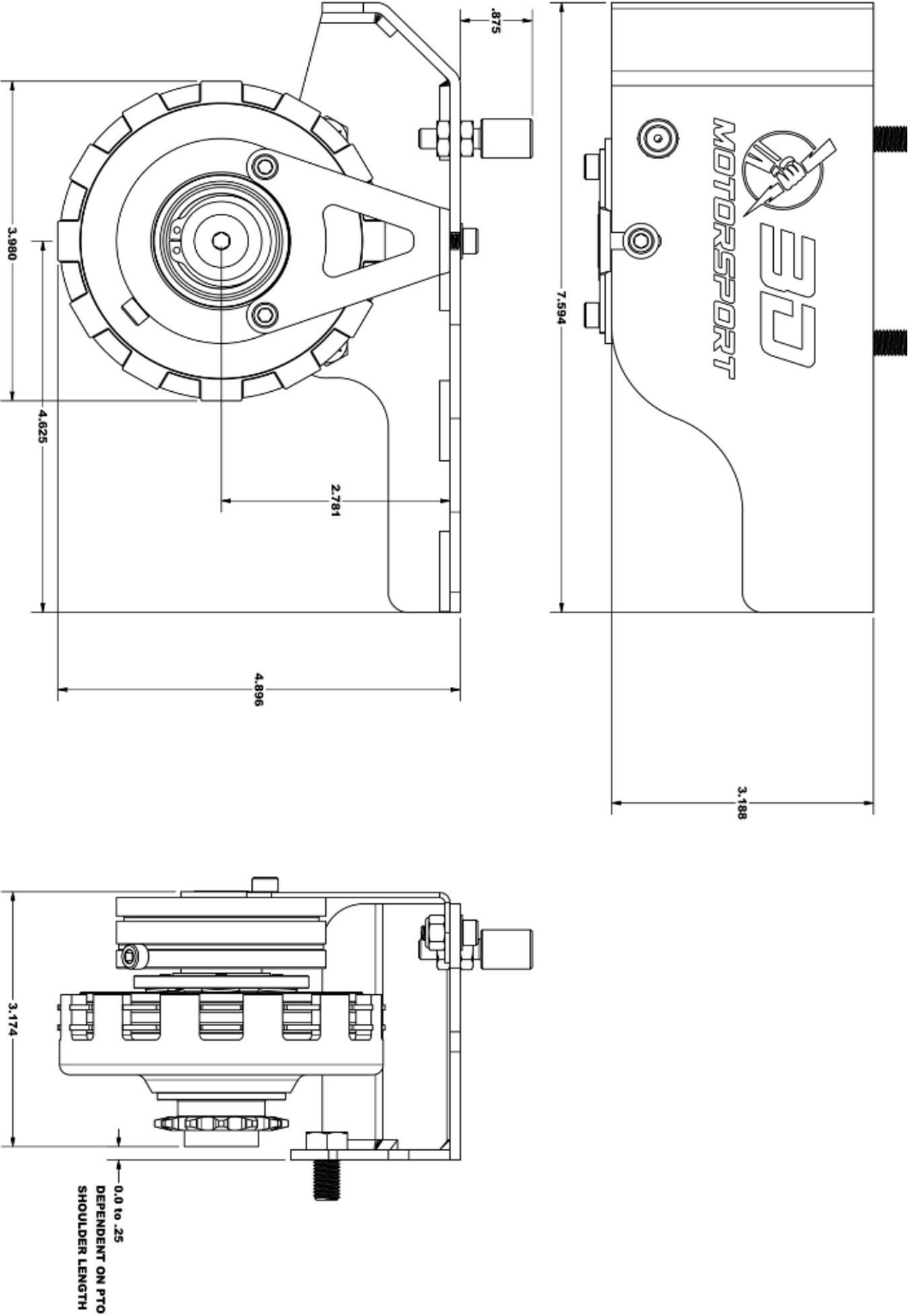
UNIT OF MEASURE	INCHES	DATE	10/27/14
TOLERANCES UNLESS OTHERWISE SPECIFIED	FRACTIONS	DECIMALS	
ANGLES	DIG. ANG.	MIN. ANG.	
THREADS PER INCH	3/8" - 16	1/2" - 14	
WELDING SYMBOLS	ASME	WELDING SYMBOLS	
FINISH		FINISH	
APPROVALS		COMMENTS	
DESIGNED BY		CHECKED BY	
DRAWN BY		DATE	
SCALE	1:2	WEIGHT	
SHEET	1 OF 1	REV	1

REAR AXLE ASSEMBLY

SCALE: 1:2 WEIGHT: SHEET 1 OF 1

SOLIDWORKS Educational Product. For Instructional Use Only

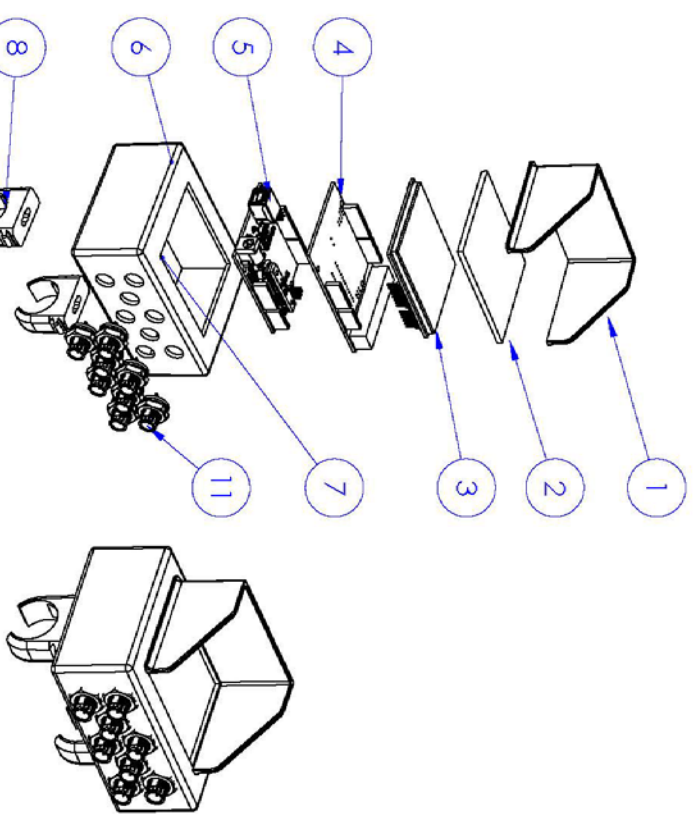
Appendix L: Clutch Diagram



2

1

ITEM NO.	PART NUMBER	DESCRIPTION	Default/QTY.
1	0C-MS-013	Sunlight shield	1
2	0C-MS-050	PC screen cover	1
3	0C-MS-005	TFT shield	1
4	0C-MS-049	Custom PCB shield	1
5	0C-MS-004	Arduino Uno	1
6	0C-MS-015	Display housing	1
7	0C-MS-022	Lock nut	2
8	0C-MS-018	Plastic clamp	2
9	0C-MS-023	Washer	4
10	0C-MS-021	Screw	2
11	0C-MS-035/7	Panel mount connector	8



PROPRIETARY AND CONFIDENTIAL
 THE INFORMATION CONTAINED IN THIS DRAWING IS THE SOLE PROPERTY OF <INSERT COMPANY NAME HERE>. ANY REPRODUCTION IN PART OR AS A WHOLE WITHOUT THE WRITTEN PERMISSION OF <INSERT COMPANY NAME HERE> IS PROHIBITED.

UNLESS OTHERWISE SPECIFIED: DIMENSIONS ARE IN INCHES TOLERANCES: FRACTIONAL ± .01 ANGULAR: MACH ±1 BEND ±1 TWO PLACE DECIMAL ±.01 THREE PLACE DECIMAL ±.001	DRAWN JJS	DATE 2/12/17
CHECKED ENG. APPR. MFG. APPR.		
INTERPRET GEOMETRIC TOLERANCING PER: MATERIAL FINISH		
DO NOT SCALE DRAWING		

COMMENTS: ① CONSISTS OF 0C-A6-006 (QTY 3) AND 0C-A6-037 (QTY 5)		
Q.A.		

TITLE: **Display Assembly**

SIZE DWG. NO. **A 4** REV **1**

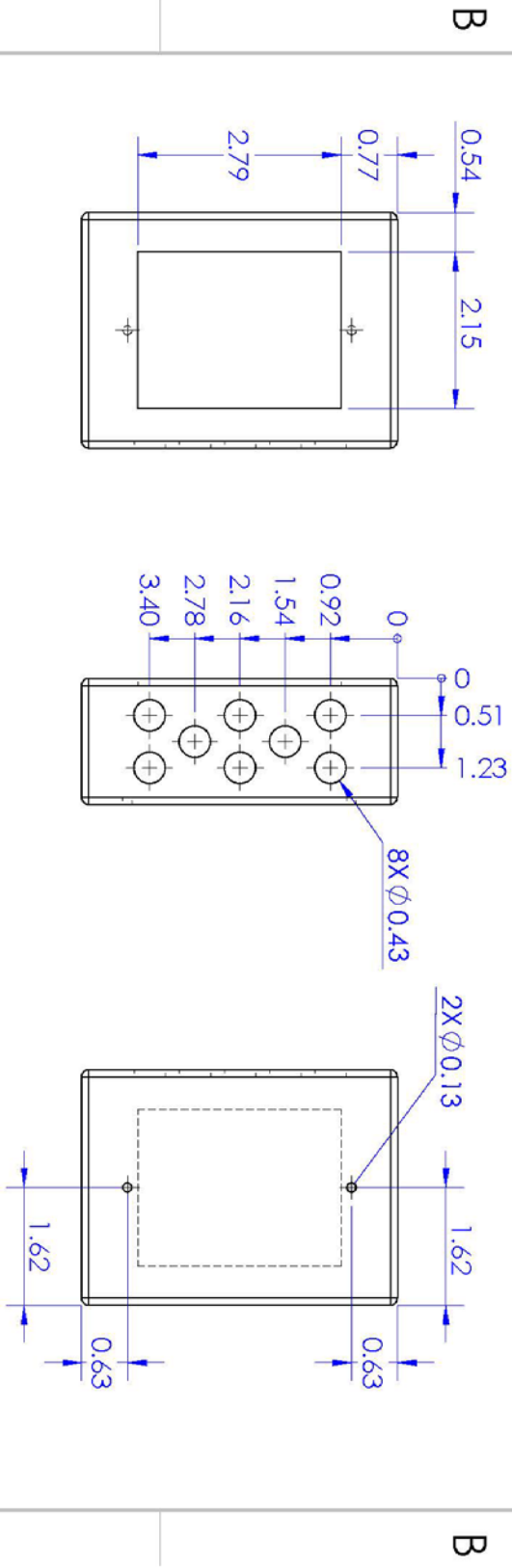
SCALE: 1:3 WEIGHT: SHEET 1 OF 1

2

1

2

1



PROPRIETARY AND CONFIDENTIAL
 THE INFORMATION CONTAINED IN THIS DRAWING IS THE SOLE PROPERTY OF DINSERT COMPANY NAME HERE. ANY REPRODUCTION IN PART OR AS A WHOLE WITHOUT THE WRITTEN PERMISSION OF DINSERT COMPANY NAME HERE IS PROHIBITED.

UNLESS OTHERWISE SPECIFIED:		DRAWN		NAME		DATE	
DIMENSIONS ARE IN INCHES		CHECKED		JIS		2/11/17	
TOLERANCES:		FRACTIONAL ±.01		ANGULAR: MACH ±1		BEND ±1	
TWO PLACE DECIMAL ±.01		THREE PLACE DECIMAL ±.001		MFG APPR.		Q.A.	
INTERPRET GEOMETRIC TOLERANCING PER:		NOTES:		1. ORIGINAL BOX FROM HAMMOND		MFG. PN HMI107-ND	
MATERIAL		ABS		FINISH		DO NOT SCALE DRAWING	
NEXT ASSY		USED ON		APPLICATION		SCALE: 1:2	
APPLICATION		WEIGHT:		SHEET 1 OF 1		REV 1	

2

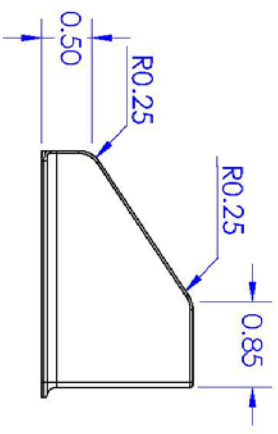
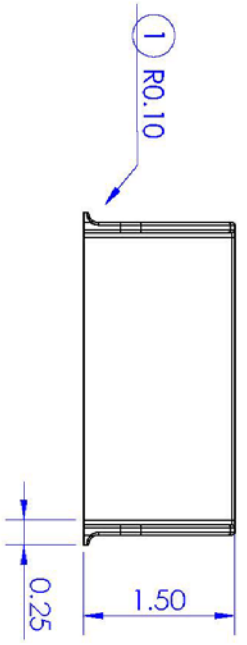
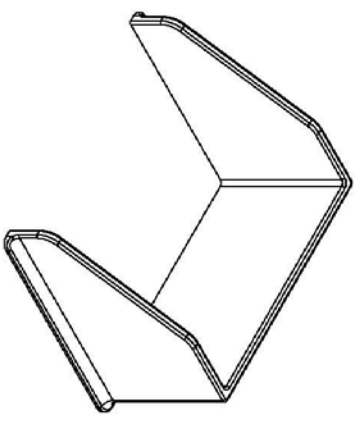
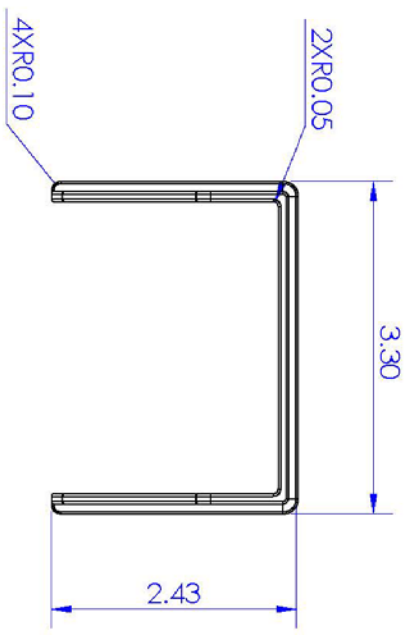
1

TITLE:
DISPLAY HOUSING

SIZE DWG. NO. **A 2**

2

1



B

B

A

A

PROPRIETARY AND CONFIDENTIAL
 THE INFORMATION CONTAINED IN THIS DRAWING IS THE SOLE PROPERTY OF DINSERT COMPANY NAME HERE. ANY REPRODUCTION IN PART OR AS A WHOLE WITHOUT THE WRITTEN PERMISSION OF DINSERT COMPANY NAME HERE IS PROHIBITED.

UNLESS OTHERWISE SPECIFIED:	
DIMENSIONS ARE IN INCHES	
TRIM FEATURE WITH THICKNESS .1	
ALL FILLETS R25	
FRACTIONAL .01	
FIND PLAN: PUNCH+1 BEND ±1	
FIND PLACE DECIMAL 5.01	
THREE PLACE DECIMAL 5.001	
MATERIAL: ABS	
FINISH	
DO NOT SCALE DRAWING	
APPLICATION	
USED ON	
NEXT ASSY	

UNLESS OTHERWISE SPECIFIED:	
DRAWN	JIS
CHECKED	
ENG APPR.	
MFG APPR.	
Q.A.	
DATE	2/11/17
NAME	

NOTES:	
① FILLET EXTENDS AROUND BORDER	
TITLE: DISPLAY SHADE	
SIZE	A
DWG. NO.	1
SCALE: 2:3	WEIGHT:
SHEET 1 OF 1	REV 1

2

1

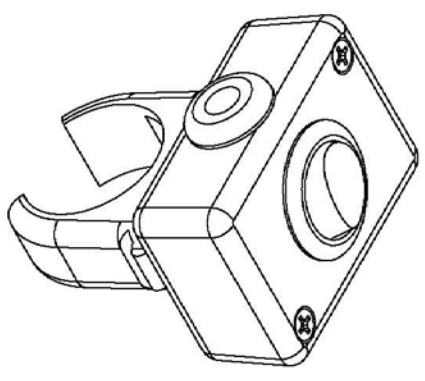
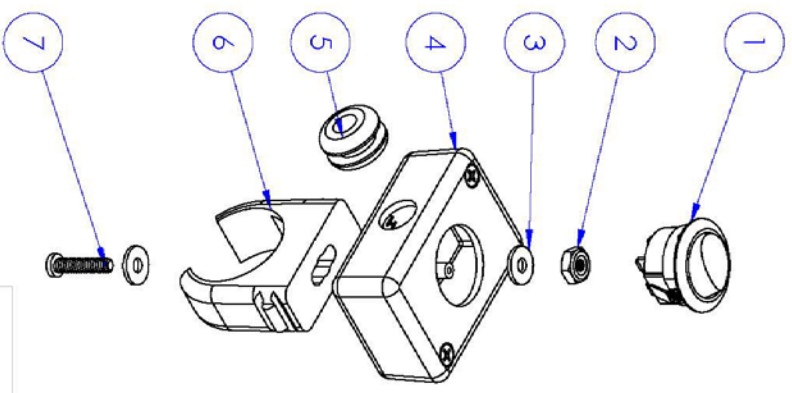
2

1

ITEM NO.	PART NUMBER	DESCRIPTION	Default/ QTY.
1	OC-MS-048	Rocker Switch	1
2	OC-MS-022	Lock nut	1
3	OC-MS-023	Washer	2
4	OC-MS-47	Plastic Box	1
5	OC-MS-051	Grommet	1
6	OC-MS-017	Plastic Clamp	1
7	OC-MS-021	Screw	1

B

B



SCALE 1:1

A

A

UNLESS OTHERWISE SPECIFIED:		NAME	DATE	TITLE: SWITCH ASSY	SIZE DWG. NO. A 5	REV 1
DIMENSIONS ARE IN INCHES		JIS	2/12/17			
TOLERANCES:		CHECKED		COMMENTS:	SCALE: 2:3	SHEET 1 OF 1
FRACTIONAL ±.01		ENGR. APPR.				
ANGULAR: MOVCH±1 BEND ±1		MFG APPR.				
TWO PLACE DECIMAL ±.01		Q.A.				
THREE PLACE DECIMAL ±.001		INTERPRET GEOMETRIC TOLERANCING PER:				
MATERIAL		FINISH				
NEXT ASSY		USED ON				
APPLICATION		DO NOT SCALE DRAWING				

PROPRIETARY AND CONFIDENTIAL
 THE INFORMATION CONTAINED IN THIS DRAWING IS THE SOLE PROPERTY OF <INSERT COMPANY NAME HERE>. ANY REPRODUCTION IN PART OR AS A WHOLE WITHOUT THE WRITTEN PERMISSION OF <INSERT COMPANY NAME HERE> IS PROHIBITED.

2

1

2

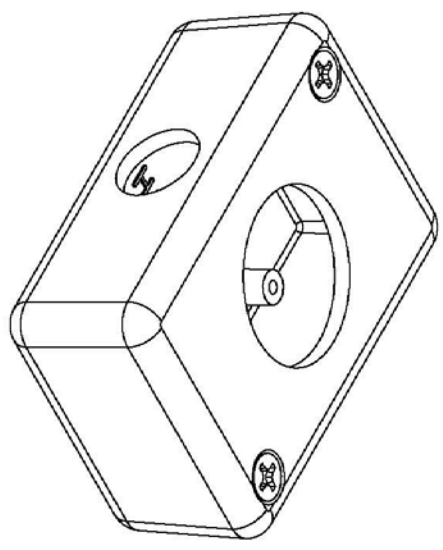
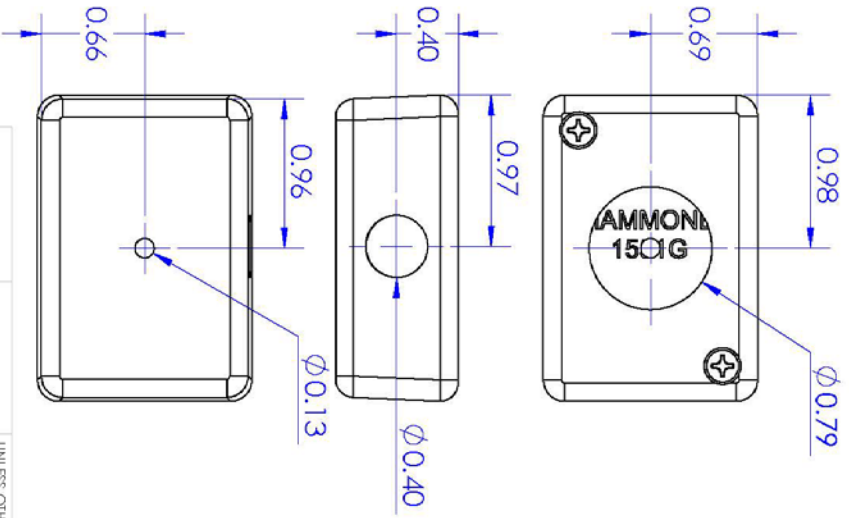
1

B

B

A

A



SCALE: 3:2

PROPRIETARY AND CONFIDENTIAL
 THE INFORMATION CONTAINED IN THIS DRAWING IS THE SOLE PROPERTY OF <INSERT COMPANY NAME HERE>. ANY REPRODUCTION IN PART OR AS A WHOLE WITHOUT THE WRITTEN PERMISSION OF <INSERT COMPANY NAME HERE> IS PROHIBITED.

UNLESS OTHERWISE SPECIFIED:		DRAWN		NAME	DATE	TITLE: SWITCH HOUSING
DIMENSIONS ARE IN INCHES		CHECKED		JJS	2/11/17	
TOLERANCES:		FRACTIONAL ±.01		ENG APPR.		SIZE DWG. NO. A 3
ANGULAR ±.0001		BEND ±1		MFG APPR.		REV 1
TWO PLACE DECIMAL ±.01		THREE PLACE DECIMAL ±.001		G.A.		SCALE: 1:1 WEIGHT: SHEET 1 OF 1
INTERPRET GEOMETRIC TOLERANCING PER:		NOTES:		1. ORIGINAL BOX FROM HAMMOND		
MATERIAL ABS		MFG. P/N HM827-6-ND		2. HIDDEN LINES OMITTED		
FINISH		APPLICATION		USED ON		
DO NOT SCALE DRAWING		NEXT ASSY				

2

1

Appendix M: Hydraulic Components

10/28/2016

Bladder Accumulator - High Pressure (UK Series) | Parker NA

BLADDER ACCUMULATOR - HIGH PRESSURE (UK SERIES)

[Email](#) [Print](#)



Click to Zoom



The Parker UK Series is a high pressure range of bladder accumulator ideally suited for the UK Industrial market (207 to 420 bar/ up to 54L).

PART NUMBER:

01100A-00-341

VOLUME (LITERS):

1

WHERE TO BUY

RESET ATTRIBUTES

PRODUCT OVERVIEW

-

TECH SPECIFICATIONS

+

[Print Tech Specifications](#)

PERFORMANCE CHARACTERISTICS

SERIES

UK Series

TYPE

207 bar to 420 bar range

BODY MATERIAL

Carbon Steel Shell

MAXIMUM OPERATING PRESSURE (BAR)

345

VALVE SIZE (INCH)

G 1/4"

PORT CONNECTION

3/4 BSPF

MAXIMUM FLOW RATE (LPM)

109

<http://ph.parker.com/us/en/high-pressure-bladder-accumulator-uk-high-pressure-bladder-accumulator-uk-1/01100a-00-341>

1/2

10/28/2016

Bladder Accumulator - High Pressure (UK Series) | Parker NA

ELASTOMER MATERIAL

Standard NBR (Nitrile) bladder

CERTIFICATES

Lloyd's/CE

MINIMUM OPERATING TEMPERATURE (C)

-15

MAXIMUM OPERATING TEMPERATURE (C)

80

WEIGHT (KG)

5.7

HEIGHT (MM)

292

MARKETS

Industrial

ACCESSORIES

Brackets & Clamps

Print Tech Specifications

PRODUCT SUPPORT

CONTACT US

Accumulator and Cooler Division Europe
Parker Hannifin Manufacturing France
Etablissement de Colombes
16 Rue de Seine
92700 Colombes
FRANCE

Phone
+33 (0)141 191 700

EMAIL PARKER

Parker Hannifin

Products

Investors

Careers

About Us

Community

Global Operations

Divisions

Worldwide Locations

ParkerStore™ Network

Sales Companies

Distribution Network

Company Information

News Room

Working with Parker

History

Event Calendar

Products Brand

<http://ph.parker.com/us/en/high-pressure-bladder-accumulator-uk-high-pressure-bladder-accumulator-uk-1/01100a-00-341>

2/2

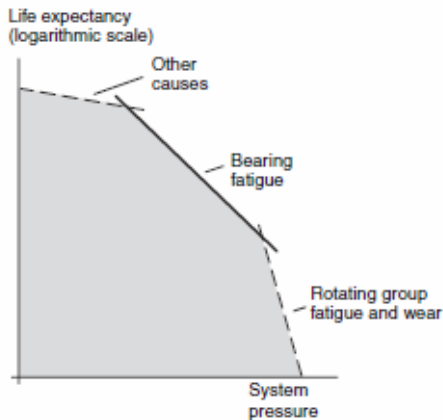
Bearing life

General information

Bearing life can be calculated for that part of the load/life curve (shown below) that is designated 'Bearing fatigue'. 'Rotating group fatigue and wear' and 'Other' caused by material fatigue, fluid contamination, etc. should also be taken into consideration when estimating the service life of a motor/pump in a specific application.

Bearing life calculations are mainly used when comparing different frame sizes. Bearing life, designated B_{10} (or L_{10}), is dependent of system pressure, operating speed, external shaft loads, fluid viscosity in the case and fluid contamination level.

The B_{10} value means that 90% of the bearings survive, at a minimum, the number of hours calculated. Statistically, 50% of the bearings will survive at least five times the B_{10} life.



Hydraulic unit life versus system pressure.

Bearing life calculation

An application is usually governed by a certain duty or work cycle where pressure and speed vary with time during the cycle.

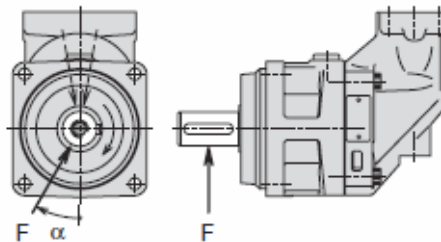
In addition, bearing life depends on external shaft forces, fluid viscosity in the case and fluid contamination.

Parker Hannifin (Mobile Controls Division) has a computer program for calculating bearing life and will assist in determining F11 or F12 motor/pump life in a specific application.

Required information

When requesting a bearing life calculation from Parker Hannifin (Mobile Controls Division), the following information (where applicable) should be provided:

- A short presentation of the application
- F11 or F12 size and version
- Duty cycle (pressure and speed versus time at given displacements)
- Low system pressure
- Case fluid viscosity
- Life probability (B_{10} , B_{20} , etc.)
- Operating mode (pump or motor)
- Direction of rotation (L or R)
- External shaft loads
- Fixed or rotating radial load
- Distance between flange and radial load
- Angle of attack (α) as defined below



The direction (a) of the radial load is positive in the direction of rotation as shown.

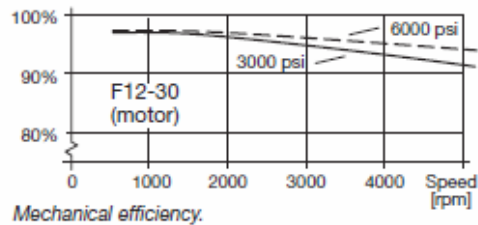
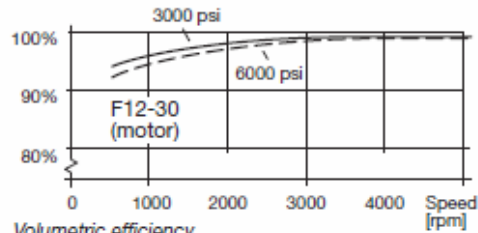
To obtain maximum bearing life, the radial load should, in most cases, be located approximately at 170° (motor; R.H. rot'n) or 190° (pump; R.H. rot'n).

Efficiency

Because of its high overall efficiency, driving a motor/pump from series F11/F12 requires less fuel or electric power. Also, it allows the use of a small reservoir and heat exchanger, which in turn reduce cost, weight, and installation size.

The diagrams to the right shows volumetric and mechanical efficiencies of an F12-30.

Contact Parker Hannifin for efficiency information on a particular F11/F12 frame size that is being considered.



Noise level

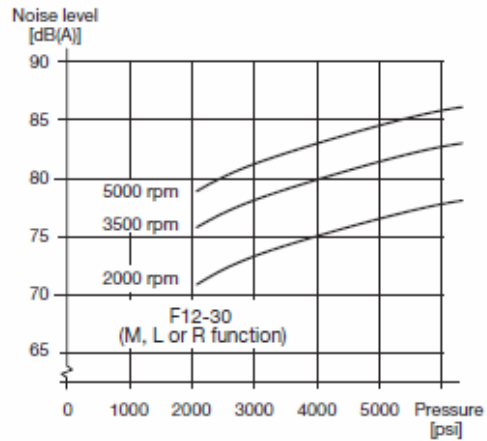
Series F11/F12 feature low noise levels from low to high speeds and pressures.

As an example, the diagram to the right shows the noise level of an F12-30.

The noise level is measured in a semi-anechoic room, 1 m behind the unit.

The noise level for a particular motor/pump may vary ± 2 dB(A) compared to what is shown in the diagram.

NOTE: Noise information for F11/F12 frame sizes are available from Parker Hannifin.



Selfpriming speed and required inlet pressure

Series F11

In pump applications, the F11 with function **L** (counter clockwise rotation) or **R** (clockwise rotation) is normally used. The **L** and **R** (pump) provide the highest self-priming speeds (see table) as well as the lowest noise level. The **M** (motor) function can also be used as a pump, in either direction, but at a lower selfpriming speed.

Operating above the selfpriming speed (refer to Diagram 1) requires increased inlet pressure.

As an example, at least 1.0 bar is needed when operating the F11-19-M as a pump at 3500 rpm. An F11 with **H** function, used as a motor (e.g. in a hydrostatic transmission), may sometimes operate as a pump at speeds above the selfpriming speed; this requires additional inlet pressure.

Insufficient inlet pressure can cause pump cavitation resulting in greatly increased pump noise and deteriorating performance.

Function	L or R	M	H
F11-5	4600	3800	3200
F11-10	4200	3100	2700
F11-14	3900	-	3200
F11-19	3500	2400	2100
F11-150	1700	1300	1100
F11-250	1500	950	-

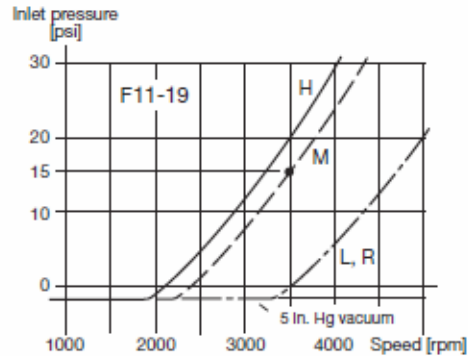
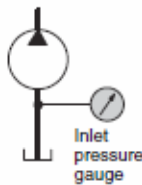


Diagram 1. Min required inlet pressure (F11-19).

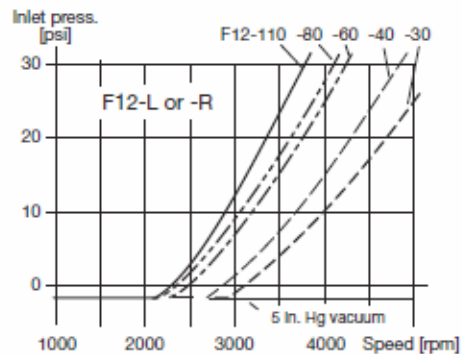


Diagram 2. Min. required pump (F12-L or -R) inlet press.

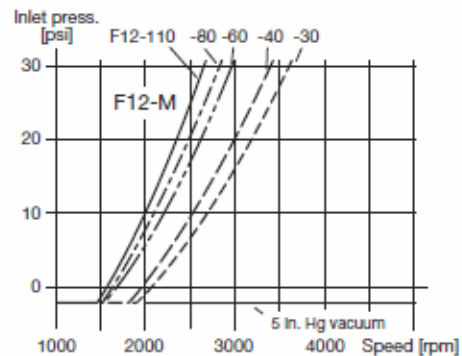
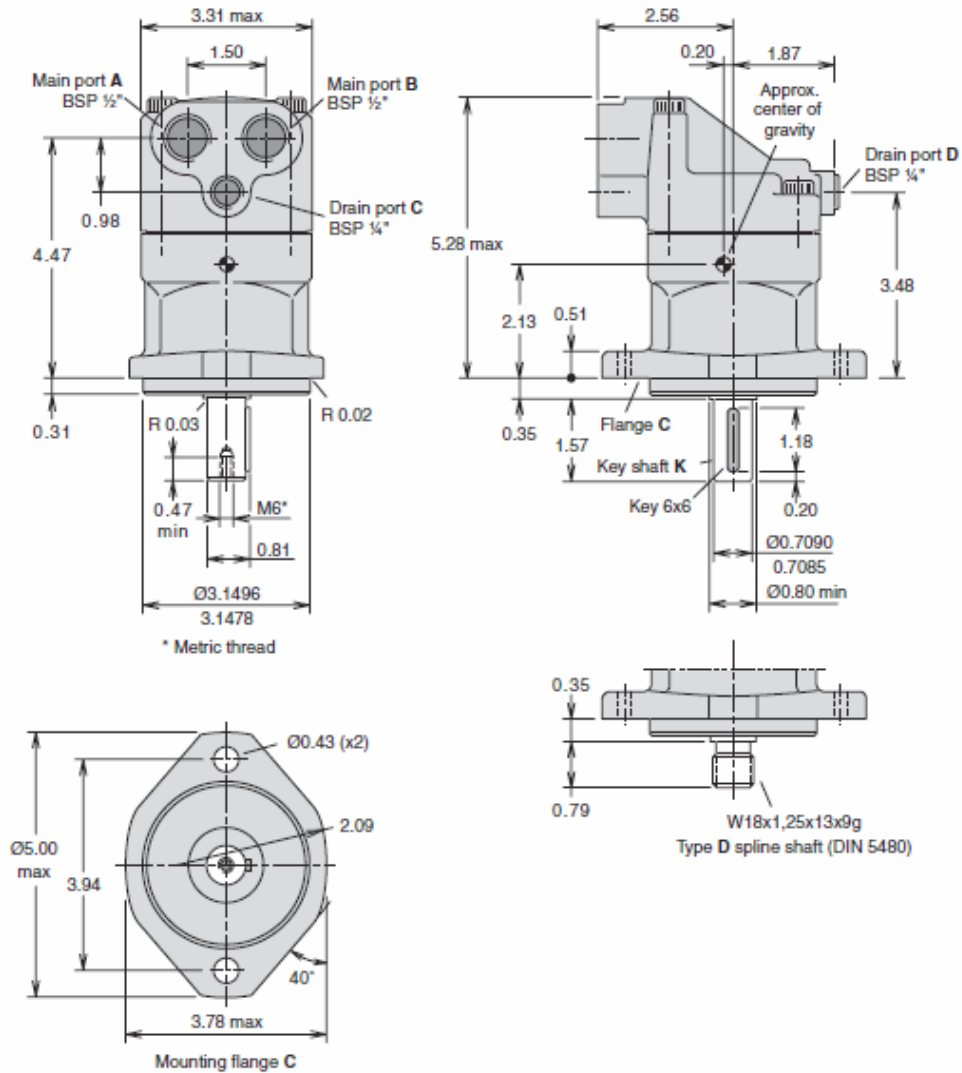


Diagram 3. Min. required motor (F12-M) inlet pressure.

NOTE: Diagrams 1, 2 and 3 are valid at sea level.

F11-5
 (CETOP versions)



2 WAY POPPET TYPE SOLENOID VALVE

[Email](#) [Print](#)



Hydraulic Solenoid Valves are used to electrically direct hydraulic fluid to and from an actuator by shifting a spool or poppet within the valve. These valves can be 2, 3, 4, or even 5 way valves shifted by either one or two electronic coils.

PART NUMBER:
DSH121N

RATED FLOW (GPM):
24

MAXIMUM INLET PRESSURE (PSI):
5000

TYPE/CONFIGURATION:
Normally Open

FREE REVERSE FLOW:
No

RESPONSE TIME (MS):
70

OVERRIDE:
N/A

ADJUSTMENT TYPE:
N/A

SEAL MATERIAL:
Nitrile

WIRE SCREEN:
N/A

WHERE TO BUY

[RESET ATTRIBUTES](#)

PRODUCT OVERVIEW	-
TECH SPECIFICATIONS	+

[Print Tech Specifications](#)

PERFORMANCE CHARACTERISTICS

10/28/2016

2 Way Poppet Type Solenoid Valve | Parker NA

FLOW DIRECTION
Side to Nose (2-1)

RATED FLOW (GPM)
24

RATED FLOW (LPM)
90

MAXIMUM INLET PRESSURE (PSI)
5000

MAXIMUM INLET PRESSURE (BAR)
350

TYPE/CONFIGURATION
Normally Open

FREE REVERSE FLOW
No

LEAK RATE (DPM)
5

CAVITY SIZE
C12-2

OVERRIDE
N/A

ADJUSTMENT TYPE
N/A

RESPONSE TIME (MS)
70

WIRE SCREEN
N/A

MINIMUM OPERATING VOLTAGE
85% of rated voltage at 72°F (20°C)

SEAL MATERIAL
Nitrile

OPERATING TEMPERATURE (F)
-30° to +250°

OPERATING TEMPERATURE (C)
-34° to +121°

VALVE MATERIALS
All parts steel. All operating parts hardened steel

RATED FLUID VISCOSITY (cSt)
Mineral-based or synthetic with lubricating properties at viscosities of 45-2000 SSU (5 to 420 cSt)

FILTRATION RATINGS
ISO 4406:1999 Code 18/15/13

WEIGHT (LB)
0.65

WEIGHT (KG)
0.29

INSTALLATION TORQUE (LBS/FT)
92-96



INSTALLATION TORQUE (NM)
125-131

COIL NUT TORQUE (LBS/FT)

<http://ph.parker.com/us/en/2-way-poppet-type-solenoid-valve/dsh121n>

22

Appendix N: Mechatronics Power Supplies

Component	Mfg.	Qty	V_expected [V]	I_expected [A]	P_expected [W]	V_rated [V]	I_rated [A]	P_rated [W]	Datasheet(s)					
Hall Effect Sensor	Sparkfun	2	5	0.005	0.025		28	0.05	1.4 Sparkfun link					
Pressure Transducer	Gems	1	6.5	0.006	0.039	-	-	-	Gems link					
Arduino Uno	Arduino	1	7	0.046	0.322		20	0.5	10 Arduino link					
LCD Shield	Robotshop	1	3.3	0.12	0.396		3.3	0.16	0.528 Sparkfun link					
Solenoid	Parker	2	12	0.3415	8.196		12	2.33	28 Parker link					
Expected power requirements														
Solenoid power supply					Arduino power supply									
Voltage		12 V		Voltage		7 V								
Current		0.683 A		Current		0.177 A								
Power		8.196 W		Power		0.782 W								
Ideal continuous operating time		8 hrs		Ideal continuous operating time		48 hrs								
Power needed		5.464 Ah		Power needed		5.36 Ah								
Suitable power supplies:					Suitable power supply:									
12V Lithium Ion Rechargeable Battery					Energizer E91 (5 in series)									
Specs					Specs									
										Voltage: 12 V				
										Power: 4.5 Ah				
										Max current draw: likely > 4.5A				
										Price: \$69.18				
Super Circuits Link					Batteries.com link									

Appendix O: Clutch Analysis

Assumptions

1. No clutch slipping (rigid connection).
2. Uniform force distribution across pad due to friction. Choose $F = T/r_{\max}$.
3. Zero angular acceleration.
4. Static loading.

Material Properties

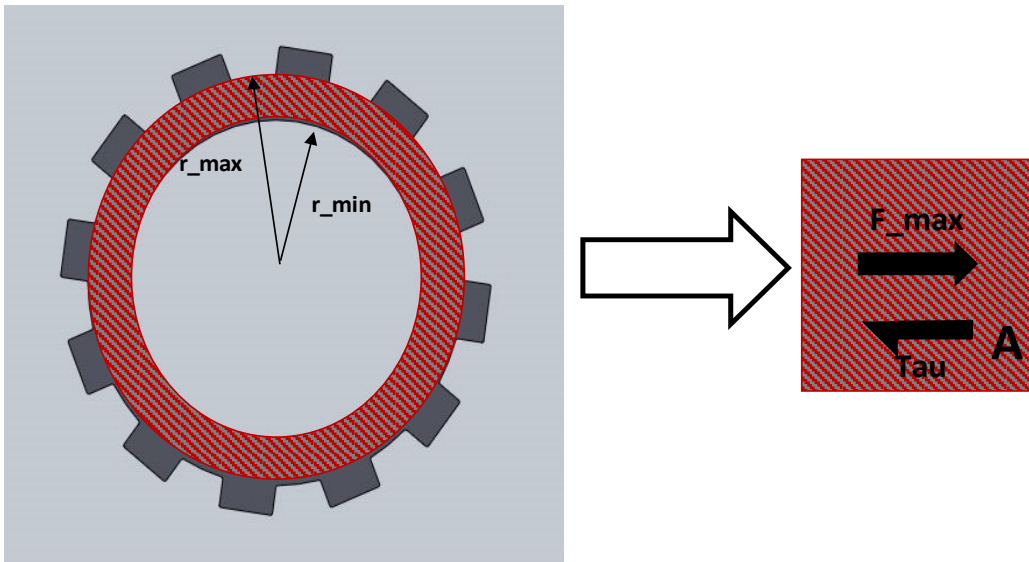
Material	Al 6061
Shearing strength	207 [Mpa]

Input Parameters

Max contact radius, r_{\max}	0.1016 [m]
Min contact radius, r_{\min}	0.0889 [m]
Max Torque, T	370 [Nm]

Calculated Values

Pad area, A	0.007601 [m ²]
Force, F_{\max}	3641.732 N
Max shearing stress, Tau	479.1367 Kpa
Factor of safety	432.027



Assumptions

1. Static loading
2. Uniform shearing stress distribution
3. Equal loading among teeth
4. Zero angular acceleration

Material Properties

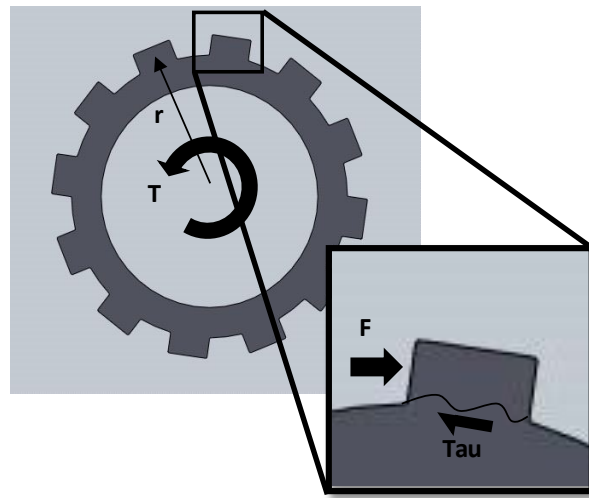
Material Al 6061
Shearing strength 207 [Mpa]

Input Parameters

Num teeth (single pad) 12
Num pads 2
Outer diameter 0.1016 [m]
Inner diameter 0.0889 [m]
Max torque, T 370 [Nm]

Calculated Values

Effective radius, r 0.047625 [m]
Force per tooth, F 323.709536 [N]
Shearing area, A (not show) 4.0323E-05 [m²]
Shearing stress, Tau 8.02801256 [Mpa]
Factor of safety 25.784713



Appendix P: Patterson Control Model

Patterson Control Model (PCM)

Inputs					
A	1.080	m	T	0.043	m
h	0.943	m	K1	5.526	
Rh	0.673	m	K2	0.238	0.623
kx	0.368	m	K3	0.000667	m/N
m	127	kg	K4	0.396	
B	0.421	m	g	9.81	m/s ²
β	17.0	deg.	lw	0.117	kg m ²
R	0.300	m	mw	1.3	kg
e	0.047	m		1%	

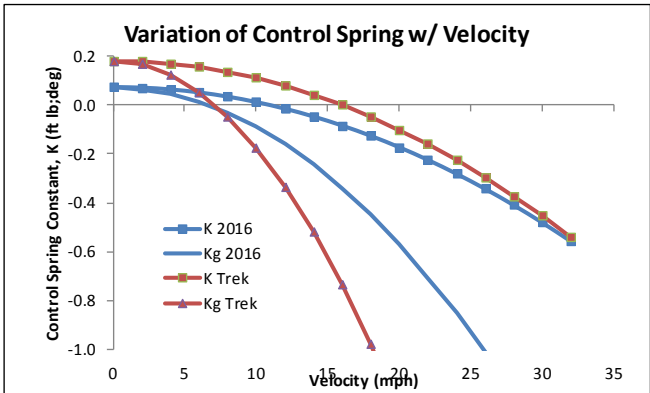
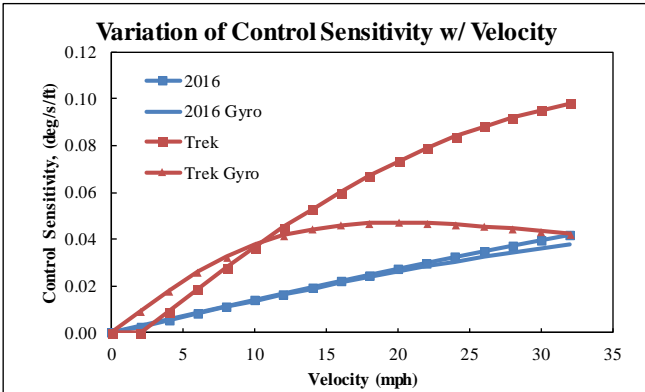
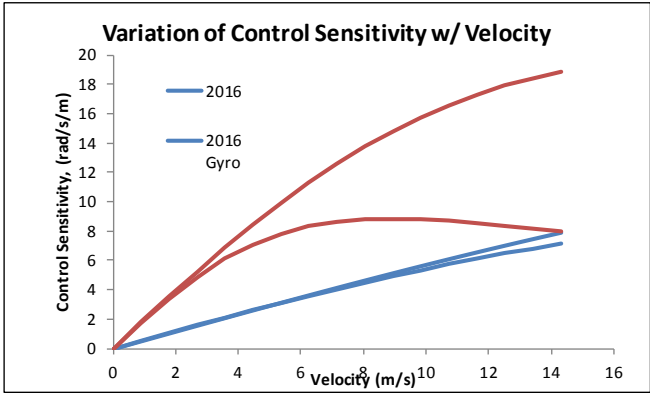
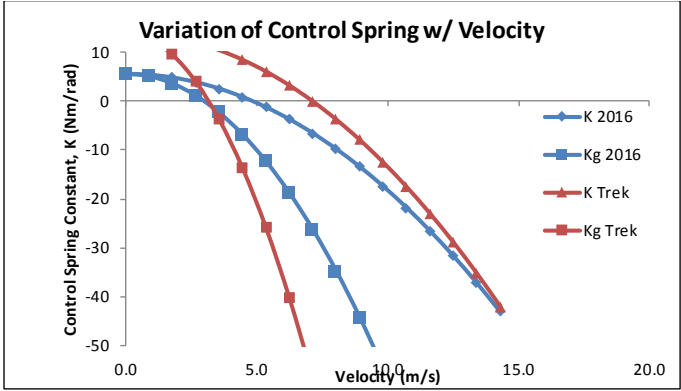
K2g 162% K2g change

Inputs (Safety Bike)					
A	1	m	B	0.4	m
h	1.2	m	β	18	deg.
Rh	0.3	m	R	0.3	m
kx	0.36	m	e	0.025	m
m	100	kg	g	9.81	m/s ²

V		K		Kg		θ dot/int		θ dot/int, gyro	
mph	m/s	Nm/rad	ftlb/deg	Nm/rad	ftlb/deg	rad/s/m	deg/s/ft	rad/s/m	deg/s/ft
0	0.0	5.5	0.071	5.5	0.071	0.0	0.000	0.0	0.000
2	0.9	5.3	0.069	5.0	0.065	0.5	0.003	0.5	0.003
4	1.8	4.8	0.061	3.5	0.046	1.1	0.006	1.1	0.006
6	2.7	3.8	0.049	1.0	0.013	1.6	0.008	1.6	0.008
8	3.6	2.5	0.032	-2.4	-0.031	2.1	0.011	2.1	0.011
10	4.5	0.8	0.010	-6.9	-0.089	2.6	0.014	2.6	0.014
12	5.4	-1.3	-0.017	-12.4	-0.160	3.1	0.017	3.1	0.016
14	6.3	-3.8	-0.049	-18.9	-0.243	3.7	0.019	3.6	0.019
16	7.2	-6.6	-0.085	-26.3	-0.339	4.2	0.022	4.0	0.022
18	8.0	-9.9	-0.127	-34.8	-0.448	4.7	0.025	4.5	0.024
20	8.9	-13.5	-0.173	-44.3	-0.570	5.2	0.027	4.9	0.026
22	9.8	-17.4	-0.225	-54.7	-0.704	5.6	0.030	5.3	0.028
24	10.7	-21.8	-0.281	-66.2	-0.852	6.1	0.033	5.7	0.031
26	11.6	-26.6	-0.342	-78.6	-1.012	6.6	0.035	6.1	0.033
28	12.5	-31.7	-0.408	-92.0	-1.185	7.0	0.037	6.5	0.034
30	13.4	-37.2	-0.479	-106.5	-1.371	7.5	0.040	6.8	0.036
32	14.3	-43.1	-0.554	-121.9	-1.569	7.9	0.042	7.1	0.038

Fork Flop:	29.6	0.382
-------------------	------	-------

Vcrit	4.8	m/s	3.0	m/s
	10.8	mph	6.7	mph



Trek									
V		K		Kg		θdot/int		θdot/int, gyro	
mph	m/s	Nm/rad	ftlb/deg	Nm/rad	ftlb/deg	rad/s/r	deg/s/ft	rad/s/m	deg/s/ft
0.0	0.0	14.0	0.179662	13.95696	0.179662	0	0	0	0
2.0	0.9	13.7	0.176849	12.84979	0.16541	1.77	0.009439	1.760251213	0.009363
4.0	1.8	13.1	0.168412	9.528286	0.122654	3.53	0.018765	3.418164063	0.018182
6.0	2.7	12.0	0.15435	3.992447	0.051393	5.24	0.027873	4.890316386	0.026012
8.0	3.6	10.5	0.134662	-3.75773	-0.04837	6.89	0.036663	6.124221988	0.032575
10.0	4.5	8.5	0.10935	-13.7222	-0.17664	8.47	0.045047	7.10055545	0.037769
12.0	5.4	6.1	0.078413	-25.9011	-0.33341	9.96	0.052952	7.827426478	0.041635
14.0	6.3	3.3	0.041851	-40.2943	-0.51869	11.3	0.060322	8.330955086	0.044313
16.0	7.2	0.0	-0.00034	-56.9018	-0.73247	12.6	0.067114	8.64600107	0.045989
18.0	8.0	-3.7	-0.04815	-75.7236	-0.97476	13.8	0.073305	8.809142535	0.046857
20.0	8.9	-7.9	-0.10158	-96.7598	-1.24555	14.8	0.078882	8.854356486	0.047097
22.0	9.8	-12.5	-0.16065	-120.01	-1.54484	15.8	0.083849	8.810936886	0.046866
24.0	10.7	-17.5	-0.22533	-145.475	-1.87264	16.6	0.088218	8.702914933	0.046292
26.0	11.6	-23.0	-0.29565	-173.154	-2.22894	17.3	0.092013	8.549327385	0.045475
28.0	12.5	-28.9	-0.37158	-203.048	-2.61375	17.9	0.095261	8.364872475	0.044494
30	13.41055	-35.2023	-0.45314	-235.156	-3.02706	18.4	0.097998	8.160675943	0.043408
32	14.30458	-41.9753	-0.54033	-269.478	-3.46887	18.8	0.10026	7.945022376	0.04226

Current Bike									
V		K		Kg		θdot/int		θdot/int, gyro	
mph	m/s	Nm/rad	ftlb/deg	Nm/rad	ftlb/deg	rad/s/r	deg/s/ft	rad/s/m	deg/s/ft
0	0	8.36401	0.107666	8.36401	0.107666	0	0	0	0
2	0.894036	8.067423	0.103848	7.326652	0.094313	0.83	0.004419	0.829939425	0.004415
4	1.788073	7.177661	0.092395	4.214577	0.054252	1.66	0.008827	1.652230356	0.008788
6	2.682109	5.694725	0.073306	-0.97221	-0.01251	2.48	0.013212	2.459457462	0.013082
8	3.576145	3.618615	0.046581	-8.23372	-0.10599	3.3	0.017561	3.244656971	0.017259
10	4.470182	0.949329	0.01222	-17.5699	-0.22617	4.11	0.021865	4.001507111	0.021284
12	5.364218	-2.31313	-0.02978	-28.9809	-0.37306	4.91	0.026113	4.724480309	0.02513
14	6.258255	-6.16876	-0.07941	-42.4665	-0.54665	5.7	0.030294	5.408950679	0.028771
16	7.152291	-10.6176	-0.13668	-58.0269	-0.74696	6.47	0.034398	6.051254384	0.032187
18	8.046327	-15.6596	-0.20158	-75.662	-0.97396	7.22	0.038417	6.648704391	0.035365
20	8.940364	-21.2947	-0.27412	-95.3718	-1.22768	7.96	0.042343	7.199564349	0.038295
22	9.8344	-27.523	-0.35429	-117.156	-1.5081	8.68	0.046167	7.702988587	0.040973
24	10.72844	-34.3446	-0.4421	-141.016	-1.81523	9.38	0.049882	8.158936532	0.043398
26	11.62247	-41.7592	-0.53755	-166.95	-2.14907	10.1	0.053484	8.568070116	0.045575
28	12.51651	-49.7671	-0.64063	-194.958	-2.50961	10.7	0.056966	8.931642244	0.047508
30	13.41055	-58.3681	-0.75135	-225.042	-2.89686	11.3	0.060323	9.251383352	0.049209
32	14.30458	-67.5623	-0.8697	-257.2	-3.31082	11.9	0.063553	9.529391694	0.050688

Bike Name		Configuration 0		
Rider Name		Fryer		
		2016 Bike	Trek FX3	
Wheelbase (A)	in.	42.50	42.50	41.89
Steering Axis Incl. (β)	deg.	17.00	17.00	22.50
Front Axle Offset (e)	in.	1.84	1.84	1.77
Road Trail, Meas. (T)	in.	2.50	2.50	2.44
Handlebar Radius (r_h)	in.	26.50	26.50	11.31
Front Wheel Radius (r_f)	in.	13.63	13.63	14.00
Rear Wheel Radius (r_r)	in.	13.63	13.63	14.00
		Anthony + frame + components	Anthony + frame	Anthony + Trek FX3
Weight Front, Level	lbf	109.20	109.20	97.80
Weight Rear, Level	lbf	170.60	170.60	123.80
Weight Front, Inclined	lbf	143.00	143.00	126.40
Weight Rear, Inclined	lbf	143.00	143.00	97.80
Dist. Between Scales (X)	in.			
Swing Time, 10 Osc.	s	20.37	20.37	20.10

Notes:		X not measured, uncertainty on inclined weight much greater than 0.5lb of scale
--------	--	---

Box Height	8.38	in.
------------	------	-----

Swing		
lo swing	33.91	slug ft2
r swing pivot to swing c.g.	3.692	ft
r pivot to rail	5.375	ft
W swing	63.5	lb

Calculated Values		
W_T , level	lbf	279.80
W_T , Inclined	lbf	286.00
B	in.	25.91
%F		61%
Trail, Calculated		2.2
Hyp	in.	42.50
X	in.	42.22
hcg/ra	in.	23.51
hcg	in.	37.14

MOI Calculation		
T, 1 period	s	2.04
r cg total wrt pivot	ft	2.54
I total	slug ft2	91.7
mr2		45.17
I bike/rider	slug ft2	12.65
	kg m2	17.15
kx	ft	1.21
	m	0.37

PCM Entry		
A	m	1.080
h	m	0.943
Rh	m	0.673
kx	m	0.368
m	kg	127
B	m	0.421
β	deg.	17.0
R	m	0.30
e	m	0.047

0.366	linked to "Components" sheet
127.37	linked to "Components" sheet
0.435	linked to "Components" sheet

Component Name	Mass [kg]	Coordinates [cm]			Distance from cg [cm]			(distance from x_cg) ² [m ²]
		X	y	z	x	y	z	
Frame + wheels + Anthony	100.24383	47.6	0	101.2698	4.094	0.302	11.2843093	0.012742662
Accumulator	8.4368112	18	13.5	55.5	-25.506	13.802	-34.4854907	0.137973429
Pump	5.1709488	49	-1	61	5.494	-0.698	-28.9854907	0.084064638
Motor	5.1709488	0	-22	44	-43.506	-21.698	-45.9854907	0.258548426
Planetary gearbox	1.814368	49	0	49	5.494	0.302	-40.9854907	0.167990144
Crank + bevel assembly	5.6245408	49	-4	30	5.494	-3.698	-59.9854907	0.361193698
Clutch housing	0.907184	0	-12	45	-43.506	-11.698	-44.9854907	0.216054605
Clutch assembly	0		0	0	-43.506	0.302	-89.9854907	0.809747953
Reservoir	0		0	0	-43.506	0.302	-89.9854907	0.809747953

"Frame + wheels + rider" Data			
<i>From BPL_MOI_Calc</i>			
hcg =	1.012698		m
I_xcg =	10.35		kg*m ²
<i>Calculated</i>			
d =	0.1128431		m
I_xcg + m*d ² =	11.626461		kg*m ²

Results					
Total mass =	127.369	kg			
Center of gravity =	(43.506	,	-0.302	,	89.985) cm
ROG about x_cg (kx) =	0.366	m			

Notes:

1. Spreadsheet assumes all components as point masses in cg and I calculations, except for "frame + wheels + rider" whose I_xcg is found using parallel axis theorem on the value derived in the "BPL_MOI_Calc" sheet.

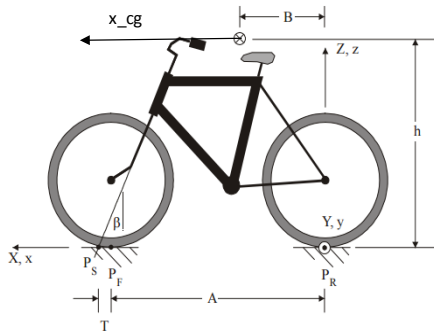


Figure showing coordinate axes (among other variables). Adapted from "Model of a Bicycle from Handling Qualities Considerations".

Bare Frame (seat low)			
	Back Scale [lb]	Front Scale [lb]	SUM
Flat	19.8	11.2	31
Cinder Block Front (8.375")			
Cinder Block Rear (8.375")	19	12.4	31.4
Time for 10 oscillations	22.97 [s]		

Frame and Rider (seat low)			
	Back Scale [lb]	Front Scale [lb]	SUM
Flat	123.8	97.8	221.6
Cinder Block Rear (8.375")	97.8	126.4	224.2
Time for 10 oscillations	20.10 [s]		

Configuration 1* (seat high)			
	Back Scale [lb]	Front Scale [lb]	SUM
Flat	66.4	28	94.4
Cinder Block Rear (8.375")	63.2	30	93.2
Time for 10 oscillations	22.45 [s]		

Configuration 1* and Rider (seat high)			
	Back Scale [lb]	Front Scale [lb]	SUM
Flat	176.4	107.8	284.2
Cinder Block Rear (8.375")	138.2	145.2	283.4
Time for 10 oscillations	20.64 [s]		

Configuration 1* and Rider (seat low)			
	Back Scale [lb]	Front Scale [lb]	SUM
Flat	170.6	109.2	279.8
Cinder Block Front (8.37")	196.6	92.6	289.2
Cinder Block Rear (8.375")	143	143	286
Time for 10 oscillations	20.37 [s]		

Trek FX 3 (22.5" size) and Rider			
	Back Scale [lb]	Front Scale [lb]	SUM
Flat	130.2	81.2	211.4
Cinder Block Front (8.37")	155.2	53.2	208.4
Cinder Block Rear (8.375")	101.6	114.2	215.8
Time for 10 oscillations	20.01 [s]		

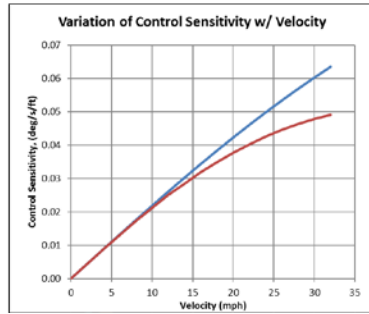
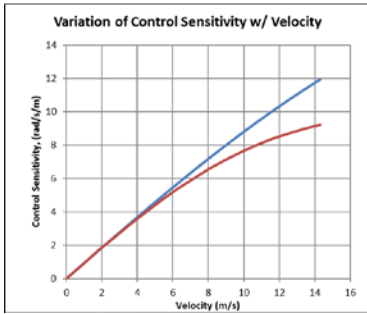
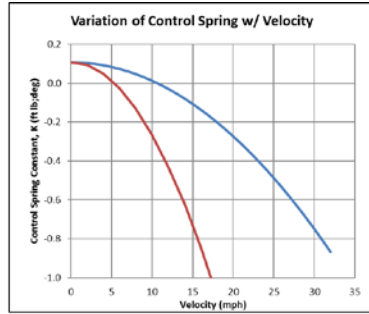
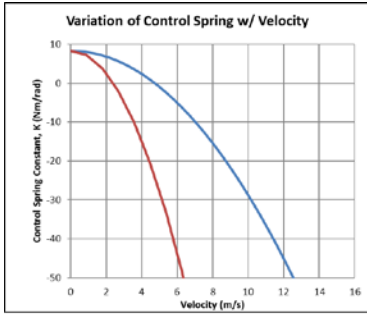
Component Weight	
Component	Weight [lbf]
Crank + Bevel Assbly	12.4
Pump + Plan gear	15.4
Motor	11.4
Accumulator	18.6
Clutch + Gear + Housing	12.6
Lines + Reservoir	15.2
Clutch housing alone	2.0

Bike Geometry		
Wheelbase (A)	42.50	[in]
Steering Axis Incl. (β)	17.00	[deg]
Front Axle Offset (e)	1.84	[in]
Road Trail, Meas. (T)	-	[in]
Handlebar Radius (r_h)	26.50	[in]
Front Wheel Radius (r_f)	13.63	[in]
Rear Wheel Radius (r_r)	13.63	[in]
Fork Height	28.25	[in]

*Configuration 1 = frame + motors + clutch housing + planetary gear assy + accum. + crank assy arranged as on the 2016 bike

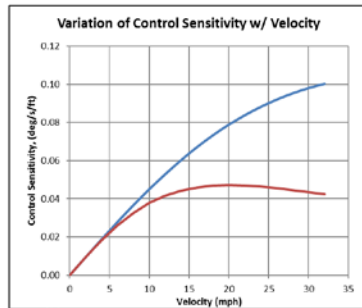
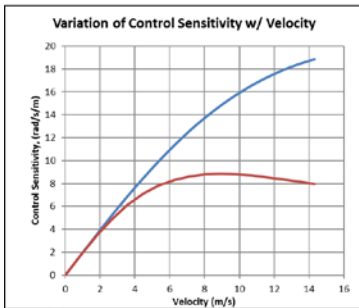
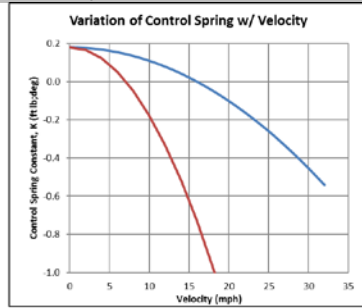
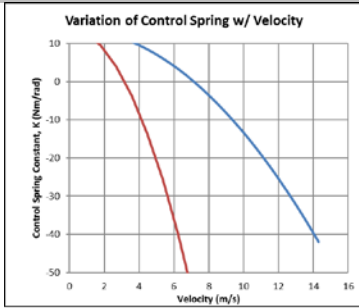


Configuration 1 + Anthony



Important Quantities				
	K		Kg	
Fork Flop:	46.309		0.596	
Vcrit:	4.732	m/s	2.406	m/s
	10.586	mph	5.382	mph

Trek FX3 + Anthony



Important Quantities				
	K		Kg	
Fork Flop:	141.07		1.82	
Vcrit:	7.10	m/s	3.17	m/s
	15.99	mph	7.10	mph

Appendix Q: Keyway Analysis

SHAFT Keys and Keyways

Shaft diameter d	19.1	mm
Shaft torque T	200	Nm
Key length L	12.7	mm

key width b	6	mm
key height h	6	mm
keyway depth shaft t_1	3.5	mm
keyway depth hub t_2	2.8	mm
shear force $F_s = T/(d/2)$	20.94	kN
shear stress key $\tau = F_s / (L \cdot b)$	274.83	MPa
bearing pressure $p = F_s / (h \cdot d/2)$	549.67	MPa
Nominal torsional stress $\tau = T / (\pi/16 \cdot d^3)$, $d_k = d - t_1$	268.3	MPa

Key dimensions: Parallel keys are most commonly used. The key and key seat cross section are ISO standardized. The key length should be less than about 1.5 times the shaft diameter to ensure a good load distribution over the entire key length when the shaft becomes twisted when loaded in torsion.

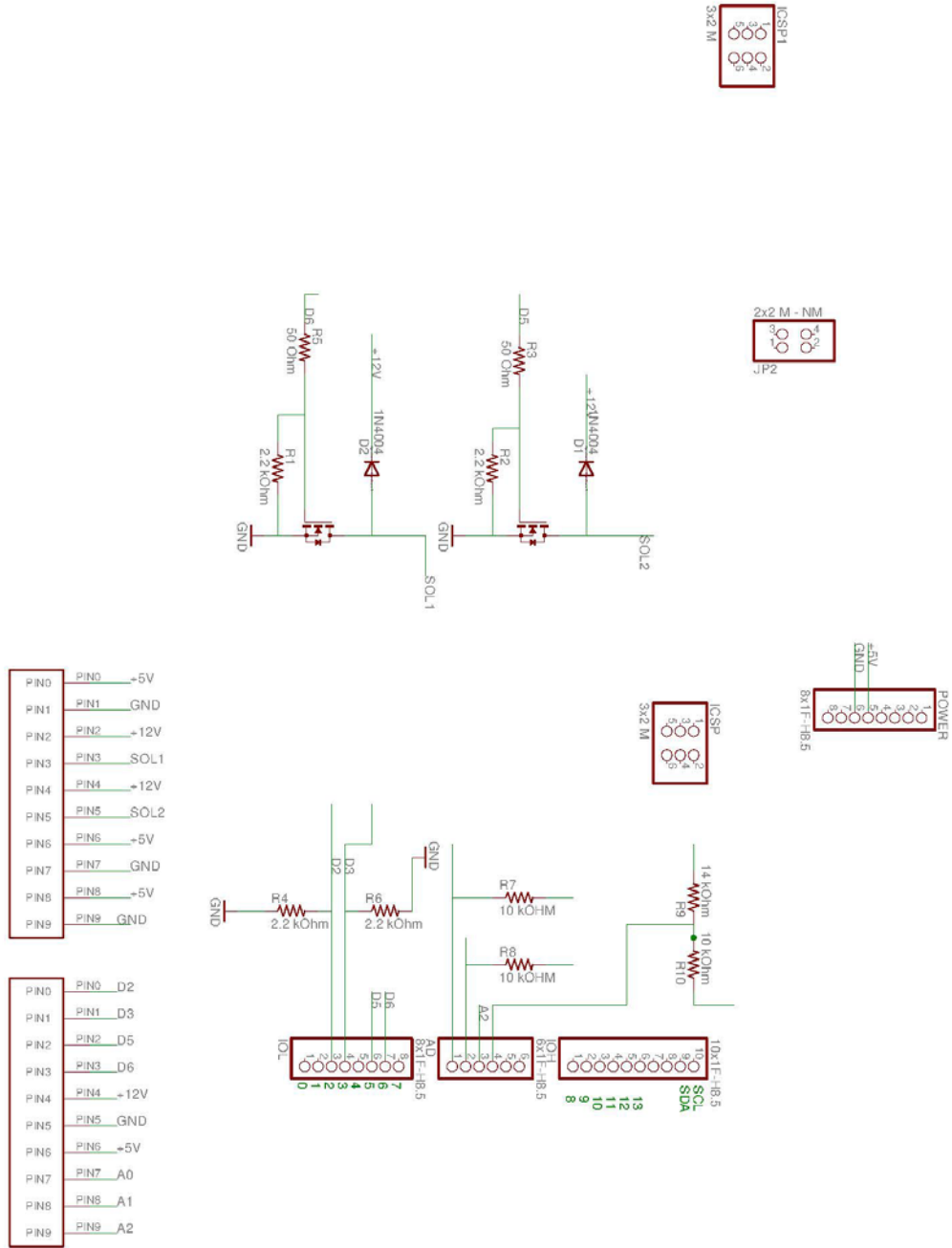
Stresses: Since compressive stresses do not cause fatigue failure, the bearing pressure is limited by the material yield strength YS of the weakest part, commonly the hub. The maximum shear stress in the key and the maximum torsional shear stress in the shaft can be derived from the yield strength of the shaft material.

Fatigue strength: [Calculator for fatigue strength >>](#)

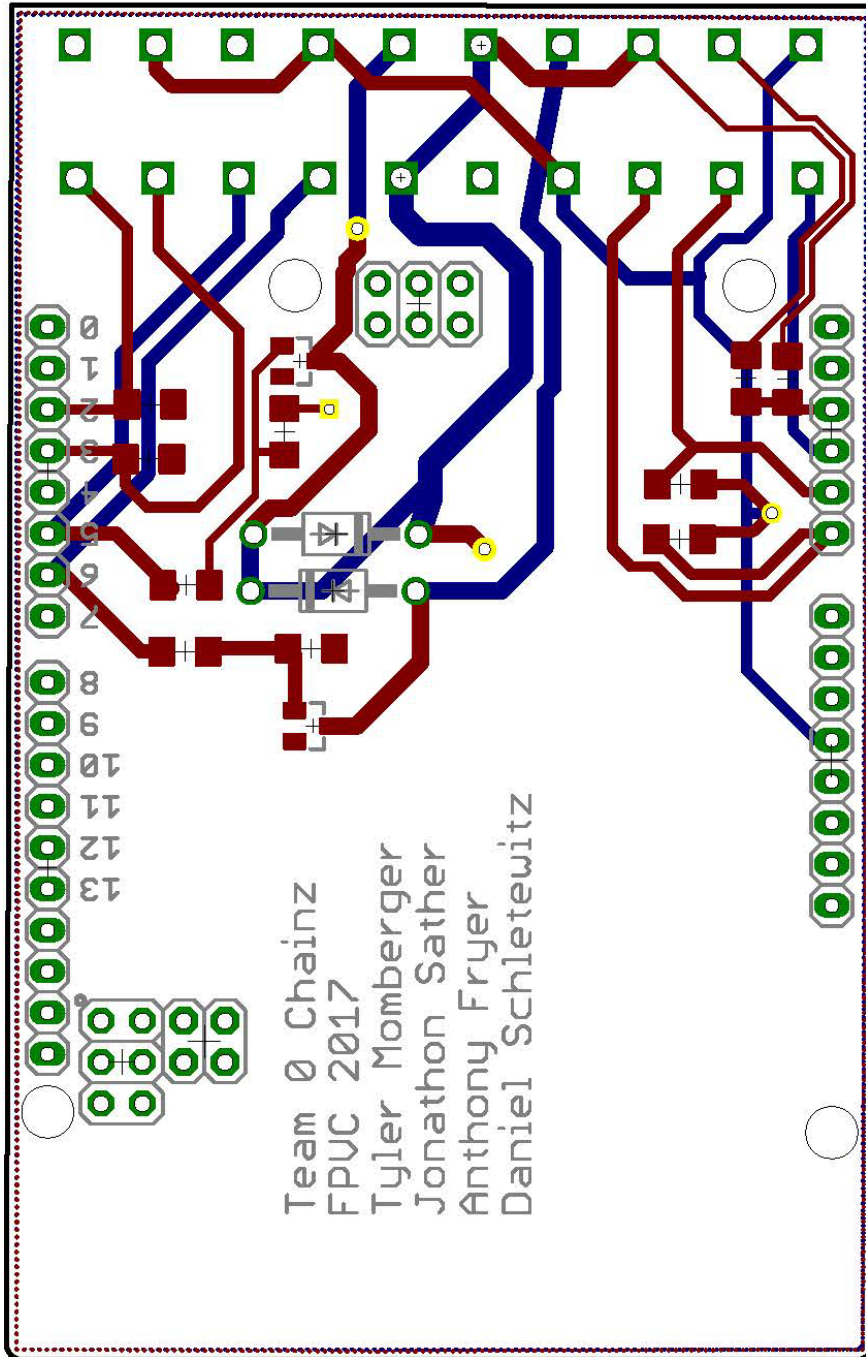
www.tribology-abc.com
📖

Appendix R: Eagle Schematic and Board for Custom PCB

Eagle Schematic



Eagle Board



Appendix S: Concept Design Hazard ID Checklist
SENIOR PROJECT CONCEPT DESIGN HAZARD IDENTIFICATION CHECKLIST

Team: 0 Chainz

Advisor: John Fabijanic

Y N

- Will any part of the design create hazardous revolving, reciprocating, running, shearing, punching, pressing, squeezing, drawing, cutting, rolling, mixing or similar action, including pinch points and shear points?
- Can any part of the design undergo high accelerations/decelerations?
- Will the system have any large moving masses or large forces?
- Will the system produce a projectile?
- Would it be possible for the system to fall under gravity creating injury?
- Will a user be exposed to overhanging weights as part of the design?
- Will the system have any sharp edges?
- Will any part of the electrical systems not be grounded?
- Will there be any large batteries or electrical voltage in the system above 40 V either AC or DC?
- Will there be any stored energy in the system such as batteries, flywheels, hanging weights or pressurized fluids?
- Will there be any explosive or flammable liquids, gases, or dust fuel as part of the system?
- Will the user of the design be required to exert any abnormal effort or physical posture during the use of the design?
- Will there be any materials known to be hazardous to humans involved in either the design or the manufacturing of the design?
- Can the system generate high levels of noise?
- Will the device/system be exposed to extreme environmental conditions such as fog, humidity, cold, high temperatures, etc?
- Is it possible for the system to be used in an unsafe manner?
- Will there be any other potential hazards not listed above? If yes, please explain on reverse.